Development of Biologics Using the *cla*MP Tag: Influence of the *cla*MP Tag on Half-life and
Proteolytic Stability

By

Michaela L. McNiff

Submitted to the graduate degree program in Pharmaceutical Chemistry and the
Graduate Faculty of the University of Kansas in partial fulfillment of the requirements
for the degree of Doctor of Philosophy.

_____

Chairperson/Teruna Siahaan, Ph.D.

_____

Jennifer S. Chadwick, Ph.D.

_____

Wendy Picking, Ph.D.

_____

Thomas Tolbert, Ph.D.

_____

Audrey Lamb, Ph.D.

Date Defended: May 30, 2017

The Dissertation Committee for Michaela L. McNiff certifies that this is the approved
version of the following dissertation:

Development of Biologics Using the *cla*MP Tag: Influence of the *cla*MP Tag on Half-life and
Proteolytic Stability

_____

Chairperson/ Teruna Siahaan, Ph.D.

Date approved: May 30, 2017

ABSTRACT

Peptide and protein therapeutics encounter proteases at every stage of delivery, beginning at the site of administration and ending in the intracellular lysosomal compartment. An intact, stable molecule is desired upon administration, yet release of the payload or activation of the prodrug is necessary at the target site. Successful payload release or prodrug activation can be accomplished using enzymatic recognition sequences specific to proteases expressed in the tumor environment or within endocytic vesicles of the target cell. Control of the proteolytic susceptibility of biologics is essential to deliver a safe and effective molecule. Although degradation and release of proteins is desired at the target site, stability in the systemic circulation is required for successful delivery. Proteins and peptides often succumb to proteolysis in the systemic circulation, causing short half-lives due to their small size resulting in rapid filtration by the kidney. Proteases in the systemic circulation reduce half-life further through fragmentation rendering the biologic inactive. Achieving stability in the systemic circulation would greatly improve the half-life and efficacy of delivered biologics.

Considering the half-life of peptides and proteins is especially important when they are used as diagnostic imaging agents. Contrast agents need a sufficient amount of time to accumulate at the target site to generate a high-quality image. Current contrast agents or diagnostic tracers consist of large chelators bound to lanthanide metals and are chemically conjugated to proteins creating a heterogeneous, unstable and toxic molecule. A common lanthanide ion used for imaging applications is gadolinium, which is often released from the chelator upon dilution into the body and accumulates in the kidney, causing renal toxicity. An improvement to chemically conjugated diagnostic imaging agents is to use a metal-binding tripeptide known as the *cla*MP Tag. The *cla*MP Tag consists of the amino acid sequence Asn-

Cys-Cys and binds transition metals tightly at basic pH. Biocompatible transition metals such as copper and cobalt can be used to create a safe and effective molecular imaging agent. The *cla*MP Tag enables design of a site-specific, homogenous and safe molecule, none of which is possible using current lanthanide binding tags.

The compatibility of the *cla*MP Tag within a metalloproteinase was investigated. Herein is the first application where the *cla*MP Tag was placed within a molecule with a structural or catalytic metal-binding site. One hypothesis was that the *cla*MP Tag would be able to interact with the catalytic Zn active site inhibiting the protease, while release of the *cla*MP Tag could activate the enzyme. The *cla*MP Tag followed by an eight-amino acid linker was engineered to the N-terminus of matrix metalloproteinase-8 (MMP-8). MMP-8 is very difficult to produce because of its inherent function of degrading extra cellular matrix (ECM) proteins and concomitant autoproteolysis. Production of this enzyme proved difficult as several fusion constructs were created and determined to be unsuccessful. A fusion construct consisting of a thioredoxin and S Tag, as well as, a polyhistidine tag enabled expression and purification of active, soluble MMP-8 in high yield. Studies were completed both with and without the *cla*MP Tag placed inline with MMP-8. The *cla*MP Tag had no structural or functional implications on the production of MMP-8. Further investigation of the *cla*MP Tag as a modulator of enzymatic activity is of interest.

Another focus of this work was to investigate the proteolytic stability of *cla*MP-Tagged proteins. To investigate the proteolytic susceptibility of a protein containing the *cla*MP Tag, a proof of concept study was designed to investigate the ability of the *cla*MP Tag to inhibit adjacent proteolysis by a serum protease. The stability of the metal-bound and apo *cla*MP Tag were compared to determine the effect of metal-binding on proteolysis. The *cla*MP Tag inhibits

proteolysis 3-fold compared to the control and use of the *cla*MP Tag in applications creates a more proteolytically stable molecule. Following the proof of concept study, a targeted imaging agent was designed using the *cla*MP Tag and the proteolytic stability of this molecule was analyzed. Previously, the *cla*MP Tag was placed inline with the targeting protein, epidermal growth factor (EGF), and the structure and function of the protein were determined to be unaltered. EGF is a small protein that binds to the receptor EGFR and can be used to target EGFR (+) tumor cells, making EGF ideal for diagnostic imaging. One limitation is EGF has a very short half-life of only 3-7 min. Thus, to improve the half-life, addition of a polymer of amino acids, known as XTEN, was engineered to the C-terminus of EGF. Three EGF-*cla*MP-XTEN molecules were created and analyzed for the structural and functional implications of the addition of XTEN and use of a relevant imaging agent, in this case cobalt, within the *cla*MP Tag.

ACKNOWLEDGEMENTS

The work presented in this dissertation would not have been possible without the support and advisement of others at the University of Kansas. Special thanks to the KU Mass Spectrometry and Analytical Proteomics Laboratory, specifically Todd Williams and Larry Seib for assistance with analyzing samples. Thank you to the KU Microscopy and Analytical Imaging Laboratory. I would like to thank Heather Shinogle and Prem Thapa for training and assistance with the Typhoon Imager. Thank you to Drs. David Volkin and Russ Middaugh at the KU Macromolecule and Vaccine Stabilization Center for allowing me to use their instruments, as well as, Ozan Kumru and Harshit Khasa for training on the instrumentation. I would like to thank Matthew Christopher for the cell culture training and advisement in conducting cell assay experiments. I would also like to thank Drs. Cindy Berrie and Jenifer Tucker for a productive collaboration and for discussion of our manuscripts.

While in graduate school, I had the opportunity to be on the Chemical Biology Training Grant and I would like to thank Drs. Audrey Lamb, Tom Prisinzano and Paul Hansen for teaching the Careers in Chemical Biology class and for all of their efforts to provide us with the necessary tools to begin a successful career. I would like to thank my committee members (Drs. Teruna Siahaan, Jennifer Chadwick, Wendy Picking, Thomas Tolbert and Audrey Lamb) for their support and counsel about my research projects.

While in graduate school I had opportunities to participate in the scientific community internationally. I would like to thank Dr. Ronald Borchardt for allowing me to be a part of the GPEN2016 Organizing Committee. I am especially grateful to have had the opportunity to travel to Helsinki, Finland to participate in the GPEN2014 Meeting. The GPEN2016 Meeting was a great success, none of which would have been possible without Nancy Helm, Dr. Jeffrey Krise, Dr. Lorena Antunez Napolitano and Samantha Pace. I also had the opportunity to work at a pharmaceutical company, AbbVie, for a summer. I would like to thank Drs. David Lindley and Brittney Mills for the opportunity to work in industry for a 3-month internship. I learned a great deal about industry and truly enjoyed being a part of their team for the summer.

I would like to especially thank Dr. Jennifer Chadwick for taking me into her lab in 2013. I not only learned how to conduct experiments and analyze data, but how to think as an independent scientist. She has been a source for not only scientific discussion, but advisement with my career. I appreciate that she continued to find time to work with me even while working full-time in industry. Thank you, as well, to previous Laurence Lab members that made this research possible. Special thanks to Dr. Brittney Mills for training me in the lab during her last year of graduate school and for conducting previous experiments that made my work possible. I would like to thank Dr. Brittney Mills for being a constant mentor and role model over the following years. Special thanks to previous Laurence lab members and friends, Alana Stearns, Emily Haynes and Monica Saha, who provided comic relief and friendship both inside and outside of the lab.

I would like to thank Dr. Teruna Siahaan for taking me into his lab for my final year of graduate school. I appreciate the constant support and advisement I received while in his lab. I would also like to thank the Siahaan lab members, Dr. Mario Morales, Kavisha Ulapane, and

CONFLICT OF INTEREST STATEMENT

JENNIFER S. CHADWICK IS THE CO-OWNER OF ECHOGEN INC., A LIMITED LIABILITY COMPANY THAT HAS LICENSED THE PATENT-PROTECTED METAL ABSTRACTION PEPTIDE (MAP) TECHNOLOGY, ON WHICH THE *cla*MP TAG IS BASED, FROM THE UNIVERSITY OF KANSAS. ALL STUDIES WERE PERFORMED AND PRESENTATION OF RESULTS PRESENTED IN ACCORDANCE WITH THE TERMS OF THE LICENSE AGREEMENT BETWEEN ECHOGEN AND KANSAS UNIVERSITY

TABLE OF CONTENTS

CHAPTER 1.   ASSESSMENT OF THE PROTEOLYTIC STABILITY OF BIOLOGICS IN VIVO

CHAPTER 2.   THIOREDOXIN FUSION CONSTRUCTS ENABLES HIGH-YIELD PRODUCTION OF SOLUBLE, ACTIVE MATRIX METALLOPROTEINASE-8 (MMP-8) IN ESCHERICHIA COLI

CHAPTER 3. METAL-BOUND *CLA*MP TAG INHIBITS PROTEOLYTIC
CLEAVAGE

LIST OF FIGURES

LIST OF SUPPLEMENTARY FIGURES

LIST OF TABLES

LIST OF ABBREVIATIONS

In alphabetical order:

ABD	Albumin binding domain
ADC	Antibody drug conjugate
ADCC	Antibody-dependent cellular cytotoxicity
AEP	Asparagine endopeptidase
Aib	α-aminoisobutyric acid
CD	Circular dichroism
CT	Computerized tomography
CV	Column volume
Da	Dalton
DMEM	Dulbecco's modified eagle medium
DOTA	1,4,7,10-tetraazacyclododecane-1,4,7,10-tetraacetic acid
DOX	Doxorubicin
DPP-IV	Dipeptidyl peptidase IV
ECM	Extracellular matrix
E. coli	Escherichia coli
EGF	Epidermal growth factor
EGFR	Epidermal growth factor receptor
FAP	Fibroblast activation protein
FBS	Fetal bovine serum
FcRn	Neonatal Fc receptor
FGF21	Fibroblast growth factor 21
Gcg	Glucagon
GIP	Glucose-dependent insulinotropic polypeptide
GLP-1	Glucagon-like peptide-1
HBS	Hydrogen bond surrogates
HNE	Human neutrophil elastase
HSA	Human serum albumin
IdeS	Immunoglobulin-degrading enzyme from *Streptococcus pyogenes*
IFN	Interferon

IMAC	Immobilized metal affinity chromatography
IPTG	Isopropyl β-D-1-thiogalactopyranoside
LB	Luria broth
MAP	Metal abstraction peptide
MBP	Maltose binding protein
MMAD	Monomethyl auristatin D
MMP	Matrix metalloproteinase
MRI	Magnetic resonance imaging
MWCO	Molecular weight cut off
NEP 24.11	Neutral endopeptidase 24.11
PEG	Polyethylene glycol
PET	Positron emission tomography
RFU	Relative fluorescent units
rhGh	Recombinant human growth hormone
sCT	Salmon calcitonin
SPECT	Single-photon emission computed tomography
TNF	Tumor necrosis factor
Trx	Thioredoxin
VIP	Vasoactive intestinal peptide
vc	Valine-citrulline

CHAPTER 1. ASSESSMENT OF THE PROTEOLYTIC STABILITY OF BIOLOGICS IN VIVO

1.1 INTRODUCTION

Although biologics are naturally derived, well-tolerated and present many advantages such as low toxicity compared to small molecules, the proteolytic stability of biologics limits their potential use as therapeutic and diagnostic agents.[1] Metabolism and degradation of biologics (*i.e.,* proteins, peptides, oligonucleotides) are rapid in the body because they are naturally derived molecules. Mechanisms of proteolytic degradation of biologics cause short half-lives, resulting in their rapid excretion. Proteolytic enzymes are encountered at every site and step of drug delivery, including the initial site of administration, within the systemic circulation, in tissue matrices, and intracellularly within lysosomes. A balance between stability in the systemic circulation and degradation at the target site is necessary to achieve effective targeted delivery. For example, protease-activated prodrugs consist of the active parent drug with an additional prodomain or promoiety that, upon proteolytic cleavage of the promoiety, generates the active form of the parent drug.[2,3] Release of the active drug is desired to occur at the site of interest, yet stability must be retained during transport to the site of action. For example, antibody-drug conjugates (ADCs) are intended to be stable in the systemic circulation and then degraded to release the drug toxin in the intracellular lysosome of the target cell. Strategies to control metabolic degradation have been utilized to improve the performance of biologics and to create next-generation products with more desirable clinical characteristics.

Proteases are intricate and multi-functional molecules, which makes it difficult to predict their site of action and level of activity toward a specific biologic.[4] The human degradome is located in both intra- and extracellular spaces and it consists of 569 proteases that are classified into five types: cysteine, serine, threonine, aspartic, and metalloproteinases.[5,6] Proteolysis of a

biologic substrate is dictated by the accessibility or proximity of the enzyme to the substrate and its cleavage site(s). Substrate selection among proteases is diverse and some proteases are highly specific and cleave only at a particular recognition sequence while others cleave following a specific amino acid or multiple amino acids. For example, Factor Xa cleaves after arginine at the C-terminus of its recognition sequence (*i.e.*, Ile-(Glu-Asp)-Gly-Arg) with relatively high fidelity, whereas trypsin cleaves at the C-terminal of the lysine or arginine residues with little sequence specificity. Predicting the specificity and activity of each protease *in vivo* is extremely difficult, but is of interest to understand the functional role of proteolytic events in biological processes. One way to identify proteolysis events is to label the N-terminal amine of the substrate. Any proteolysis at the cleavage site that occurs on the labeled substrate can be identified using LC-MS/MS.[7] This method can be used to determine proteolytic cleavage of the substrate biologic at a specific site(s) within the body, for example in the blood, liver, intestines, or kidney. This enables the design of biologics with higher stability.[8-10]

This chapter focuses on the role of proteolytic enzymes in designing proteins and peptides as therapeutic and diagnostic agents. Deciphering proteolytic activity and specificity that produces unwanted degradation in biologic products can be utilized to improve the design and/or formulation of biologics. Identifying protease cleavage sequences and structural preferences will help in the design of the next generation of proteins or peptides with improved stability at the site of administration and in the systemic circulation.

1.2 FACTORS THAT INFLUENCE PROTEOLYSIS

1.2.1 Effects of Individual Chemical Moieties

Recognition of the substrate by a protease is determined by hydrogen bonding and hydrophobic (non-polar) interactions at multiple sites on the substrate and the enzyme active

site.[11] Proteases typically prefer cleavage at the amide bond between two amino acid residues, caused by specific recognition of the two or more amino acid backbones and side chains of the substrate cleavage site by the enzyme binding pocket or active site. Mutation of the amino acid on the substrate cleavage site can greatly decrease or abolish the proteolytic degradation of the substrate. Because the body is teeming with proteases, peptide and protein therapeutics often display poor efficacy because of rapid fragmentation and clearance from the body, resulting in a very short half-life. Often, enzymatic degradation inactivates a therapeutic protein; this can be due to degradation of an active site of the drug. For example, glucagon-like peptide 1 (GLP-1), a 30-amino acid peptide hormone that regulates glucose levels through release of insulin, has a circulation half-life of only 3 min upon intravenous (I.V.) administration.[12] Prior to rapid kidney filtration, GLP-1 is inactivated by the dipeptidyl peptidase IV (DPP-IV) enzyme, which removes the first two N-terminal amino acids, decreasing the half-life to 1–2 min.[13] DPP-IV specifically cleaves peptides from the glucagon family after the second N-terminal amino acid, in this case, the alanine residue. Removal of the two N-terminal amino acids decreases the binding affinity to the GLP-1 receptor 100-fold, rendering the peptide inactive.[14] A second protease, neutral endopeptidase 24.11 (NEP 24.11), cleaves at multiple sites of GLP-1, including between Ala15-Val16, Ser18-Tyr19, Tyr19-Leu20, Glu27-Phe28, Phe28-Ile29, and Trp31-Leu32, causing complete degradation.[15,16] A mutation of the second amino acid, Ala to Gly, inhibits proteolysis by DPP-IV, extending the half-life to 60–90 min.[17,18] Therefore, when a site of proteolysis is known, mutation of a specific amino acid can greatly improve half-life; however, inhibiting a broad range of proteases at multiple susceptible sites requires alternative approaches.

To inhibit a broad range of proteases, six common modifications of the peptide backbone can be implemented, including: (1) incorporation of a N-methylated amide bond, (2) mutation of

an L- to D-amino acid residue, (3) C-methylation of the α-carbon of the amino acid (*e.g.*, α-aminoisobutyric acid, Aib), (4) mutation with β² residues, and (5) mutation with β³ residues (Figure 1.1).[19,20] First, methylation of the peptide backbone is a common modification used to

| α | N-Me-α | D-α | Aib | β² | β³ |
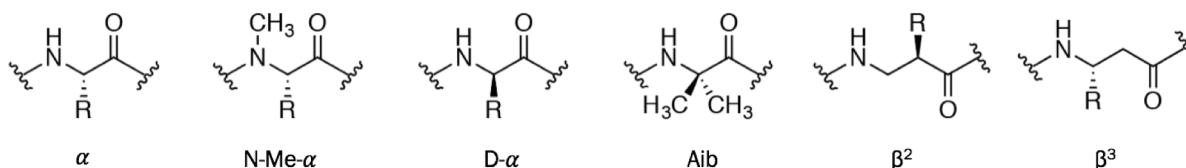
Figure 1.1 Inhibition of proteolysis across a broad range of proteolytic sites can be accomplished using chemical mutations. The structure of five of the commonly used non-natural residues are compared to the natural α-amino acid on the far left.

suppress proteolysis without losing the biological activity of the peptide. For example, three sites of somatostatin were N-methylated to produce octreotide with a 5-fold increase in half-life.[21] Second, a substitution from the natural L-amino acid to a D-amino acid within the cleavage site can improve the enzymatic stability of peptides because proteases cleave only natural L-amino acids. For example, the proteolytic stability of an 11-amino acid peptide used to prevent aggregation of amyloid-β (Aβ) peptides was improved using D-amino acid mutations. The mutated peptide was stable when incubated with high protease concentrations for extended periods of time.[22] Third, α-aminoisobutyric acid (Aib) is an unnatural amino acid that binds to the cell membrane. Aib is present in the peptaibol family of peptide antibiotics, and the presence of Aib in the peptide suppresses their degradation by trypsin. Further, strategic placement of Aib residues in a peptide completely abolished enzymatic degradation.[23] Lastly, β-amino acids have an extended methylene group, either between the amino and α carbon (β²) or between the carboxylate and α carbon (β³).[20] Addition of β-amino acids in several peptide substrates has been shown to eliminate peptide proteolytic degradation.[24] Because β-amino acid-substituted peptides have the propensity to form helical, turn, or extended structures, it is necessary to ensure that

mutated peptides retain their biological activity.[25] It should be noted that any addition of chemically altered amino acids can influence the target selectivity and bioactivity of the modified peptide. Thus, it is necessary to continuously reevaluate the peptide activity and stability during the peptide modification process.[26,27] The peptide backbone modifications were made to a designed peptide and proteolysis at a specific cleavage site was analyzed for each of the backbone modifications. Comparison of the proteolytic susceptibility of the peptide backbone modification determined D-amino acids were the most effective modification and it could increase peptide half-life from 100 to 1000-fold.[19] In contrast, modification with N-methylation of the peptide bond was the least effective in increasing peptide enzymatic stability.

1.2.2 Effects of Secondary Structure

Proteases normally cleave flexible and unstructured regions of proteins much more rapidly than the rigid and structured regions. For example, a region with α-helical structure is proteolytically more stable than the β-sheet region. Analysis of multiple crystal structures showed that the enzyme active site binds to extended β-strand regions of the ligand.[28] Thus, imposing α-helical structure at the cleavage site of a peptide or protein can potentially decrease proteolytic degradation. Typically, small peptides have a low propensity to form α-helix structure; thus, the α-helical structure can be induced and stabilized using a hydrocarbon staple or a disulfide bond within the helical residues (Figure 1.2). A disulfide bond or staple formation between two α-helices can improve the stability of peptides 1000-fold (Figure 1.2 A).[29] One disadvantage of using a disulfide bond is that it can be dissociated *in vivo* by reducing agents (*e.g.*, glutathione) in tissues; thus, a hydrocarbon staple is a more stable crosslink than a disulfide bond. To generate a hydrocarbon staple, two unnatural amino acids containing an alkyne arm are integrated into the peptide sequence. Then, the olefin metathesis reaction is carried out to link the

two alkyne groups and to create a staple across one or two turns in an α-helix (Figure 1.2 B).[30] It has been shown that a peptide with a staple was 41-fold more stable than the parent non-stapled peptide.[30] A natural hydrogen bond can be strategically replaced with hydrogen bond surrogates (HBS) to induce and stabilize an α-helix structure within a peptide (Figure 1.2 C).[31] An unconstrained peptide that binds Bcl-xL and regulates cell death was modified using HBS to create a peptide analog (Bak); Bak peptide has a 30-fold slower degradation rate compared to the unconstrained parent peptide.[32] Cyclic peptides have previously been shown to have higher stability toward proteolysis than do their parent linear peptides. This is due to a more rigid backbone of the cyclic peptide, which does not allow the optimal binding to the active site of the proteolytic enzyme. As an example, a natural cyclic peptide, kahalalide F, is resistant to proteases in plasma.[33] In summary, these modifications may be incorporated into a peptide whenever possible to improve the enzymatic stability of the peptide without sacrificing the biological activity.
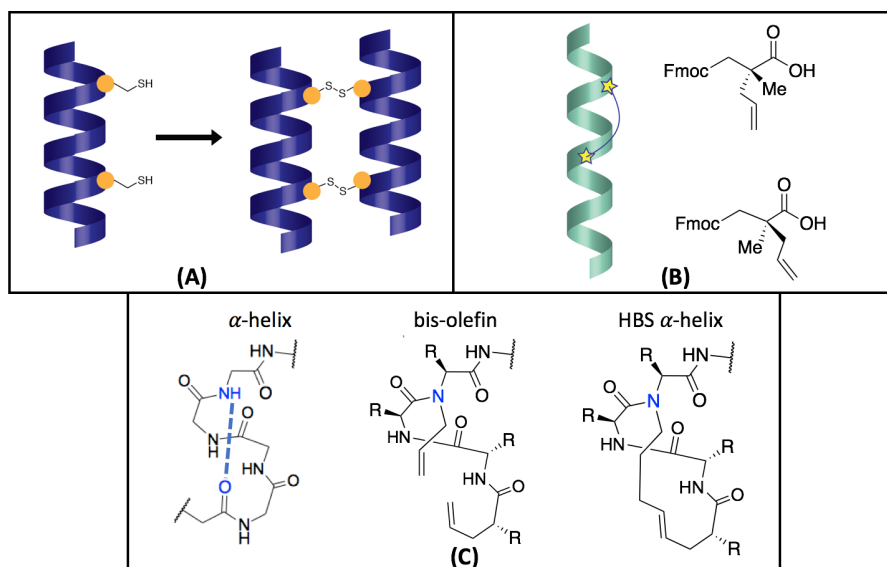
Figure 1.2 Implementation of α-helical structure improves stability against proteolytic cleavage. Three methods of employing covalent bonds to stabilize α-helical structure are: (A) disulfide bond staples, (B) hydrocarbon cross-links, and (C) hydrogen bond surrogates.[29-31]

1.2.3 Inaccessibility to Proteases

Polymers are often added to peptides and proteins to increase *in vivo* circulating half-life by avoiding glomerular filtration (Table 1.1). Not only is glomerular filtration prevented, access to proteolytic sites can be inhibited via steric hindrance in the presence of a polymer. Polyethylene glycol (PEG) is a synthetic, hydrophilic polymer that has been conjugated to peptides and proteins to increase the solubility and hydrodynamic radius of the molecules because every ethylene oxide unit can coordinate 2–3 water molecules.[34] For example, PEG was conjugated to the N-terminus of a recombinant methionyl human granulocyte colony-stimulating factor (Pegfilgrastim or Neulasta®) that is used to treat patients with low white blood cell count (neutropenia) after chemotherapy treatments. Pegfilgrastim can be administered less often than the parent protein, and this improves patient compliance.[35] Pegfilgrastim decreased clearance by 8.6-fold compared to filgrastim, enabling administration once every 21 days rather than daily.[36]

Strategic conjugation of PEG to a site(s) on the peptide or protein is important to consider for maintaining peptide activity while preventing proteolysis. Investigating optimal PEGylation site(s) on human Pin 1 WW domain protein resulted in improved proteolytic and conformational stability.[37] The PEGylated protein has a 1.7- to 3.6-fold increase in half-life compared to the parent protein upon exposure to pronase and proteinase k, respectively.[37] PEGyation at a site that is important for biological activity can reduce protein activity; for example, PEGylation at a native Cys or Lys residue in interferon alpha-2b (IFN α-2b) (PegIntron®) caused a loss of 92% or 93% of the cytokine activity, respectively. However, PEGylation increased the half-life, which compensates for the loss of activity.[38]

Table 1.1 Commonly Used Polymers and Fusion Proteins to Increase Half-life

Half-life Enhancer	Sequence	Molecular Weight (kDa)	Function
PEG	Polymer of ethylene oxide	5, 10, 20 kDa	Synthetic polymer[34,39]
ELPfusion	(Val-Pro-Gly-Xaa-Gly)$_x$	Tunable	Reversible phase transition[40-42]
XTEN	Random sequence of Ala, Glu, Gly, Pro, Ser, Thr	Tunable	Non-immunogenic, hydrophilic, proteolytic-resistant[43-47]
CTP	C-terminal peptide from the β-subunit of hCG	3.5 kDa plus glycosylation	Four O-glycosylation sites[48-50]
Fc Fusion	Fc domain of mAb	50 kDa	FcRn binding and recycling[51-53]
Albufusion	Human Serum Albumin	65 kDa	Long serum half-life[54-56]

As an alternative to PEG, an XTEN protein has been fused to the N- or C-terminus of protein drugs to increase their hydrodynamic radius and half-life.[43,47] The XTEN protein is an unstructured protein with a random sequence composed of six amino acids, including Ser, Thr, Glu, Gly, Pro and Ala. The XTEN sequence is normally genetically engineered into the DNA sequence of a functional protein, and the fusion protein is expressed in an inline homogeneous fashion. The XTEN sequence is biodegradable and, yet, it has been designed to prevent proteolysis by serum proteases for an extended period of time.[57] XTEN has been incorporated into many functional proteins, including exenatide, human growth hormone, and glucagon to display half-lives with a 60- to 130-fold improvement over the native molecule.[44,46,57,58] An in-depth review of this type of fusion proteins is outside the context of this review but can be found at the references listed here.[59,60]

Another way to improve the protein half-life is to fuse a functional molecule, such as the Fc domain of IgG, to the protein. Monoclonal antibodies (mAbs) are protected from intracellular

degradation because at the early stage of endocytosis, the Fc domain of mAbs binds to the neonatal Fc receptor (FcRn). Once endocytosed, the pH is lowered to 6.0–6.5, resulting in protonation of the histidine residues on the CH2-CH3 hinge domain of IgG. Ionic interactions then form between the protonated His residues and the negatively charged Glu117, Glu132 and/or Glu135, and Asp137 residues on FcRn. The increase in binding affinity results in the molecule being recycled back to the surface where it can re-enter the circulation.[61] Exposure to the extracellular space at pH 7.4 reduces affinity and enables release of IgG from FcRn, which substantially lengthens circulating half-life, in some cases up to 1–2 weeks.[62-64] As an example, etanercept (Enbrel®, Amgen) is a fusion protein consisting of two extracellular domains of tumor necrosis factor (TNF) receptor conjugated to the Fc fragment from IgG1. This fusion protein is used to treat rheumatoid arthritis by neutralizing and reducing the TNF cytokine levels produced during inflammation. Etanercept has a half-life of 68 h, and requires twice weekly dosing compared to the unstable TNFR p75 monomer.[65] Also, Eloctate® (Biogen) is a recombinant human factor XIII fused to the Fc domain used for treatment of hemophilia. Fusion of Factor XIII to the Fc domain increases the half-life to 19 h compared to 8–12 h for the parent Factor XIII; this is due to lower elimination and slower proteolytic degradation of Factor XII-Fc fusion than the parent Factor XIII.[66] Similar to Fc fusion, albufusion is an inline fusion between human serum albumin (HSA) and a bioactive protein.[54] Albufusion of IFN-α (HSA-IFN-α) provides a longer half-life (159 h) than PEGylated IFN-α; therefore, HSA-IFN-α can be dosed every 2–4 weeks rather than once a week for PEGylated IFN-α.[56] Although the half-life of HSA-IFN-α is increased, its activity is only 1% of that of the parent IFN-α, similar to PEGylated IFN-α. An alternative to albufusion, bioactive protein can be linked to fatty acid chains, and this modification enables binding of the fatty acid-protein conjugate to HSA in the systemic

circulation. This method improves the half-life of the conjugate in the systemic circulation without sacrificing the activity of the protein drug.[55] One example is liraglutide, a fatty acid conjugate of GLP-1. This conjugate binds to albumin and increases its half-life to 10–14 h.[17,67] Table 1.2 is a list of bioactive protein drugs that utilize chemical and fusion protein modifications to increase proteolytic stability and half-life in systemic circulation.

Addition of a small stability tag to a protein can increase protein enzymatic stability in serum while maintaining its bioactivity. In this case, the tag is a string of amino acids that is resistant to serum proteases. One example of an enzymatic-resistant peptide is a twelve-residue peptide that is resistant to thrombin proteolysis. Pro, Ser, Thr, and Asn residues within the peptide are the most thrombin-resistant amino acids. This inhibitory property is due to the induced peptide secondary structure with stabilized hydrogen bondings.[68] Also, a dipeptide tag such as the Pro-Pro motif has been shown to increase peptide stability in serum.[69] Using a florescent tag, incubation of stable peptides in serum showed that Asp-Pro-Pro-Ser and Asp-Pro-Pro-Glu are the most stable sequences against enzymatic degradation.[69] Thus, inclusion of a small stability tag can increase proteolytically stability of therapeutic peptides and proteins without the need to conjugate them to large molecules.

Table 1.2 Examples of Biologics Designed to Improve Half-life

Biologic Drug	Native molecule	Modification to Inhibit Proteolysis/Extend Half-life	Improvement over native
Peg-Intron ® (Merck)	Interferon alfa-2b	12 kDa PEG conjugated to interferon alfa-2b[38,70]	40 h vs. 0.1-1.7 h
Pegasys ® (Genentech)	Interferon alfa-2a	Pegylated (branched 40 kDa) interferon alfa-2a[71]	77 h vs. 9 h
Neulasta® (Amgen)	Recombinant methionyl human granulocyte colony-stimulating factor	N-terminal 20 kDa PEG conjugated to recombinant methionyl human granulocyte colony-stimulating factor[35,36,72]	15-80 h vs. 2.6 h

Enbrel ® (Amgen)	Tumor necrosis factor (TNF) receptor	Two extracellular domains of tumor necrosis factor (TNF) receptor conjugated to Fc fragment from IgG1[65]	Approximately 70 h
Eloctate ® (Biogen)	Recombinant human factor XIII	Fc-fusion protein[66]	19 h vs. 8-12 h
VRS-859 Exendin 4-XTEN, Phase 1 clinical trials (Amunix)	GLP-1	GLP-1 analog, exenatide fused with XTEN864 at the C-terminus[43]	128 h vs. 1-5 min
Kineret ® (Sobi)	Human interleukin-1 receptor antagonist (IL-1Ra)	HES (hydroxyethyl starch)[73,74]	10.8 h vs. 1.7
Byetta ® (AstraZeneca)	GLP-1	Second amino acid Ala to Gly[43]	2.4 h vs. 1.5-5 min
Victoza ® (Novo Nordisk)	GLP-1	Addition of C-16 free fatty acid[17,67]	10-14 h vs. 1.5-5 min
Sandostatin ® (Novartis)	Somatostatin	Shortened to eight amino acids, Trp8 to D-Trp8, disulfide, Phe to D-Phe and Thr to reduced threoninol[21,75]	90-120 min vs. 2-4 min
Somavaratan (VRS-317)	Recombinant human growth hormone	Addition of XTEN to N and C terminus[76]	30-60-fold increase to more than 131 h

1.3 PROTEOLYTIC ACTIVITY AT DIFFERENT SITES

Oral, pulmonary, transdermal, and other non-invasive routes contain the most preferred sites for peptide and protein drug administration in patients; however, some of these (*i.e.*, oral and transdermal) do not have effective sites for delivering peptides and proteins due to the presence of restrictive biological barriers (*i.e.*, intestinal and skin barriers) that the drugs are unable to cross. In addition, each delivery site has a unique composition of proteases that can digest the delivered peptide and protein drugs. Therefore, understanding protease activity and specificity for the delivered drug at the common sites of administration (*i.e.*, intravenous, oral, pulmonary, subcutaneous, and transdermal) enables selection of the appropriate route of

administration for the drug. The drug formulation can be designed to stabilize the molecule against proteolytic degradation at the site of delivery (Table 1.3 and Table 1.4).[77,78]

1.3.1 Intravenous Delivery

Intravenous injections are commonly used for direct delivery of drugs to the systemic circulation and to enable rapid onset of action by the biologic. Small proteins and peptides, specifically peptide hormones, are susceptible to rapid degradation in the systemic circulation. Peptide hormones (*e.g.*, GLP-1 and glucose-dependent insulinotropic polypeptide (GIP)) exhibit cleavage of the first two N-terminal residues by DPP-IV in serum (Figure 1.3 A).[79-81] Furthermore, carboxypeptidase M removes the C-terminal Arg residue of GLP-1.[79] DPP-IV and fibroblast activation protein (FAP) readily digest fibroblast growth factor 21 (FGF21) at the N- and C-termini, respectively, to limit its half-life to 1–2 h.[82-84] Cleavage of the first 2 or 4 residues of FGF21 by DPP-IV did not impact its activity; however, cleavage of the C-terminus after Pro-171 by FAP renders FGF21 inactive because it no longer binds to the receptor (Figure 1.3B).[81]
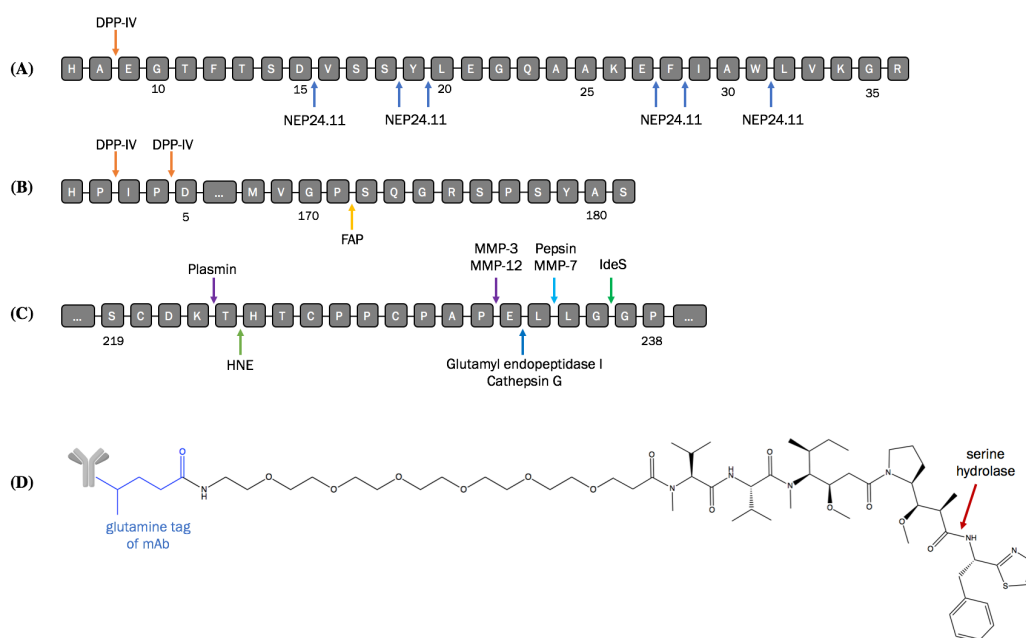
Figure 1.3 Multiple proteolytic sites are present within protein and peptide therapeutics. Sites of enzymatic cleavage are labeled within (A) GLP-1,[16,17] (B) FGF-21,[81] (C) hinge domain of IgG1,[85] and (D) MMAD payload conjugated to an antibody.[86]

Large proteins such as monoclonal antibodies (mAbs) spend a substantial amount of time in circulation and have prolonged exposure to proteases. Degradation of mAbs is common in human serum; for example, IgG1 is cleaved at the hinge region by matrix metalloproteinase-3 (MMP-3), glutamyl endopeptidase I, and streptococcal immunoglobulin-degrading enzyme (IdeS) to release a 135 kDa fragment (Figure 1.3 C).[85] A long enzymatic incubation of intact mAbs leads to further proteolysis and release of Fab and Fc fragments. The antibody-drug conjugate (ADC) trastuzumab is susceptible to degradation by multiple proteases. For examples, MMPs cleave trastuzumab at the lower hinge region while IdeS cleaves between the Gly236 and Gly237 residues at the hinge region. When proteolysis occurs, the activity of the molecule is in jeopardy, which impacts both the binding to the HER2+ receptor and hinders the antibody-dependent cell-mediated cytotoxicity (ADCC) activity. Cleavage of trastuzumab at the hinge domain did not affect its binding affinity for HER2; however, the ADCC activity of trastuzumab decreased from 80% to 20% because of the loss of the Fc domain.[87] Other mAbs such as infliximab and adalimumab are degraded by MMP-3 and MMP-12 when incubated in sera from patients. A 32-kDa Fc monomer was released from the antibody, while the antigen-binding domain (Fab) activity was still retained for neutralizing tumor necrosis factor in patients with inflammatory bowel disease.[88] The small Fab fragment is likely to have a shorter half-life and lowering circulation time for exerting its biological activity. Not only can both the mAb and the linker be enzymatically degraded, the drug payload itself is susceptible to degradation. Monomethyl auristatin D (MMAD) conjugated through a non-cleavable linker to the mAb was cleaved by proteases to release a 186 Da fragment corresponding to the C-terminal dolaphenine residue (Figure 1.3 D).[86] Modification of the C-terminal end of MMAD or changing the site of MMAD conjugation eliminated proteolytic degradation. LC-MS techniques have been developed

to characterize the exact sites of proteolysis, enabling identification of specific enzymes that show high activity. [89-91]

1.3.2 Oral Delivery

One of the major hurdles in oral delivery of peptides and proteins is the harsh chemical and enzymatic environment of the stomach and intestines, as well as the presence of intestinal barriers that block the passive diffusion of peptides and proteins. The small intestine is home to some of the highest concentrations of proteases, including trypsin, chymotrypsin, and elastase; these enzymes specifically recognize and cleave basic and aromatic amino acids.[8] In addition to proteolytic degradation, the innate physicochemical properties (*i.e.*, size, hydrophilicity, and charge) of biologics prevent their absorption and permeation through the intestinal epithelium, which limits absorption of molecules greater than 500–700 Da.[92,93]

Upon oral administration, protein therapeutics first encounter the severe environment of the stomach, which has a low pH between 2–3 and contains digestive enzymes such as pepsin that rapidly cleave the peptide bonds. Protein and peptide drugs can be protected from the acidic and enzymatic environment in the stomach through complexation with pH-responsive complexation gels. For example, polymers can be used to encapsulate insulin for protection from low pH in the stomach and the insulin is released from the polymer in the intestine as the pH increases.[94] These technologies are very useful for protection of peptides and proteins from degradation, but they do not help the absorption process of peptides and protein because the normal bioavailability of biologic drugs is less than 1%. An alternative is OptiGel™ Biotechnology (Catalent), which formulates macromolecules with an enteric coating and permeability enhancers to protect drug molecules from degradation. This application enables improved drug transport through the tight junctions of the intestinal lumen. Another option to

decrease proteolysis is to administer the biologic with protease inhibitors; the extent of degradation was decreased when the ratio of inhibitor-to-trypsin was increased.[95] Salmon calcitonin (sCT) is rapidly degraded in the lumen by serine proteases, and co-administration with ovomucoids greatly improves its stability. After a 1-hour incubation of 1:4 trypsin:inhibitor with sCT, 87% of sCT remained intact compared to 0% intact in the absence of inhibitor.[95]

From the stomach, the biologic travels to the small intestine, which consists of the duodenum, jejunum, and ileum. In the duodenum, enzymes secreted from the pancreas account for the highest proteolytic activity, while less proteolytic activity is seen in the ileum and colon.[96] Specifically, serine endopeptidases and carboxypeptidases such as trypsin, chymotrypsin, elastase, and carboxypeptidase A and B are secreted into the lumen.[97] For bioavailability, the intact biologic must reach the systemic circulation, which means traversing the intestinal epithelium, consisting of a mucosal layer, followed by the brush-border that lines the epithelial cells. The mucosal layer consists of enzymes, mucopolysaccharides, glycoproteins, electrolytes, and water, creating a thick barrier layer that is very difficult to diffuse through, slowing absorption.[77] Following uptake into the mucosal layer, the biologic encounters the surface of the epithelia cells known as the brush border membrane. Brush border enzymes have an activity of 4.18 nmol hydrolysis/cm^2/min in an area of 0.5–2.0 cm^2, which was determined by cleavage of the substrate L-leucine-*p*-nitroanilide.[9] Woodley *et. al.* have presented a complete list of active brush border enzymes.[97]

Antibodies have not yet been delivered orally because of their size and proteolytic susceptibility. An alternative to delivering intact mAbs is to use a smaller version of an antibody, termed a nanobody. The nanobody was initially discovered in camel sera[98] and consists of a mAb that lacks the CH1 domain and the light chain, containing only one heavy variable chain

(approximately 15 kDa).[99,100] Oral delivery of these molecules is of interest because of their small size and the fact that when incubated with pepsin or trypsin for 1 hour the molecule retains 60% activity.[101] Through DNA shuffling to create a mutant of the nanobody, proteolytic stability was increased and activity was retained in gastric and jejuna fluid to create a promising candidate for oral delivery.[102] However, it is still not clear whether nanobodies can cross the intestinal mucosa barrier into the systemic circulation. Peptides have been used successfully to target cells within the intestine without the need to cross the intestinal mucosa barrier. Linaclotide, a 14-amino acid peptide, has been used to treat irritable bowel syndrome (IBS) and chronic idiopathic constipation (CIC). The peptide targets a receptor within the intestine to stimulate a pharmacologic response without requiring exposure to the systemic circulation. Rapid proteolysis of linaclotide was observed in the duodenum and jejunum, and less degradation was observed in the ileum.[103] When linaclotide was incubated with carboxypeptidase A, a single reaction product was formed, but the molecule remained active.[103] Other peptides, such as GLP-1 agonists for oral formulations were in phase I or II clinical trials in 2015[104] and insulin for oral formulations was in phase II-IV clinical trials as reported in 2016.[93]

1.3.3 Pulmonary Delivery

Pulmonary delivery is a non-invasive option that avoids the harsh condition of the GI tract. The lung provides a large surface area with good vascularization and low membrane thickness, making it an ideal drug delivery site. Although the characteristics of the lungs seem well suited for delivery, mechanisms are in place to keep out foreign substances. Absorption is difficult to achieve because of the presence of alveolar macrophages and proteases in the lower respiratory airways designed to remove toxic aerosols.[105] The main clearance mechanism in the upper conducting airways is mucociliary clearance using a mucus layer. The mucus layer

protects the body from foreign inhaled substances that are rapidly cleared before reaching the epithelium. Drugs that cannot penetrate the mucus layer will be eliminated with the mucus when it is transported by the ciliated cells to the GI tract.[106] The lower respiratory airways contain alveolar macrophages and proteases that clear or degrade slowly dissolving molecules.[107] Macrophages contain peptide hydrolases that can degrade foreign proteins rapidly, evolving this function as a protection against foreign bacteria and viruses. Enzymes such as extracellular lysozyme, aprotinin, neutral endopeptidase, angiotensin-converting enzymes, tryptase, and chymase are active in the pulmonary environment.[108] Most of these enzymes are non-specific and cleave at many peptide bond sites. If the biologic makes it past the mucus layer, it will encounter the epithelium, where the molecule can be absorbed by transcytosis or paracellular transport or through large pores in the epithelium.[109] Lastly, the molecule must pass through the basement membrane and vascular epithelium, which are cells that make up the small blood and lymph vessels enabling access to the systemic circulation.[110,111]

Enzymatic degradation is common during pulmonary delivery, but to a lesser extent than in oral delivery. Comparison of incubation of insulin in small intestine homogenate vs. homogenate of lung tissue showed half-lives of 66 min and 82 min, respectively.[112] These results are in line with insulin incubation in intestinal epithelial cytosol compared to lung cytosol where 60% of insulin remained intact after 9.1 and 27 min, respectively.[113] When co-administered with bacitracin, an inhibitor of aminopeptidases, 95% and 60% of insulin remained intact after 10 and 240 min, respectively, while only 65% intact insulin remained after 10 minute-incubation without bacitracin.[113] Other proteins have been investigated for enzymatic degradation via the pulmonary route.[114] For example, formulation of sCT into PEG-coated micelles shielded the peptide from enzymes in the pulmonary environment and increased bioavailability by 60%.[115]

Similarly, peptide YY (PYY; a 36-amino acid peptide), which is used to treat obesity by suppressing appetite, has the same half-life when administered via the pulmonary (25 min) and intravenous (26 min) routes.[116] One metabolite of PYY is PYY3-36 with deletion of the first two amino acids. This deletion suggests that DPP-IV is the cause of the N-terminal cleavage in PYY.[116]

1.3.4 Subcutaneous and Transdermal Delivery

Subcutaneous injection using a needle to administer a bolus injection into the hypodermis is commonly used to deliver biologics because it bypasses the protective layers of skin (*i.e.*, the stratum corneum, epidermis, and dermis) that contain many proteases for protection from foreign substances.[117] The drug travels to the systemic circulation either by traversing the blood vessels or through lymphatic uptake. Proteolysis also occurs at the subcutaneous site, and co-administration of enzyme inhibitors suppresses degradation of biologics. For example, co-administration of the protease inhibitor ε-aminocaproic acid decreased proteolytic activity to restore response to the parathyroid hormone (PTH).[118]

A less invasive strategy is transdermal delivery; it has the convenience of self-administration and less frequent dosing, which increases patient compliance. Transdermal drug delivery encounters less proteolytic activity than mucosal routes.[119] Enzymes that are active throughout the skin layers include endopeptidases and exopeptidases. Carboxypeptidases and aminopeptidases are specifically found in the skin; they metabolize collagen, gelatin, and elastin as well as exopeptidases, such as DPP-IV, carboxypeptidases, and aminopeptidases.[120] Streinstrasser *et al.* list enzymes that cleave topically applied peptides, including aminopeptidase and dipeptidyl peptidase that digest calcitonin and vasopressin.[120] The GLP-1 analog, exendin-4, was investigated for transdermal delivery. Exendin-4 has a half-life of 30 min when administered

intravenously and 2–3 h when administered subcutaneously. To improve the half-life, two Cys mutants were placed within exendin-4 at *i* and either *i* +7, *i* +11, or *i* +14 to create a disulfide staple to stabilize the helical structure and protect against serum proteases. Microstructure arrays consisting of exendin-4 incorporated into biodegradable solid microstructures allow more rapid systemic absorption, reaching C_{max} after 5 min compared to the gradual increase over 8 h observed with subcutaneous administration.[121] Although transdermal delivery has lower proteolytic activity, analogs such as exendin-4, rather than GLP-1, must still be used to protect against active proteases.

Table 1.3 Proteases Expressed at Each Site of Administration

Sites	Proteases	Solutions
Intravenous	DPP-IV, FAP, MMPs, IdeS, Glutamyl endopeptidase I, plasmin, carboxypeptidase M	Amino acid mutations[17,18]
Oral	Pepsin, carboxypeptidase A, plasmin, trypsin, carboxypeptidase B, chymotrypsin, elastase	Polymer enteric coating,[94] thioether cross-linkage,[122] enzyme inhibitors[95]
Pulmonary	Neutral endopeptidase, chymase, DPP-IV, tryptase	PEG-coated micelles,[115] enzyme inhibitors[113]
Subcutaneous & Transdermal	Neutral endopeptidase 24.11, DPP-IV	Disulfide staple,[121] enzyme inhibitors[118]
Intracellular	Cathepsin B, Cathepsin D, HNE, Cathepsin G	Val-Cit dipeptide,[123] β-glucuronide linker[124]

Table 1.4 Summary of Relevant Enzymes Contributing to Proteolysis of Biologics *In Vivo*

Enzyme Type	Enzyme Name	Preferred Cleavage Site	Examples	Relevant Tissue(s)/Site of Administration	Intra- or Extra-cellular Origin
Aspartic protease	Pepsin	IgG1 hinge	IgG1[85]	Stomach	Extra
Cysteine protease	Cathepsin B	ADC Val-Cit linker	Adcentris[125]	Lysosome	Intra

Cysteine protease	Cathepsin D	Cleavage after Glu and Asp	a-Synuclein (Glu123-Ala124) (overexpression in Parkinson's disease)[126]	Lysosome	Intra
Cysteine protease	Streptococcal immunoglobulin degrading enzyme (IdeS)	Hinge cleavage	IgG1, Trastuzumab[85]	Serum	Extra
Metalloproteases	Aminopeptidases	Cleave N-terminal residues	Insulin[113]	Epidermis	Extra
Metalloprotease	Angiotensin converting enzyme	Cleaves between Arg & Leu	Angiotensin[127]	Lung	Extra
Metalloexopeptidase	Carboxypeptidase A	Cleavage of C-terminal aromatic/aliphatic residue	Linaclotide[103]	Secreted from pancreas	Extra
Metalloexopeptidase	Carboxypeptidase B	Cleavage of terminal basic residue	Proinsulin[128]	Secreted from pancreas	Extra
Metalloexopeptidase	Carboxypeptidase M	Removes C-terminal basic residues (Arg or Lys)	GLP-1, GIP[79]	Serum	Extra
Metalloproteinase	MMP-3, MMP-7, MMP-9, MMP-12, MMP-13	Hinge cleavage	IgG1, infliximab, adalimumab, trastuzumab[85, 88]	Serum	Extra
Metalloprotease	Neutral endopeptidase	Cleaves N-terminal to hydrophobic residues	Glucagon[108]	Lung	Extra
Metalloproteinase	Neutral Endopeptidase 24.11 (NEP 24.11)	Multiple sites	GLP-1[15,16]	Serum	Extra

Serine protease	Cathepsin G	IgG1 hinge	IgG1[85]	Cytoplasm	Intra & Extra
Serine protease	Chymase	Cleaves C-terminal to Phe, Tyr, Trp or Leu	VIP[108]	Lung	Extra
Serine protease	Chymotrypsin	Cleavage C-terminal to Phe or Tyr	Insulin[8]	Secreted from pancreas	Extra
Serine protease	DPP-IV	Cleavage after Ala or first 2-4 residues	GLP-1, FGF21[13,81-83]	Serum, Lung, Skin	Extra
Serine protease	Elastase	Cleaves C-terminal to Leu	Insulin[129]	Secreted from pancreas	Extra
Serine protease	Fibroblast Activation Protein (FAP)	Cleaves after Pro-171 in FGF	FGF[81]	Serum	Extra
Serine protease	Glutamyl endopeptidase I	Hinge cleavage	IgG1[85]	Serum	Extra
Serine protease	Human neutrophil elastase (HNE)	Fab of IgG1	IgG1[85]	Cytoplasm	Intra & Extra
Serine protease	Plasmin	Fab of IgG1	IgG1[85]	Serum	Extra
Serine protease	Trypsin	Cleavage C-terminal to Arg or Lys	Insulin[128]	Secreted from pancreas	Extra
Serine protease	Tryptase	Cleaves C-terminal to Arg or Lys	Vasoactive intestinal peptide (VIP)[130]	Lung	Extra

1.4 TARGETING PROTEASES FOR IMPROVED DELIVERY

1.4.1 Protease-Activated Therapeutics

Although inhibition of proteases is often necessary for the biologic to reach or be retained in the systemic circulation, proper timing of the release at the tumor site presents an advantage to create extremely effective biologics. For example, ADCs utilize cleavable linkers that take

advantage of the differences in intra- and extracellular environments, such as reduction potential and the specific enzymes expressed at each site. The conjugation between the two entities by a linker is extremely important because it determines the stability of the intact molecule. Ideally, the linker is stable in the systemic circulation before reaching the target cells, yet the payload is released once the conjugate is internalized into the cell.[131] It is necessary to characterize the stability of the intact ADC to ensure that limited premature drug release occurs to avoid off-target toxicity.[132] Different types of linkers such as chemically-labile, enzymatically-labile, and non-cleavable linkers are used for conjugation.[131] Linkers are typically compared to determine the most stable and useful linker for the specific application.[133] Conjugation of a mAb to MMAE through a hydrazone (acid-labile) linker was compared to conjugation through a dipeptide (enzyme-labile) linker. The enzyme-labile linker showed increased stability in plasma, and further investigation using a mouse model determined half-lives of 2.3 days and 30 days for acid-labile and enzyme-labile linkers, respectively.[134]

Within lysosomes there are more than 50 hydrolytic enzymes that thrive in the acidic environment, completing rapid degradation by proteolysis.[135] Cathepsins are lysosomal enzymes and are classified as serine, aspartic, and cysteine cathepsins. In addition, other enzymes such as napsin and AEP (asparagine endopeptidase) are present.[135] During disease states, levels of protease expression and activation are dysregulated, making proteolysis within the tumor environment unpredictable.[136] For example, not only are cathepsins found intracellularly, but during tumor metastasis they are secreted into the extracellular environment where they degrade extracellular matrix (ECM) proteins.[137] A popularly used enzymatic linker is the valine-citrulline (vc) dipeptide that is cleaved intracellularly by cathepsin B.[123] Alternatively, a β-glucuronide linker is cleaved by β-glucuronidase, an enzyme expressed in lysosomes and the tumor

environment.[124] Choi *et. al.* provides a list of intracellular proteases and their preferred cleavage sequence, including enzymes such as cathepsin B, kallikrein 2, MMPs, and trypsin.[2]

Targeted release within the tumor environment rather than intracellularly has been used successfully as well. One family of enzymes that is of interest is MMPs because their dysregulated activity is associated with tumorigenesis. Doxorubicin (DOX), a small molecule chemotherapeutic agent, was conjugated to a small peptide consisting of an MMP cleavage sequence. The attached peptide inhibited DOX from diffusing into the cell, but after proteolytic removal of the peptide, the molecule is free to enter the cell and increases DOX accumulation at the tumor site 10-fold compared to that in other tissues.[138] The enzyme chosen to cleave the prodrug should be expressed solely at the site of desired activation to create an effective prodrug. This is truly a way to improve selectivity of a molecule by targeting well-known enzymes expressed only at the targeted site.

1.4.2 Enzymatic Releasable Half-life Enhancement

As discussed above, half-life can be improved through chemical conjugation or fusion of a polymer to the protein, but often these polymers impede bioactivity. A releasable version of PEG has been used to control and modify the half-life of the molecule and allow the free molecule to retain activity once released.[39,139,140] This technology is extremely useful for applications in which addition of PEG greatly reduces activity. The design includes an enzymatic cleavage sequence between the biomolecule and PEG.[141] For example, the antimicrobial peptide Onc112 was conjugated to PEG through a 4-residue linker that is recognized and cleaved by blood proteases. Depending on the sequence of the linker, the half-life can be tuned anywhere from 1 to 42 h for Onc112.[142] Releasable methods were also applied to the albufusion

technology, where HSA is released by proteolysis from the protein therapeutic. This releasable technology exhibits a 2- to 64-fold increase in activity over the non-releasable construct.[73]

Alternatively, enzyme-releasable small affinity tags to human serum albumin, termed albumin binding domains (ABDs), can be used to bind to serum albumin. Albumin binding domains of 12 amino acids were identified to bind with high affinity to HSA. Similar to the releasable albufusion technology, the addition of a linker containing a thrombin or Factor Xa cleavage sequence can be used to release the ABD peptide. An ABD-linker-GLP-1 molecule was created and an 8–20-fold improvement in half-life of exendin-4 was observed.[143] Conjugation through enzymatic linkers allows slow release of proteins from their circulating half–life partners.

1.5 CONCLUSIONS

Proteolysis is an important factor to consider when designing biologics. Proteolysis can cause a short half-life by cleaving the biologic into smaller fragments or site-specific cleavage that causes inactivation. Both amino acid sequence and secondary structure impact the ability of a protease to cleave a protein, and new techniques are being developed to easily impose and stabilize protease-resistant structures. Large fusion proteins can be added to proteins to increase their half-lives, but they often compete with the activity of the molecule. Using enzymes to purposefully cleave a prodomain to release an active protein allows "tuning" of the half-life of these biologics. Strategies to protect biologics from proteolytic degradation can be implemented to successfully design active and effective biologics.

1.6 REFERENCES

1.   Vugmeyster, Y.; Xu, X.; Theil, F.-P.; Khawli, L. A.; Leach, M. W., Pharmacokinetics and toxicology of therapeutic proteins: Advances and challenges. *World Journal of Biological Chemistry* **2012,** *3* (4), 73-92.

2.   Choi, K. Y.; Swierczewska, M.; Lee, S.; Chen, X., Protease-Activated Drug Development. *Theranostics* **2012,** *2* (2), 156-178.

3.   Vandooren, J.; Opdenakker, G.; Loadman, P. M.; Edwards, D. R., Proteases in cancer drug delivery. *Advanced Drug Delivery Reviews* **2016,** *97*, 144-155.

4.   López-Otín, C.; Bond, J. S., Proteases: Multifunctional Enzymes in Life and Disease. *The Journal of Biological Chemistry* **2008,** *283* (45), 30433-30437.

5.   Lopez-Otin, C.; Matrisian, L. M., Emerging roles of proteases in tumour suppression. *Nat Rev Cancer* **2007,** *7* (10), 800-808.

6.   López-Otín, C.; Palavalli, L. H.; Samuels, Y., Protective roles of matrix metalloproteinases: From mouse models to human cancer. *Cell Cycle* **2009,** *8* (22), 3657-3662.

7.   Timmer, John C.; Enoksson, M.; Wildfang, E.; Zhu, W.; Igarashi, Y.; Denault, J.-B.; Ma, Y.; Dummitt, B.; Chang, Y.-H.; Mast, Alan E.; Eroshkin, A.; Smith, Jeffrey W.; Tao, W A.; Salvesen, Guy S., Profiling constitutive proteolytic events in vivo. *The Biochemical Journal* **2007,** *407* (Pt 1), 41-48.

8.   Mahato, R. I.; Narang, A. S.; Thoma, L.; Miller, D. D., Emerging trends in oral delivery of peptide and protein drugs. *Critical Reviews™ in Therapeutic Drug Carrier Systems* **2003,** *20* (2&3).

9.   Bernkop-Schnürch, A., The use of inhibitory agents to overcome the enzymatic barrier to perorally administered therapeutic peptides and proteins. *Journal of Controlled Release* **1998,** *52* (1–2), 1-16.

10.   Werle, M.; Bernkop-Schnürch, A., Strategies to improve plasma half life time of peptide and protein drugs. *Amino Acids* **2006,** *30* (4), 351-367.

11.   Turk, B., Targeting proteases: successes, failures and future prospects. *Nat Rev Drug Discov* **2006,** *5* (9), 785-799.

12.   Kolterman, O. G.; Kim, D. D.; Shen, L.; Ruggles, J. A.; Nielsen, L. L.; Fineman, M. S.; Baron, A. D., Pharmacokinetics, pharmacodynamics, and safety of exenatide in patients

with type 2 diabetes mellitus. *American Journal of Health-System Pharmacy* **2005,** *62* (2), 173.

13. Mentlein, R., Mechanisms underlying the rapid degradation and elimination of the incretin hormones GLP-1 and GIP. *Best Practice & Research Clinical Endocrinology & Metabolism 23* (4), 443-452.

14. Montrose-Rafizadeh, C.; Yang, H.; Rodgers, B. D.; Beday, A.; Pritchette, L. A.; Eng, J., High Potency Antagonists of the Pancreatic Glucagon-like Peptide-1 Receptor. *Journal of Biological Chemistry* **1997,** *272* (34), 21201-21206.

15. Hupe-Sodmann, K.; Göke, R.; Göke, B.; Thole, H. H.; Zimmermann, B.; Voigt, K.; McGregor, G. P., Endoproteolysis of Glucagon-like Peptide (GLP)-1(7–36) amide by Ectopeptidases in RINm5F Cells. *Peptides* **1997,** *18* (5), 625-632.

16. Manandhar, B.; Ahn, J.-M., Glucagon-like Peptide-1 (GLP-1) Analogs: Recent Advances, New Possibilities, and Therapeutic Implications. *Journal of Medicinal Chemistry* **2015,** *58* (3), 1020-1037.

17. Drucker, D. J.; Nauck, M. A., The incretin system: glucagon-like peptide-1 receptor agonists and dipeptidyl peptidase-4 inhibitors in type 2 diabetes. *The Lancet 368* (9548), 1696-1705.

18. Garber, A. J., Long-acting glucagon-like peptide 1 receptor agonists. *Diabetes care* **2011,** *34* (Supplement 2), S279-S284.

19. Werner, H. M.; Cabalteja, C. C.; Horne, W. S., Peptide backbone composition and protease susceptibility: Impact of modification type, position, and tandem substitution. *ChemBioChem* **2015**.

20. Weinstock, M. T.; Francis, J. N.; Redman, J. S.; Kay, M. S., Protease-Resistant Peptide Design – Empowering Nature's Fragile Warriors Against HIV. *Biopolymers* **2012,** *98* (5), 431-442.

21. Chatterjee, J.; Gilon, C.; Hoffman, A.; Kessler, H., N-methylation of peptides: a new perspective in medicinal chemistry. *Accounts of chemical research* **2008,** *41* (10), 1331-1342.

22. Soto, C.; Kindy, M. S.; Baumann, M.; Frangione, B., Inhibition of Alzheimer's Amyloidosis by Peptides That Prevent β-Sheet Conformation. *Biochemical and Biophysical Research Communications* **1996,** *226* (3), 672-680.

23.   Yamaguchi, H.; Kodama, H.; Osada, S.; Kato, F.; Jelokhani-Niaraki, M.; Kondo, M., Effect of α,α-Dialkyl Amino Acids on the Protease Resistance of Peptides. *Bioscience, Biotechnology, and Biochemistry* **2003,** *67* (10), 2269-2272.

24.   Gopi, H. N.; Ravindra, G.; Pal, P. P.; Pattanaik, P.; Balaram, H.; Balaram, P., Proteolytic stability of β-peptide bonds probed using quenched fluorescent substrates incorporating a hemoglobin cleavage site. *FEBS Letters* **2003,** *535* (1–3), 175-178.

25.   Cabrele, C.; Martinek, T. s. A.; Reiser, O.; Berlicki, Ł., Peptides containing β-amino acid patterns: challenges and successes in medicinal chemistry. *Journal of medicinal chemistry* **2014,** *57* (23), 9718-9739.

26.   Uhlig, T.; Kyprianou, T.; Martinelli, F. G.; Oppici, C. A.; Heiligers, D.; Hills, D.; Calvo, X. R.; Verhaert, P., The emergence of peptides in the pharmaceutical business: From exploration to exploitation. *EuPA Open Proteomics* **2014,** *4*, 58-69.

27.   Vlieghe, P.; Lisowski, V.; Martinez, J.; Khrestchatisky, M., Synthetic therapeutic peptides: science and market. *Drug discovery today* **2010,** *15* (1), 40-56.

28.   Tyndall, J. D.; Nall, T.; Fairlie, D. P., Proteases universally recognize beta strands in their active sites. *Chemical Reviews* **2005,** *105* (3), 973-1000.

29.   Chen, Y.; Yang, C.; Li, T.; Zhang, M.; Liu, Y.; Gauthier, M. A.; Zhao, Y.; Wu, C., The Interplay of Disulfide Bonds, α-Helicity, and Hydrophobic Interactions Leads to Ultrahigh Proteolytic Stability of Peptides. *Biomacromolecules* **2015,** *16* (8), 2347-2355.

30.   Schafmeister, C. E.; Po, J.; Verdine, G. L., An all-hydrocarbon cross-linking system for enhancing the helicity and metabolic stability of peptides. *JOURNAL-AMERICAN CHEMICAL SOCIETY 122* (24), 5891-5892.

31.   Patgiri, A.; Jochim, A. L.; Arora, P. S., A hydrogen bond surrogate approach for stabilization of short peptide sequences in α-helical conformation. *Accounts of chemical research* **2008,** *41* (10), 1289-1300.

32.   Wang, D.; Liao, W.; Arora, P. S., Enhanced Metabolic Stability and Protein-Binding Properties of Artificial α Helices Derived from a Hydrogen-Bond Surrogate: Application to Bcl-xL. *Angewandte Chemie International Edition* **2005,** *44* (40), 6525-6529.

33.   Sparidans, R. W.; Stokvis, E.; Jimeno, J. M.; López-Lázaro, L.; Schellens, J. H.; Beijnen, J. H., Chemical and enzymatic stability of a cyclic depsipeptide, the novel, marine-derived, anti-cancer agent kahalalide F. *Anti-cancer drugs* **2001,** *12* (7), 575-582.

34. Pasut, G., Polymers for protein conjugation. *Polymers* **2014,** *6* (1), 160-178.

35. Arvedson, T.; O'Kelly, J.; Yang, B.-B., Design rationale and development approach for pegfilgrastim as a long-acting granulocyte colony-stimulating factor. *BioDrugs* **2015,** *29* (3), 185-198.

36. Zamboni, W. C., Pharmacokinetics of Pegfilgrastim. *Pharmacotherapy: The Journal of Human Pharmacology and Drug Therapy* **2003,** *23* (8P2), 9S-14S.

37. Lawrence, P. B.; Gavrilov, Y.; Matthews, S. S.; Langlois, M. I.; Shental-Bechor, D.; Greenblatt, H. M.; Pandey, B. K.; Smith, M. S.; Paxman, R.; Torgerson, C. D., Criteria for selecting PEGylation sites on proteins for higher thermodynamic and proteolytic stability. *Journal of the American Chemical Society* **2014,** *136* (50), 17547-17560.

38. Bailon, P.; Palleroni, A.; Schaffer, C. A.; Spence, C. L.; Fung, W.-J.; Porter, J. E.; Ehrlich, G. K.; Pan, W.; Xu, Z.-X.; Modi, M. W., Rational design of a potent, long-lasting form of interferon: a 40 kDa branched polyethylene glycol-conjugated interferon α-2a for the treatment of hepatitis C. *Bioconjugate Chem* **2001,** *12* (2), 195-202.

39. Pelegri-O'Day, E. M.; Lin, E.-W.; Maynard, H. D., Therapeutic protein–polymer conjugates: advancing beyond PEGylation. *Journal of the American Chemical Society* **2014,** *136* (41), 14323-14332.

40. Megeed, Z.; Cappello, J.; Ghandehari, H., Genetically engineered silk-elastinlike protein polymers for controlled drug delivery. *Advanced drug delivery reviews* **2002,** *54* (8), 1075-1091.

41. McPherson, D. T.; Xu, J.; Urry, D. W., Product Purification by Reversible Phase Transition FollowingEscherichia coliExpression of Genes Encoding up to 251 Repeats of the Elastomeric Pentapeptide GVGVP. *Protein expression and purification* **1996,** *7* (1), 51-57.

42. Conrad, U.; Plagmann, I.; Malchow, S.; Sack, M.; Floss, D. M.; Kruglov, A. A.; Nedospasov, S. A.; Rose-John, S.; Scheller, J., ELPylated anti-human TNF therapeutic single-domain antibodies for prevention of lethal septic shock. *Plant biotechnology journal* **2011,** *9* (1), 22-31.

43. Podust, V. N.; Balan, S.; Sim, B.-C.; Coyle, M. P.; Ernst, U.; Peters, R. T.; Schellenberger, V., Extension of in vivo half-life of biologically active molecules by XTEN protein polymers. *Journal of Controlled Release* **2016,** *240*, 52-66.

44. Schellenberger, V.; Wang, C.-w.; Geething, N. C.; Spink, B. J.; Campbell, A.; To, W.; Scholle, M. D.; Yin, Y.; Yao, Y.; Bogin, O.; Cleland, J. L.; Silverman, J.; Stemmer, W. P. C., A recombinant polypeptide extends the in vivo half-life of peptides and proteins in a tunable manner. *Nat Biotech* **2009,** *27* (12), 1186-1190.

45. Alters, S. E.; McLaughlin, B.; Spink, B.; Lachinyan, T.; Wang, C.-w.; Podust, V.; Schellenberger, V.; Stemmer, W. P. C., GLP2-2G-XTEN: A Pharmaceutical Protein with Improved Serum Half-Life and Efficacy in a Rat Crohn's Disease Model. *PLOS ONE* **2012,** *7* (11), e50630.

46. Geething, N. C.; To, W.; Spink, B. J.; Scholle, M. D.; Wang, C.-w.; Yin, Y.; Yao, Y.; Schellenberger, V.; Cleland, J. L.; Stemmer, W. P. C.; Silverman, J., Gcg-XTEN: An Improved Glucagon Capable of Preventing Hypoglycemia without Increasing Baseline Blood Glucose. *PLOS ONE* **2010,** *5* (4), e10175.

47. Haeckel, A.; Appler, F.; Figge, L.; Kratz, H.; Lukas, M.; Michel, R.; Schnorr, J.; Zille, M.; Hamm, B.; Schellenberger, E., XTEN-Annexin A5: XTEN Allows Complete Expression of Long-Circulating Protein-Based Imaging Probes as Recombinant Alternative to PEGylation. *Journal of Nuclear Medicine* **2014,** *55* (3), 508-514.

48. Bouloux, P. M. G.; Handelsman, D. J.; Jockenhövel, F.; Nieschlag, E.; Rabinovici, J.; Frasa, W. L. H.; de Bie, J. J.; Voortman, G.; Itskovitz-Eldor, J., First human exposure to FSH-CTP in hypogonadotrophic hypogonadal males. *Human Reproduction* **2001,** *16* (8), 1592-1597.

49. Calo, D.; Hart, G.; Hoffman, M.; Yagev, L. I.; Tzur, Y.; Binder, L.; Monahan, P.; Zakar, M.; Bar-Ilan, A.; Hershkovitz, O., Enhancing the longevity and in vivo potency of therapeutic proteins: The power of CTP. *Precision Medicine* **2015,** *1*.

50. Fares, F.; Havron, A.; Fima, E., Designing a long acting erythropoietin by fusing three carboxyl-terminal peptides of human chorionic gonadotropin subunit to the N-terminal and C-terminal coding sequence. *International journal of cell biology* **2011,** *2011*.

51. Czajkowsky, D. M.; Hu, J.; Shao, Z.; Pleass, R. J., Fc-fusion proteins: new developments and future perspectives. *EMBO molecular medicine* **2012,** *4* (10), 1015-1028.

52. Hecht, R.; Li, Y.-S.; Sun, J.; Belouski, E.; Hall, M.; Hager, T.; Yie, J.; Wang, W.; Winters, D.; Smith, S., Rationale-based engineering of a potent long-acting FGF21 analog for the treatment of type 2 diabetes. *PLoS One* **2012,** *7* (11), e49345.

53. Hager, T.; Spahr, C.; Xu, J.; Salimi-Moosavi, H.; Hall, M., Differential enzyme-linked immunosorbent assay and ligand-binding mass spectrometry for analysis of biotransformation of protein therapeutics: application to various FGF21 modalities. *Analytical chemistry* **2013,** *85* (5), 2731-2738.

54. Liumbruno, G.; Bennardello, F.; Lattanzio, A.; Piccoli, P.; Rossettias, G., Recommendations for the use of albumin and immunoglobulins. *Blood Transfus* **2009,** *7* (3), 216-234.

55. Lee, P.; Wu, X., Review: modifications of human serum albumin and their binding effect. *Current pharmaceutical design* **2015,** *21* (14), 1862-1865.

56. Subramanian, G. M.; Fiscella, M.; Lamousé-Smith, A.; Zeuzem, S.; McHutchison, J. G., Albinterferon α-2b: a genetic fusion protein for the treatment of chronic hepatitis C. *Nature biotechnology* **2007,** *25* (12), 1411-1419.

57. Ding, S.; Song, M.; Sim, B.-C.; Gu, C.; Podust, V. N.; Wang, C.-W.; McLaughlin, B.; Shah, T. P.; Lax, R.; Gast, R.; Sharan, R.; Vasek, A.; Hartman, M. A.; Deniston, C.; Srinivas, P.; Schellenberger, V., Multivalent Antiviral XTEN–Peptide Conjugates with Long in Vivo Half-Life and Enhanced Solubility. *Bioconjugate Chemistry* **2014,** *25* (7), 1351-1359.

58. Cleland, J. L.; Geething, N. C.; Moore, J. A.; Rogers, B. C.; Spink, B. J.; Wang, C.-W.; Alters, S. E.; Stemmer, W. P. C.; Schellenberger, V., A Novel Long-Acting Human Growth Hormone Fusion Protein (VRS-317): Enhanced In Vivo Potency and Half-Life. *Journal of Pharmaceutical Sciences* **2012,** *101* (8), 2744-2754.

59. Strohl, W. R., Fusion Proteins for Half-Life Extension of Biologics as a Strategy to Make Biobetters. *BioDrugs* **2015,** *29* (4), 215-239.

60. Beck, A.; Reichert, J. M. In *Therapeutic Fc-fusion proteins and peptides as successful alternatives to antibodies*, MAbs, Taylor & Francis: 2011; pp 415-416.

61. Roopenian, D. C.; Akilesh, S., FcRn: the neonatal Fc receptor comes of age. *Nature reviews immunology* **2007,** *7* (9), 715-725.

62. Borrok, M. J.; Wu, Y.; Beyaz, N.; Yu, X.-Q.; Oganesyan, V.; Dall'Acqua, W. F.; Tsui, P., pH-dependent binding engineering reveals an FcRn affinity threshold that governs IgG recycling. *Journal of Biological Chemistry* **2015,** *290* (7), 4282-4290.

63. Glassman, P. M.; Balthasar, J. P., Mechanistic considerations for the use of monoclonal antibodies for cancer therapy. *Cancer biology & medicine* **2014,** *11* (1), 20-33.

64. Hansel, T. T.; Kropshofer, H.; Singer, T.; Mitchell, J. A.; George, A. J., The safety and side effects of monoclonal antibodies. *Nature reviews Drug discovery* **2010,** *9* (4), 325-338.

65. Haraoui, B.; Bykerk, V., Etanercept in the treatment of rheumatoid arthritis. *Therapeutics and clinical risk management* **2007,** *3* (1), 99.

66. Powell, J. S.; Josephson, N. C.; Quon, D.; Ragni, M. V.; Cheng, G.; Li, E.; Jiang, H.; Li, L.; Dumont, J. A.; Goyal, J.; Zhang, X.; Sommer, J.; McCue, J.; Barbetti, M.; Luk, A.; Pierce, G. F., Safety and prolonged activity of recombinant factor VIII Fc fusion protein in hemophilia A patients. *Blood* **2012,** *119* (13), 3031-3037.

67. Knudsen, L. B.; Nielsen, P. F.; Huusfeldt, P. O.; Johansen, N. L.; Madsen, K.; Pedersen, F. Z.; Thøgersen, H.; Wilken, M.; Agersø, H., Potent derivatives of glucagon-like peptide-1 with pharmacokinetic properties suitable for once daily administration. *Journal of medicinal chemistry* **2000,** *43* (9), 1664-1669.

68. Eldridge, B.; Cooley, R. N.; Odegrip, R.; McGregor, D. P.; FitzGerald, K. J.; Ullman, C. G., An in vitro selection strategy for conferring protease resistance to ligand binding peptides. *Protein Engineering Design and Selection* **2009**, gzp052.

69. Jambunathan, K.; K Galande, A., Design of a serum stability tag for bioactive peptides. *Protein and peptide letters* **2014,** *21* (1), 32-38.

70. Radwanski, E.; Perentesis, G.; Jacobs, S.; Oden, E.; Affrime, M.; Symchowicz, S.; Zampaglione, N., Pharmacokinetics of Interferon α-2b in Healthy Volunteers. *The Journal of Clinical Pharmacology* **1987,** *27* (5), 432-435.

71. Harris, J. M.; Chess, R. B., Effect of pegylation on pharmaceuticals. *Nat Rev Drug Discov* **2003,** *2* (3), 214-221.

72. Cox, G. N.; Smith, D. J.; Carlson, S. J.; Bendele, A. M.; Chlipala, E. A.; Doherty, D. H., Enhanced circulating half-life and hematopoietic properties of a human granulocyte colony-stimulating factor/immunoglobulin fusion protein. *Experimental hematology* **2004,** *32* (5), 441-449.

73. Zhao, H. L.; Xue, C.; Du, J. L.; Ren, M.; Xia, S.; Liu, Z. M., Balancing the pharmacokinetics and pharmacodynamics of interferon-α2b and human serum albumin

fusion protein by proteolytic or reductive cleavage increases its in vivo therapeutic efficacy. *Molecular pharmaceutics* **2012,** *9* (3), 664-670.

74. Liebner, R.; Mathaes, R.; Meyer, M.; Hey, T.; Winter, G.; Besheer, A., Protein HESylation for half-life extension: synthesis, characterization and pharmacokinetics of HESylated anakinra. *European Journal of Pharmaceutics and Biopharmaceutics* **2014,** *87* (2), 378-385.

75. Critchley, M., Octreotide scanning for carcinoid tumours. *Postgraduate Medical Journal* **1997,** *73* (861), 399-402.

76. Moore, W. V.; Nguyen, H. J.; Kletter, G. B.; Miller, B. S.; Rogers, D.; Ng, D.; Moore, J. A.; Humphriss, E.; Cleland, J. L.; Bright, G. M., A Randomized Safety and Efficacy Study of Somavaratan (VRS-317), a Long-Acting rhGH, in Pediatric Growth Hormone Deficiency. *The Journal of Clinical Endocrinology & Metabolism* **2016,** *101* (3), 1091-1097.

77. Bruno, B. J.; Miller, G. D.; Lim, C. S., Basics and recent advances in peptide and protein drug delivery. *Therapeutic delivery* **2013,** *4* (11), 1443-1467.

78. Lee, V., Enzymatic barriers to peptide and protein absorption. *Critical reviews in therapeutic drug carrier systems* **1987,** *5* (2), 69-97.

79. Yi, J.; Warunek, D.; Craft, D., Degradation and stabilization of peptide hormones in human blood specimens. *PloS one* **2015,** *10* (7), e0134427.

80. Xu, J.; Stanislaus, S.; Chinookoswong, N.; Lau, Y. Y.; Hager, T.; Patel, J.; Ge, H.; Weiszmann, J.; Lu, S.-C.; Graham, M., Acute glucose-lowering and insulin-sensitizing action of FGF21 in insulin-resistant mouse models—association with liver and adipose tissue effects. *American Journal of Physiology-Endocrinology and Metabolism* **2009,** *297* (5), E1105-E1114.

81. Zhen, E. Y.; Jin, Z.; Ackermann, B. L.; Thomas, M. K.; Gutierrez, J. A., Circulating FGF21 proteolytic processing mediated by fibroblast activation protein. *Biochemical Journal* **2016,** *473* (5), 605-614.

82. Zhu, L.; Tamvakopoulos, C.; Xie, D.; Dragovic, J.; Shen, X.; Fenyk-Melody, J. E.; Schmidt, K.; Bagchi, A.; Griffin, P. R.; Thornberry, N. A., The Role of Dipeptidyl Peptidase IV in the Cleavage of Glucagon Family Peptides IN VIVO METABOLISM OF

PITUITARY ADENYLATE CYCLASE-ACTIVATING POLYPEPTIDE-(1–38). *Journal of Biological Chemistry* **2003,** *278* (25), 22418-22423.

83. Kim, Y. B.; Kopcho, L. M.; Kirby, M. S.; Hamann, L. G.; Weigelt, C. A.; Metzler, W. J.; Marcinkeviciene, J., Mechanism of Gly-Pro-pNA cleavage catalyzed by dipeptidyl peptidase-IV and its inhibition by saxagliptin (BMS-477118). *Archives of biochemistry and biophysics* **2006,** *445* (1), 9-18.

84. Kharitonenkov, A.; Shiyanova, T. L.; Koester, A.; Ford, A. M.; Micanovic, R.; Galbreath, E. J.; Sandusky, G. E.; Hammond, L. J.; Moyers, J. S.; Owens, R. A.; Gromada, J.; Brozinick, J. T.; Hawkins, E. D.; Wroblewski, V. J.; Li, D.-S.; Mehrbod, F.; Jaskunas, S. R.; Shanafelt, A. B., FGF-21 as a novel metabolic regulator. *Journal of Clinical Investigation* **2005,** *115* (6), 1627-1635.

85. Ryan, M. H.; Petrone, D.; Nemeth, J. F.; Barnathan, E.; Björck, L.; Jordan, R. E., Proteolysis of purified IgGs by human and bacterial enzymes in vitro and the detection of specific proteolytic fragments of endogenous IgG in rheumatoid synovial fluid. *Molecular immunology* **2008,** *45* (7), 1837-1846.

86. Dorywalska, M.; Strop, P.; Melton-Witt, J. A.; Hasa-Moreno, A.; Farias, S. E.; Galindo Casas, M.; Delaria, K.; Lui, V.; Poulsen, K.; Sutton, J.; Bolton, G.; Zhou, D.; Moine, L.; Dushin, R.; Tran, T.-T.; Liu, S.-H.; Rickert, M.; Foletti, D.; Shelton, D. L.; Pons, J.; Rajpal, A., Site-Dependent Degradation of a Non-Cleavable Auristatin-Based Linker-Payload in Rodent Plasma and Its Effect on ADC Efficacy. *PLOS ONE* **2015,** *10* (7), e0132282.

87. Fan, X.; Brezski, R. J.; Fa, M.; Deng, H.; Oberholtzer, A.; Gonzalez, A.; Dubinsky, W. P.; Strohl, W. R.; Jordan, R. E.; Zhang, N., A single proteolytic cleavage within the lower hinge of trastuzumab reduces immune effector function and in vivo efficacy. *Breast Cancer Research* **2012,** *14* (4), R116.

88. Biancheri, P.; Brezski, R. J.; Di Sabatino, A.; Greenplate, A. R.; Soring, K. L.; Corazza, G. R.; Kok, K. B.; Rovedatti, L.; Vossenkämper, A.; Ahmad, N., Proteolytic cleavage and loss of function of biologic agents that neutralize tumor necrosis factor in the mucosa of patients with inflammatory bowel disease. *Gastroenterology* **2015,** *149* (6), 1564-1574. e3.

89. Xu, K.; Liu, L.; Saad, O. M.; Baudys, J.; Williams, L.; Leipold, D.; Shen, B.; Raab, H.; Junutula, J. R.; Kim, A.; Kaur, S., Characterization of intact antibody–drug conjugates from plasma/serum in vivo by affinity capture capillary liquid chromatography–mass spectrometry. *Analytical Biochemistry* **2011,** *412* (1), 56-66.

90. Kluge, B.; Gambin, A.; Niemiro, W., Modeling Exopeptidase Activity from LC-MS Data. *Journal of Computational Biology* **2009,** *16* (2), 395-406.

91. Dittwald, P.; Ostrowski, J.; Karczmarski, J.; Gambin, A., Inferring serum proteolytic activity from LC-MS/MS data. *BMC Bioinformatics* **2012,** *13* (5), S7.

92. Antosova, Z.; Mackova, M.; Kral, V.; Macek, T., Therapeutic application of peptides and proteins: parenteral forever? *Trends in Biotechnology 27* (11), 628-635.

93. Muheem, A.; Shakeel, F.; Jahangir, M. A.; Anwar, M.; Mallick, N.; Jain, G. K.; Warsi, M. H.; Ahmad, F. J., A review on the strategies for oral delivery of proteins and peptides and their clinical perspectives. *Saudi Pharmaceutical Journal* **2016,** *24* (4), 413-428.

94. Lowman, A. M.; Morishita, M.; Kajita, M.; Nagai, T.; Peppas, N. A., Oral delivery of insulin using pH‐responsive complexation gels. *Journal of Pharmaceutical Sciences 88* (9), 933-937.

95. Shah, R. B.; Khan, M. A., Protection of salmon calcitonin breakdown with serine proteases by various ovomucoid species for oral drug delivery. *Journal of Pharmaceutical Sciences 93* (2), 392-406.

96. Goldberg, M.; Gomez-Orellana, I., Challenges for the oral delivery of macromolecules. *Nat Rev Drug Discov* **2003,** *2* (4), 289-295.

97. Woodley, J. F., Enzymatic barriers for GI peptide and protein delivery. *Critical reviews in therapeutic drug carrier systems* **1994,** *11* (2-3), 61-95.

98. Hamers-Casterman, C.; Atarhouch, T.; Muyldermans, S.; Robinson, G.; Hammers, C.; Songa, E. B.; Bendahman, N.; Hammers, R., Naturally occurring antibodies devoid of light chains. *Nature* **1993,** *363* (6428), 446-448.

99. Kolkman, J. A.; Law, D. A., Nanobodies − from llamas to therapeutic proteins. *Drug Discovery Today: Technologies* **2010,** *7* (2), e139-e146.

100. Cortez-Retamozo, V.; Backmann, N.; Senter, P. D.; Wernery, U.; De Baetselier, P.; Muyldermans, S.; Revets, H., Efficient Cancer Therapy with a Nanobody-Based Conjugate. *Cancer Research* **2004,** *64* (8), 2853.

101. Ebrahimizadeh, W.; Mousavi Gargari, S.; Rajabibazl, M.; Safaee Ardekani, L.; Zare, H.; Bakherad, H., Isolation and characterization of protective anti-LPS nanobody against V. cholerae O1 recognizing Inaba and Ogawa serotypes. *Applied Microbiology and Biotechnology* **2013,** *97* (10), 4457-4466.

102. Harmsen, M. M.; van Solt, C. B.; van Zijderveld-van Bemmel, A. M.; Niewold, T. A.; van Zijderveld, F. G., Selection and optimization of proteolytically stable llama single-domain antibody fragments for oral immunotherapy. *Applied Microbiology and Biotechnology* **2006,** *72* (3), 544-551.

103. Busby, R. W.; Kessler, M. M.; Bartolini, W. P.; Bryant, A. P.; Hannig, G.; Higgins, C. S.; Solinga, R. M.; Tobin, J. V.; Wakefield, J. D.; Kurtz, C. B.; Currie, M. G., Pharmacologic Properties, Metabolism, and Disposition of Linaclotide, a Novel Therapeutic Peptide Approved for the Treatment of Irritable Bowel Syndrome with Constipation and Chronic Idiopathic Constipation. *Journal of Pharmacology and Experimental Therapeutics* **2012,** *344* (1), 196.

104. Fosgerau, K.; Hoffmann, T., Peptide therapeutics: current status and future directions. *Drug Discovery Today* **2015,** *20* (1), 122-128.

105. Scheuch, G.; Siekmeier, R., Novel approaches to enhance pulmonary delivery of proteins and peptides. *J Physiol Pharmacol* **2007,** *58 Suppl 5* (Pt 2), 615-625.

106. Olsson, B.; Bondesson, E.; Borgström, L.; Edsbäcker, S.; Eirefelt, S.; Ekelund, K.; Gustavsson, L.; Hegelund-Myrbäck, T., Pulmonary Drug Metabolism, Clearance, and Absorption. In *Controlled Pulmonary Drug Delivery*, Smyth, H. D. C.; Hickey, A. J., Eds. Springer New York: New York, NY, 2011; pp 21-50.

107. Uchenna Agu, R.; Ikechukwu Ugwoke, M.; Armand, M.; Kinget, R.; Verbeke, N., The lung as a route for systemic delivery of therapeutic proteins and peptides. *Respiratory Research* **2001,** *2* (4), 198-209.

108. Niven, R. W., Delivery of biotherapeutics by inhalation aerosol. *Critical Reviews™ in Therapeutic Drug Carrier Systems* **1995,** *12* (2-3).

109. Labiris, N. R.; Dolovich, M. B., Pulmonary drug delivery. Part I: Physiological factors affecting therapeutic effectiveness of aerosolized medications. *British Journal of Clinical Pharmacology* **2003,** *56* (6), 588-599.

110. Patton, J. S., Mechanisms of macromolecule absorption by the lungs. *Advanced Drug Delivery Reviews* **1996,** *19* (1), 3-36.

111. Patton, J. S.; Nagarajan, S.; Clark, A. In *Pulmonary absorption and metabolism of peptides and proteins*, 1998; Interpharm Press, Buffalo Grove, IL, USA: pp 17-24.

112. Fukuda, Y.; Tsuji, T.; Fujita, T.; Yamamoto, A.; Muranishi, S., Susceptibility of Insulin to Proteolysis in Rat Lung Homogenate and Its Protection from Proteolysis by Various Protease Inhibitors. *Biological & Pharmaceutical Bulletin* **1995,** *18* (6), 891-894.

113. Shen, Z.; Zhang, Q.; Wei, S.; Nagai, T., Proteolytic enzymes as a limitation for pulmonary absorption of insulin: in vitro and in vivo investigations. *International Journal of Pharmaceutics* **1999,** *192* (2), 115-121.

114. Kobayashi, S.; Kondo, S.; Juni, K., Critical factors on pulmonary absorption of peptides and proteins (diffusional barrier and metabolic barrier). *European Journal of Pharmaceutical Sciences* **1996,** *4* (6), 367-372.

115. Baginski, L.; Gobbo, O. L.; Tewes, F.; Salomon, J. J.; Healy, A. M.; Bakowsky, U.; Ehrhardt, C., In Vitro and In Vivo Characterisation of PEG-Lipid-Based Micellar Complexes of Salmon Calcitonin for Pulmonary Delivery. *Pharmaceutical research* **2012,** *29* (6), 1425-1434.

116. Nadkarni, P. P.; Costanzo, R. M.; Sakagami, M., Pulmonary delivery of peptide YY for food intake suppression and reduced body weight gain in rats. *Diabetes, Obesity and Metabolism* **2011,** *13* (5), 408-417.

117. Richter, W. F.; Bhansali, S. G.; Morris, M. E., Mechanistic Determinants of Biotherapeutics Absorption Following SC Administration. *The AAPS Journal* **2012,** *14* (3), 559-570.

118. Parsons, J. A.; Rafferty, B.; Stevenson, R. W.; Zanelli, J. M., Evidence that protease inhibitors reduce the degradation of parathyroid hormone and calcitonin injected subcutaneously. *British journal of pharmacology* **1979,** *66* (1), 25-32.

119. Kalluri, H.; Banga, A. K., Transdermal delivery of proteins. *Aaps Pharmscitech* **2011,** *12* (1), 431-441.

120. Steinsträsser, I.; Merkle, H. P., Dermal metabolism of topically applied drugs: pathways and models reconsidered. *Pharmaceutica Acta Helvetiae* **1995,** *70* (1), 3-24.

121. Yang, P.-Y.; Zou, H.; Chao, E.; Sherwood, L.; Nunez, V.; Keeney, M.; Ghartey-Tagoe, E.; Ding, Z.; Quirino, H.; Luo, X.; Welzel, G.; Chen, G.; Singh, P.; Woods, A. K.; Schultz, P. G.; Shen, W., Engineering a long-acting, potent GLP-1 analog for microstructure-based transdermal delivery. *Proceedings of the National Academy of Sciences* **2016,** *113* (15), 4140-4145.

122. Lindgren, J.; Eriksson Karlström, A., Intramolecular Thioether Crosslinking of Therapeutic Proteins to Increase Proteolytic Stability. *ChemBioChem* **2014,** *15* (14), 2132-2138.

123. Dubowchik, G. M.; Firestone, R. A.; Padilla, L.; Willner, D.; Hofstead, S. J.; Mosure, K.; Knipe, J. O.; Lasch, S. J.; Trail, P. A., Cathepsin B-Labile Dipeptide Linkers for Lysosomal Release of Doxorubicin from Internalizing Immunoconjugates: Model Studies of Enzymatic Drug Release and Antigen-Specific In Vitro Anticancer Activity. *Bioconjugate Chemistry* **2002,** *13* (4), 855-869.

124. Graaf, M. d.; Boven, E.; Scheeren, H. W.; Haisma, H. J.; Pinedo, H. M., Beta-glucuronidase-mediated drug release. *Current pharmaceutical design* **2002,** *8* (15), 1391-1403.

125. Lu, J.; Jiang, F.; Lu, A.; Zhang, G., Linkers Having a Crucial Role in Antibody–Drug Conjugates. *International journal of molecular sciences* **2016,** *17* (4), 561.

126. Sevlever, D.; Jiang, P.; Yen, S.-H. C., Cathepsin D is the main lysosomal enzyme involved in the degradation of α-synuclein and generation of its carboxy-terminally truncated species. *Biochemistry* **2008,** *47* (36), 9678.

127. Beldent, V.; Michaud, A.; Wei, L.; Chauvet, M.-T.; Corvol, P., Proteolytic release of human angiotensin-converting enzyme. Localization of the cleavage site. *Journal of Biological Chemistry* **1993,** *268* (35), 26428-26434.

128. Kemmler, W.; Peterson, J. D.; Steiner, D. F., Studies on the conversion of proinsulin to insulin I. Conversion in vitro with trypsin and carboxypeptidase B. *Journal of Biological Chemistry* **1971,** *246* (22), 6786-6791.

129. Shaji, J.; Patole, V., Protein and peptide drug delivery: oral approaches. *Indian journal of pharmaceutical sciences* **2008,** *70* (3), 269.

130. Ohmori, Y.; Onoue, S.; Endo, K.; Matsumoto, A.; Uchida, S.; Yamada, S., Development of dry powder inhalation system of novel vasoactive intestinal peptide (VIP) analogue for pulmonary administration. *Life Sciences* **2006,** *79* (2), 138-143.

131. Ducry, L.; Stump, B., Antibody− drug conjugates: linking cytotoxic payloads to monoclonal antibodies. *Bioconjugate chemistry* **2009,** *21* (1), 5-13.

132. Ross, P. L.; Wolfe, J. L., Physical and Chemical Stability of Antibody Drug Conjugates: Current Status. *Journal of Pharmaceutical Sciences 105* (2), 391-397.

133. Chen, X.; Zaro, J.; Shen, W.-C., Fusion Protein Linkers: Property, Design and Functionality. *Advanced drug delivery reviews* **2013,** *65* (10), 1357-1369.

134. Doronina, S. O.; Toki, B. E.; Torgov, M. Y.; Mendelsohn, B. A.; Cerveny, C. G.; Chace, D. F.; DeBlanc, R. L.; Gearing, R. P.; Bovee, T. D.; Siegall, C. B.; Francisco, J. A.; Wahl, A. F.; Meyer, D. L.; Senter, P. D., Development of potent monoclonal antibody auristatin conjugates for cancer therapy. *Nat Biotech* **2003,** *21* (7), 778-784.

135. Müller, S.; Dennemärker, J.; Reinheckel, T., Specific functions of lysosomal proteases in endocytic and autophagic pathways. *Biochimica et Biophysica Acta (BBA) - Proteins and Proteomics* **2012,** *1824* (1), 34-43.

136. Law, B.; Tung, C.-H., Proteolysis: a biological process adapted in drug delivery, therapy, and imaging. *Bioconjugate chemistry* **2009,** *20* (9), 1683-1695.

137. Tan, G.-J.; Peng, Z.-K.; Lu, J.-P.; Tang, F.-Q., Cathepsins mediate tumor metastasis. *World J Biol Chem* **2013,** *4* (4), 91-101.

138. Albright, C. F.; Graciani, N.; Han, W.; Yue, E.; Stein, R.; Lai, Z.; Diamond, M.; Dowling, R.; Grimminger, L.; Zhang, S.-Y.; Behrens, D.; Musselman, A.; Bruckner, R.; Zhang, M.; Jiang, X.; Hu, D.; Higley, A.; DiMeo, S.; Rafalski, M.; Mandlekar, S.; Car, B.; Yeleswaram, S.; Stern, A.; Copeland, R. A.; Combs, A.; Seitz, S. P.; Trainor, G. L.; Taub, R.; Huang, P.; Oliff, A., Matrix metalloproteinase–activated doxorubicin prodrugs inhibit HT1080 xenograft growth better than doxorubicin with less toxicity. *Molecular Cancer Therapeutics* **2005,** *4* (5), 751.

139. Gong, Y.; Leroux, J.-C.; Gauthier, M. A., Releasable conjugation of polymers to proteins. *Bioconjugate chemistry* **2015,** *26* (7), 1172-1181.

140. Santi, D. V.; Schneider, E. L.; Reid, R.; Robinson, L.; Ashley, G. W., Predictable and tunable half-life extension of therapeutic agents by controlled chemical release from

macromolecular conjugates. *Proceedings of the National Academy of Sciences* **2012,** *109* (16), 6211-6216.

141.   Nollmann, F. I.; Goldbach, T.; Berthold, N.; Hoffmann, R., Controlled systemic release of therapeutic peptides from PEGylated prodrugs by serum proteases. *Angewandte Chemie International Edition* **2013,** *52* (29), 7597-7599.

142.   Böttger, R.; Knappe, D.; Hoffmann, R., Readily adaptable release kinetics of prodrugs using protease-dependent reversible PEGylation. *Journal of Controlled Release* **2016,** *230*, 88-94.

143.   Li, H.; Ma, Y.; Chen, Y.; Sang, Y.; Zhou, T.; Qiu, M.; Huang, X.; Zhou, C.; Su, Z., A Protease-Based Strategy for the Controlled Release of Therapeutic Peptides. *Angewandte Chemie International Edition* **2010,** *49* (29), 4930-4933.

CHAPTER 2. THIOREDOXIN FUSION CONSTRUCTS ENABLES HIGH-YIELD PRODUCTION OF SOLUBLE, ACTIVE MATRIX METALLOPROTEINASE-8 (MMP-8) IN ESCHERICHIA COLI

2.1 INTRODUCTION

Matrix metalloproteinases are a class of proteins responsible for degrading extracellular matrix (ECM) proteins to support tissue remodeling and repair.[1,2] MMPs are of interest because of their complex biological roles and because of their participation in a variety of disease states, including cancer, metastasis and tumorigenesis, which is caused by the inappropriate up- or down-regulation of MMPs and/or their activity.[3] Elevated activity leads to loosening of the supporting matrix, which facilitates dissemination of cancer cells to enable metastasis.[4] Many MMP inhibitors have been created, but most have failed in clinical trials because of the complex set of contributions MMP activity exerts on disease progression, and as such, these enzymes remain the subject of much study.[5,6]

MMPs utilize a zinc-bound metal active site and are secreted as glycosylated zymogens, with a prodomain bound to the metal active site.[2] Catalysis is activated by proteolytic cleavage of the prodomain, which exposes the active site. These enzymes are often difficult to produce recombinantly in a soluble form because of their complex composition, and generating them typically requires numerous steps, which include expression as proenzymes, refolding and use of several diverse purification approaches.[7-9] MMPs also are difficult to produce because of their proteolytic function, which permits autoproteolysis to occur.[10] Significant efforts have resulted in the production of a few MMPs in the amounts necessary to study their structure in atomic detail.[11-14] Crystal structures of MMP-8 have been solved (PDB: 3DNG, 3DPE, 1ZVX)[15,16] utilizing the complex protein production methods, and moreover, require the addition of an inhibitor to prevent autoproteolysis when concentrated.[17] The ability to obtain high-resolution

information about the protein enables design of selective inhibitors and provides the ability to characterize other ligand and protein-protein interactions that regulate enzyme activity.[18-20]

MMP-8 plays a role in cancer, arthritis, and asthma and promotes premature degradation of dental fillings by degrading the underlying collagen matrix within the dentin of demineralized tooth.[21,22] While the fold of MMP-8 is related to other MMPs, it differs from them in the active site because it contains an insertion that creates a significantly larger binding pocket.[23] The ability to study this enzyme and its unique active site in atomic detail in solution, without using an inhibitor would be extremely valuable for simplifying production and understanding how to design more potent and selective inhibitors of this particular MMP.[24,25]

Here, we present a method to express an active, stable form of matrix metalloproteinase-8 (MMP-8) in *E. coli* in sufficient amounts to enable structural evaluation. Several fusion constructs were generated that did not result in high yield of soluble, active, stable protein, but one construct met these criteria. This MMP-8 fusion includes two tags (thioredoxin and S Tag) to aid in folding and stability and a polyhistidine tag for affinity purification. Using this system, over 100 mg of MMP-8 from a 1 L cell culture can be expressed as a fusion protein in the soluble fraction of the cell lysate and purified quickly using immobilized metal affinity chromatography (IMAC) to recover appreciable amounts of catalytically active enzyme that retains full activity when stored refrigerated in simple buffer. Recognition sites for removal of the thioredoxin and thioredoxin-S Tag fusion partners were engineered into the construct. A spacer sequence also containing the metal-binding *cla*MP Tag was inserted between the fusion partner and the enzyme. An additional aim of this study was to demonstrate compatibility of use of the metal abstraction peptide (MAP) technology inline with a metalloprotein.[26] Genetic engineering of MAP into a plasmid creates, the *cla*MP Tag, a linker-less carrier for many

transition metals with utility in healthcare applications.[27] The *cla*MP Tag is a tripeptide consisting of the amino acid sequence Asn-Cys-Cys, which scavenges small transition metals from chelating agents.[28] Because of the uniquely beneficial properties of the *cla*MP Tag, which includes extraordinarily tight binding, resistance to metal release upon dilution at serum pH and specific release in acidic conditions as in endosomes, the *cla*MP Tag is being investigated as a method for targeted delivery of metals for therapeutic and diagnostic applications by designing targeting proteins to contain the metal bound tripeptide.[27] The *cla*MP Tag has not been investigated previously in a system, such as matrix metalloproteinases, in which a structural and/or catalytic metal-binding site is present. Analysis of the activity and stability of these two fusion proteins and their cleaved products is presented herein.

2.2 MATERIALS AND METHODS

2.2.1 Genetic Engineering

Human matrix metalloproteinase-8 (MMP-8) in the pCMV6-XL4 vector was obtained (OriGene Technologies, Inc. Cat # SC 127843) and the catalytic domain was amplified with designed primers (Integrated DNA Technologies). Two constructs of MMP-8 were prepared, one containing solely MMP-8 and one bearing an additional N-terminal *cla*MP Tag (Asn-Cys-Cys).[27,29] The primers contained a region matching the pET-32Xa/LIC vector (underlined), a portion matching the MMP-8 catalytic domain (italics), the *cla*MP Tag (bold) and an inserted linker (bold and underlined) between the *cla*MP Tag and MMP-8. 5'-<u>GGT ATT GAG GGT CGC</u> *AAT CCA GGA AAC CCC AAG TG*-3' (forward primer no *cla*MP Tag), 5'-**TGC GGC TCT TCT GGC ATT GAG GGT CGC** *AAC CCC AAG TGG GAA*-3' (first forward primer for *cla*MP-link insertion), 5'-<u>GGT ATT GAG GGT CGC CCA GAT CTG GGT</u> **AAC TGC TGC GGC TCT TCT GGC**-3' (second forward primer for *cla*MP-link insertion), and 5'-<u>AGA GGA</u>

GAG TTA GAG CCT TAT CCA TAG ATG GCC TG-3' (reverse primer for both constructs).

The MMP-8 PCR reaction was purified using QIAquick PCR Purification Kit (Qiagen) and was

inserted into the pET-32Xa/LIC vector by ligation independent cloning (protocol provided by

Novagen). *cla*MP-link-MMP-8 required two sequential PCR steps to incorporate the full-length

linker. The PCR reaction was then purified using QIAquick PCR Purification Kit (Qiagen) and

was inserted into the pET-32Xa/LIC vector by ligation independent cloning (protocol provided

by Novagen). The inserted tag contained a *Bgl*II site so that the original Factor Xa recognition

sequence could be removed by cleaving with this endonuclease. The new plasmid was cut with

the restriction enzyme, *Bgl*II and was re-ligated with T4 DNA ligase.

Using the standard heat shock procedure, the reactions were transformed into DH5α

Escherichia coli (E. coli) cell strain. Luria broth (LB) agar plates with 100 μg/mL ampicillin

were used to select transformed cells. The plates were incubated overnight at 37 °C. Individual

colonies were grown in 5 mL LB with 100 μg/mL ampicillin overnight at 37 °C and 250 rpm.

The starter cultures were spun down at 1717 x g for 15 min and the supernatant was discarded. A

miniprep kit (Qiagen) was used to purify the plasmid DNA. DNA sequences were confirmed by

UC Berkeley DNA Sequencing Facility.

Four additional constructs bearing a variety of tags that may improve folding and/or

solubility were generated and tested for expression in *E. coli*. These constructs did not lead to

accumulation of soluble protein and are described in Supplemental Information.

2.2.2 Expression of MMP-8

Plasmids were transformed into BL21 *E. coli* cell strain using standard heat shock

techniques. The cells were plated on LB agar plates with 100 μg/mL ampicillin and incubated

overnight at 37 °C. Cultures were started using a single colony to inoculate 50 mL of LB with

100 μg/mL ampicillin and grown for 16 h at 37 °C, 250 rpm in an orbital shaker. Twenty milliliters of starter culture was transferred to 1 L of LB with 100 μg/mL ampicillin in a 3 L fernbach flask. The cells were grown at 37 °C, 250 rpm until the OD_{600} reached approximately 0.7. One milliliter of 1 M isopropyl β-D-1-thiogalactopyranoside (IPTG) was used to induce the cells, which were harvested after 4 h by centrifugation at 1391 x g for 8 min. The cell pellets were stored at -80 °C until use.

2.2.3 Protein Purification

A one-liter pellet was resuspended in 25 mL lysis buffer (50 mM Tris-Cl, 20 mM imidazole, 59 mM NaCl, 10 μM N-Isobutyl-N-(4-methoxyphenylsulfonyl)glycyl hydroxamic acid (NNGH), pH 7.9) and three passes through a french press at 21,000 psi was used to lyse the cells. Lysates were centrifuged for 1 hour at 21,000 x g and 4 °C. The supernatant containing the protein was filtered through a 0.45 μm filter followed by a 0.2 μm filter and applied to a nickelated 5 mL Hi-Trap Chelating HP column (GE Lifesciences) equilibrated in lysis buffer. The column was washed with 50 mM Tris-Cl, 58 mM NaCl, 40 mM imidazole, 10 μM NNGH, pH 7.9 for 10 CV at a flow rate of 1.25 mL/min at 4 °C. The protein was eluted from the column using a linear gradient elution starting with the wash buffer (50 mM Tris-Cl, 58 mM NaCl, 40 mM imidazole, 10 μM NNGH, pH 7.9) and increasing the imidazole concentration from 0 to 100% of 50 mM Tris, 37 mM NaCl, 500 mM imidazole, 10 μM NNGH, pH 7.9. The eluate was concentrated using Amicon Ultra 10 kDa MWCO (Millipore) concentrators to approximately 2 mL and injected on a HiLoad 26/600 Superdex 75 prep grade column (pack size 1 x 320 mL, GE Lifesciences #28-98930-34) equilibrated in 50 mM Tris-Cl, 60 mM NaCl, 10 μM NNGH, pH 7.9 to separate degradation fragments and eliminate the imidazole in the sample. The fractions containing the protein were concentrated using an Amicon Ultra 10 kDa MWCO (Millipore) to

approximately 2 mL. To cleave the fusion into thioredoxin and S Tag-MMP-8, 70 Units of Thrombin were added and the reaction was incubated at room temperature for 12 h. The sample was injected on a Superdex 75 column (GE Lifesciences) to separate the fragments. The S tag was cleaved by adding 9.8 ng of Factor Xa and allowing the reaction to proceed at room temperature for 16 h and run over the Superdex 75 column (GE Lifesciences). The final product was concentrated to 1.5 mL and stored at 4 °C. All solutions used in these procedures contained 10 μM NNGH to stabilize the protein and protect against autoproteolysis, however, it was determined herein that this compound is not required for the fusion proteins.

*cla*MP-link-MMP-8 abstracts nickel from the IMAC resin during purification, generating a translucent, rusty orange solution, typical of the Ni-*cla*MP complex.[27] As previously reported, UV-vis absorbance spectroscopy at 425 nm was used to assess metal occupancy of the *cla*MP Tag in the fusion construct.[27] The molar extinction coefficient for 425 nm is 350 $M^{-1}cm^{-1}$. Following purification, at 0.5 mM, the highest concentration of the fusion protein, the A425 indicates complete nickel insertion into the *cla*MP Tag has been achieved. Factor Xa cleaves the nickel-bound *cla*MP Tag from MMP-8.

2.2.4 Liquid Chromatography and Mass Spectrometry

Whole protein electrospray ionization mass spectra (ESI-MS) were acquired on a Qtof Premier (Waters/Micromass, Manchester UK) hybrid mass spectrometer operated in MS mode and acquiring data with the time of flight analyzer. The instrument was operated in V mode or at 9000 resolution. The source was optimized using lysozyme infused at the HPLC flow rate. The cone voltage was 45 V, the source ion guide with added gas flow (N_2, 20 mL/min) and Ar was admitted to the collision cell. The cell was operated at 10 eV or maximum transmission without increasing water loss ions. Spectra were acquired covering the mass range 300 to 3000 amu and

accumulating data for 4 seconds per cycle. Time to mass calibration was made with NaI cluster ions acquired under the same conditions. Spectral mass correction was made with the peptide leucine encephalin (YGGFL) dimer (1111.5463) observed in the lock mass spray channel. The average mass of proteins was determined from the charge state distribution with the "Transform" and/or MaxEnt I routines in Masslynx software.

Microbore HPLC/MS experiments were performed with a Waters Acquity H class chromatograph at 180 µL/min on a 1-mm ID C4 RP column eluting into the standard ESI source of the Qtof premier. The solvents were: A H$_2$O, B 90% CH$_3$CN, 10% isopropanol, both 0.08% formic acid. Separations were performed on a 1-mm ID x 50-mm long C4 reverse phase column (Zorbax C4, 300Å pore size, 3.5 µm particles packed by Micro-Tech) with a 1-mm x 2-cm dry-packed guard column (Upchurch Scientific Model C.128, Oak Harbor, WA) filled with Zorbax C3 resin. The gradient was to ramp from 1% to 20% B in 1 min then to 50% B by 9 min, and finally to 75% B by 10 min.

2.2.5 Circular Dichroism Spectroscopy

Circular dichroism (CD) spectra were collected using a Chirascan spectropolarimeter (Applied Photophysics). The samples were analyzed at a concentration of 0.2 mg/mL in 10 mM sodium phosphate, pH 7.9 and were added to a quartz cuvette with a 0.1-cm path length (Starna Cells). Spectra were collected at 10 °C and analyzed using several wavelength ranges, beginning at 190, 195, 200, 205 and 210 nm through 260 nm. Background signal from the solution was subtracted. CDNN software (Applied Photophysics) was used for spectral deconvolution.

2.2.6 SDS PAGE Analysis

SDS-PAGE samples were obtained by mixing 30 µL of sample with 30 µL of reducing Laemmli buffer and heated at 90 °C for 10 min. Samples were stored at -20 °C until used. Gel

samples were loaded onto standard 15% (v/v) resolving, 4% (v/v) stacking gels and run at 135 V for 2 h. A pre-stained molecular weight ladder (BioRad, #161-0374) was used for Coomassie staining and an unstained molecular weight ladder (BioRad, #161-0363) was used as a reference for gels stained with SYPRO Ruby Protein Gel Stain (Life Technologies, cat# S-12000).

2.2.7 Densitometry Analysis

Densitometry analysis was done on SYPRO Ruby-stained gels. A Typhoon TRIO Variable Mode Imager (Amersham Biosciences) was used to image the gels and ImageQuantTL Software was used to perform the quantitative analysis. Gels were stained with SYPRO Ruby Protein Gel Stain (Life Technologies, cat# S-12000) according to the manufacturer's instructions.

2.2.8 Activity Assay

The MMP-8 Fluorometric Drug Discovery Kit, RED (Enzo Life Sciences cat# BML-AK305) was used to examine enzyme activity of the recombinant proteins and cleavage products. The kit components were thawed to room temperature and diluted in assay buffer according to the manufacturer's instructions. Briefly, assay buffer, enzyme (final concentration 1 μM), and either inhibitor (final concentration 5 μM) or an equivalent amount of buffer were pipetted into the wells of a 96-well plate and incubated at 37 °C for 1 hour. The fluorescent plate reader was set at Ex/Em=545/576 nm, with cut off at 570 nm. To begin the reaction, 10 μL of substrate equilibrated to 37 °C was added to obtain a final concentration of 1 μM. Buffer blanks and control solutions were analyzed to account for background signal and samples were analyzed in triplicate. Data were processed and fitting and error analysis was performed using Microsoft Excel and plots were made using GraphPad Prism. Error bars are representative of the standard deviation between replicates.

2.3 RESULTS

2.3.1 Recombinant MMP-8 Expression and Purification

The catalytic domain of MMP-8 was cloned into a set of eight vectors containing a variety of tags to identify a construct that would produce soluble, active protein in high yield. The pET-32Xa/LIC vector containing N-terminal thioredoxin and S Tag successfully supported this objective. This fusion construct enables folding of MMP-8 to generate milligram quantities (from one liter culture) of the catalytically active enzyme while avoiding accumulation in inclusion bodies, which allows one-step affinity purification from the soluble fraction of the cell lysate.

To test the robustness of the general construct, an additional variant of the MMP-8 fusion protein was created that alters the spacing between the stabilizing fusion partner and the enzyme. The *cla*MP Tag developed by our lab was inserted N-terminal to MMP-8 with an additional flexible spacer sequence (Gly-Ser-Ser-Gly-Ile-Glu-Gly-Arg) (Figure 2.1). The *cla*MP Tag is an extremely stable, inline module for targeted metal delivery.[27,30] It consists of the amino acid sequence Asn-Cys-Cys and rapidly and quantitatively binds metal at basic pH,[30,31] here during purification upon exposure to the Ni-IMAC resin. The recognition sequence of Factor Xa follows this *cla*MP-link spacer in the *cla*MP-link-MMP-8 construct to permit cleavage of the additional tag and release of the same MMP-8 product. SDS-PAGE analysis of pre- and post-induction samples shows expression of the proteins in *E. coli* at the expected molecular weight of approximately 35 kDa (Figure 2.2).
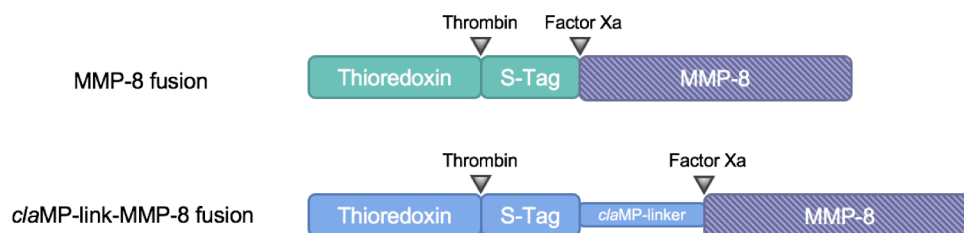
Figure 2.1 Cartoon of the fusion constructs of matrix metalloproteinase-8 (MMP-8) containing fusion partners and cleavage sites.
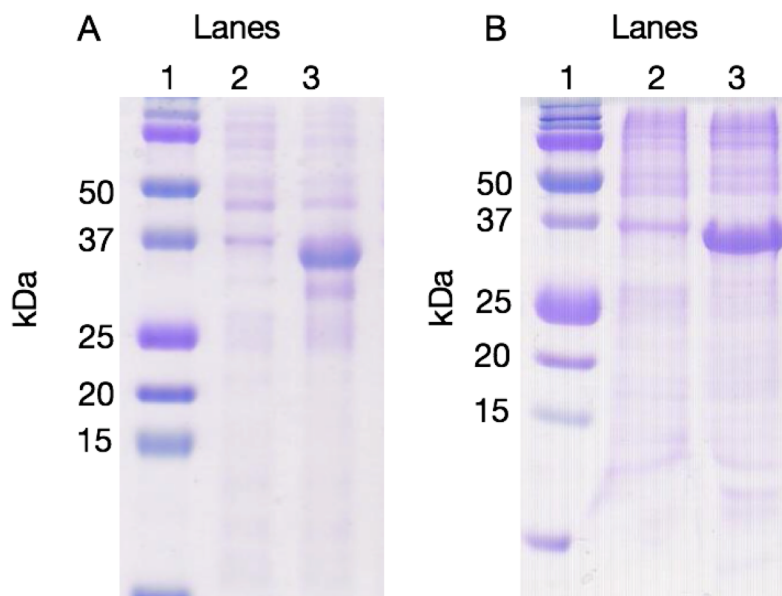
Figure 2.2 Coomassie stained SDS-PAGE showing expression of the two different MMP-8 constructs. (A) MMP-8 fusion cell lysate pre-induction (lane 2) and post-induction (lane 3). (B) *cla*MP-link-MMP-8 fusion cell lysate pre-induction (lane 2) and post-induction (lane 3). In panels A and B, lane 1 is the molecular weight ladder (BioRad, #161-0374).

A representative SDS-PAGE analysis of the purification of MMP-8 fusion is shown in Figure 2.3. Following cell lysis and centrifugation to remove insoluble debris, the MMP-8 fusion protein remained present in the soluble fraction of the cell lysate, while it was not detectable in the pellet (Figure 2.3, lane 2). A Ni-IMAC column was used to affinity purify MMP-8 fusion from the cell lysate. The flow through during application of the cell lysate to the column (lane 3) and the 40 mM imidazole wash (lane 4) were collected to verify retention of protein on the column. A gradient elution of imidazole from 40 mM to 500 mM over 12 CV was used to elute the protein (lane 5). The gel displays molecular weight proteins below the expected 35-kDa MMP-8 fusion indicative of proteolytic degradation. To remove the lower molecular weight fragments SEC was used (lane 6) and mass spectrometry confirmed the presence of full-length fusion MMP-8 (Figure 2.4).

Thrombin and/or Factor Xa was/were added to the purified protein in an effort to remove the fusion tags and release MMP-8. Reaction with Factor Xa leads to incomplete cleavage but the uncut fusion protein is easily removed by SEC. Unfortunately, productive cleavage generates two proteins (MMP-8 and thioredoxin-S Tag) of approximately 17-18 kDa, which cannot be separated by SEC and attempts to isolate MMP-8 from the fusion partner using IMAC after Factor Xa cleavage were unsuccessful. Consequently, a serial reaction with thrombin and Factor Xa was performed. Thrombin was added to cleave the thioredoxin tag (13 kDa), leaving S Tag-MMP-8 (21-kDa) (lane 7). While complete cleavage at the desired position is observed,

additional fragments appear in the sample (lane 7). SEC effectively separates the cleaved thioredoxin tag (lane 10) from the MMP-8 fusion protein (lane 8) though a band appears on the gel at 13 kDa (lane 8), it is not thioredoxin; mass spectrometry shows that thioredoxin is not present in the MMP-8 fraction and this band instead corresponds to a fragment of MMP-8 (mass spectrum peak at 13875.8 ± 0.2 Da corresponds to MMP-8 fragmentation at residue 72 between Ala and His, with an
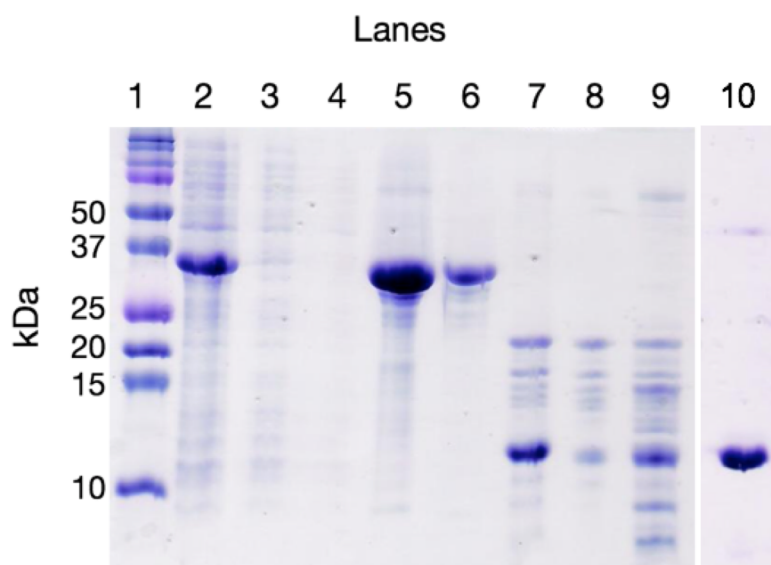
Figure 2.3 Coomassie stained SDS-PAGE of the purification process of MMP-8. (Lane 1) molecular weight standards, (lane 2) soluble fraction of the cell lysate, (lane 3) the flow through of application of the cell lysis to the Ni-IMAC, (lane 4) the flow through of a 40 mM wash of the Ni-IMAC, (lane 5) the gradient elution peaks from 40 to 500 mM imidazole, (lane 6) SEC separation of degradants from the gradient elution step, (lane 7) after incubating with thrombin for 12 h, (lane 8) separation of thrombin cleavage fragments by SEC, (lane 9) after incubating with Factor Xa for 16 h, (lane 10) thrombin-cleaved thioredoxin tag separated by SEC.

average theoretical mass of 13876.1 Da) presumably due to autoproteolysis (data not shown). Multiple degradation fragments are present that would not separate using SEC. Because MMP-8 is prone to autoproteolysis, it seems likely that degradation proceeds once thioredoxin is cleaved. It is evident from the higher molecular weight bands in lane 8 and mass spectrometry data that Factor Xa fails to accomplish complete cleavage, resulting in a mixture of S Tag-MMP-8 and MMP-8 in the final product (lane 9). Attempts to isolate MMP-8 by SEC after this step result in extremely low recovery of protein, which remains a mixture of fragments.

Approximately 130 mg of protein was obtained from the cell lysate of a one-liter culture of MMP-8 fusion, determined by a Bradford assay after Ni-IMAC elution. 75 mg was injected onto the SEC and approximately 50% was recovered at the correct size (with fewer degradation fragments) (Figure 2.3, lane 6). The amount of MMP-8 obtained at each purification step was determined and is reported as the weight fraction of MMP-8 within the total fusion protein (Table 2.1). Although the results are not quantitative for cleaved MMP-8, the table summarizes

Table 2.1 Relative MMP-8 Equivalents[a] Recovered at Each Purification Step

Construct	Post Ni-IMAC (mg)	Post SEC (mg)	Post Thrombin Cleavage (mg)	Post Factor Xa Cleavage (mg)
MMP-8	39.6 ± 7.7	20.5 ± 3.7	9.8 ± 0.3	0.9 ± 0.7[b]
*cla*MP-link-MMP-8	22.2 ± 2.6	ND	ND	1.2 ± 0.2[b]

[a]Mass equivalents of MMP-8 were calculated by taking the mass of MMP-8 as a fraction of the fusion protein, which initially was 75 mg. [b]This value reflects the total protein content of cleaved fragments present, not native MMP-8.

the high-yield of protein produced in the form of the fusion construct and relative losses that accompany removal of the stabilizing fusion partner. The table shows that when using the thioredoxin-S Tag fusion construct large amounts, 20-40 mg of MMP-8 were obtained following affinity purification. The results show clearly that substantial loss of MMP-8 occurs when the

fusion partner is cleaved. The percent yield of MMP-8 recovered after complete processing was calculated to be approximately 2.5% ± 2.3% of the original amount present in the fusion constructs, but this value is clearly falsely elevated because MMP-8 cannot be obtained in a pure form and the sample contains numerous fragments. Because these species cannot be isolated and their individual activity assessed, accurate quantitation of native MMP-8 is not possible.

2.3.2 Mass Spectrometric Analysis

The correct protein size was initially determined using an SDS-PAGE analysis. To confirm the results from SDS-PAGE, a mass spectrometric analysis was completed of the fusion protein isolated by affinity chromatography. The spectrum shows a peak at 34971.4 ± 0.5 Da, which corresponds to fusion MMP-8
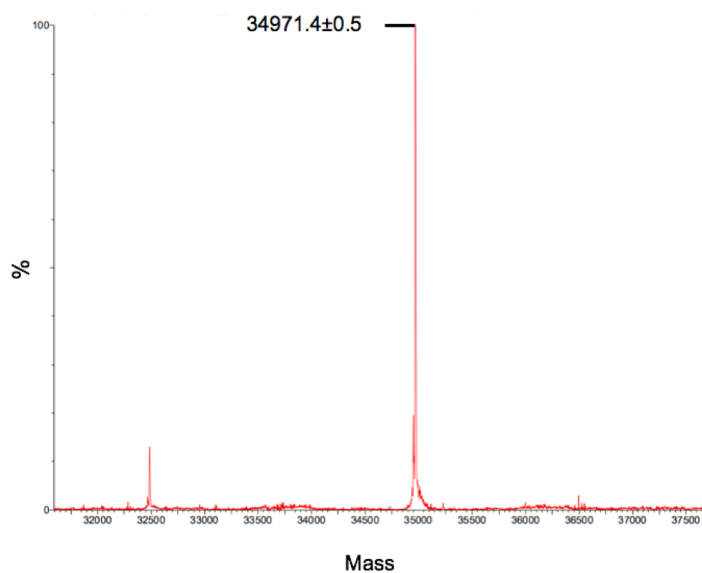
Figure 2.4 Mass spectrum of MMP-8 fusion (average theoretical mass of 34973.8 Da).

with the N-terminal methionine removed (average theoretical mass = 34,973.8 Da) (Figure 2.4). The thrombin and Xa-cut mass spectrometry analysis displayed peaks of the expected masses but also many fragments of lower molecular weight, which presumably result from autoproteolysis (data not shown). Mass spectrometry data also was collected for the *cla*MP Tagged fusion construct and it displayed the expected mass of 34893.13 ± 0.44 Da for the fusion protein lacking the lead methionine residue as well (data not shown).

2.3.4 Circular Dichroism (CD) Analysis

To verify the correct fold for the fusion proteins is achieved, the secondary structure of MMP-8 fusion and *cla*MP-link-MMP-8 fusion was analyzed using CD. Each protein was determined to be folded properly, containing the expected proportion of secondary structure that was predicted from the structures of the individual domains for thioredoxin and MMP-8. The spectra of MMP-8 fusion and *cla*MP-link-MMP-8 fusion are very similar overall, but differ substantially below 200 nm. Differences in this region correspond to the tag itself. The calculated helical content decreases by 5% and random coil content increases by approximately 5% when this region of the spectrum is excluded from the calculation. This region is often omitted from CD analysis because of interference from buffers and other components, and the values obtained for secondary structure calculated using 205-260 nm produces comparable results for the two variants, indicating the *cla*MP Tag does not affect the fold of MMP-8. The helical content of MMP-8 fusion and *cla*MP-link-MMP-8 fusion was determined to be 19% and 18%, while the β-strand composition was 28% and 29% and random coil was 47% and 48%, respectively. This is consistent with previous CD analysis of MMPs, which have approximately 20% helical, 20% β-strand and 50% random coil structures.[32] The two constructs examined have an N-terminal thioredoxin tag, and independently thioredoxin has approximately 35% helical and 18% β-strand character.[33] An intervening linker sequence is also present between these two domains, which comprises approximately 10% of the fusion protein. This region may adopt a non-random coil structure and lead to the great increase in stability of the fusion system. Because the structure of this region is unknown, the experimentally determined value of the amalgamated fusion secondary structures matches that expected for thioredoxin fused to MMP-8.

2.3.5 Densitometry Analysis of Stability

MMP-8 fusion and purified MMP-8 were stored at 4 °C in 50 mM Tris, 60 mM NaCl, 10 μM NNGH, pH 7.9 and sampled over several days to determine the stability of the purified enzymes. SDS-PAGE and densitometry analysis were performed to compare the amount of intact enzyme to the total protein content to determine the extent of degradation. The intact fusion protein represents approximately 50% of the total protein in the sample at day 1, and 25% of the full-length fusion protein remains after 12 days (Figure 2.5). As soon as MMP-8 is isolated from the fusion protein, less intact protein is present in the sample, with only 6% of the total protein in the sample being intact MMP-8. Within 10 days the amount of MMP-8 decreases to less than 1% intact (Figure 2.5, inset). Not only is the amount of intact fusion MMP-8 eight times greater than isolated MMP-8, but approximately 50% of fusion MMP-8 on day 1 remains intact after 12 days, while only 15% of MMP-8 on day 1 remains intact on day 10. These results clearly
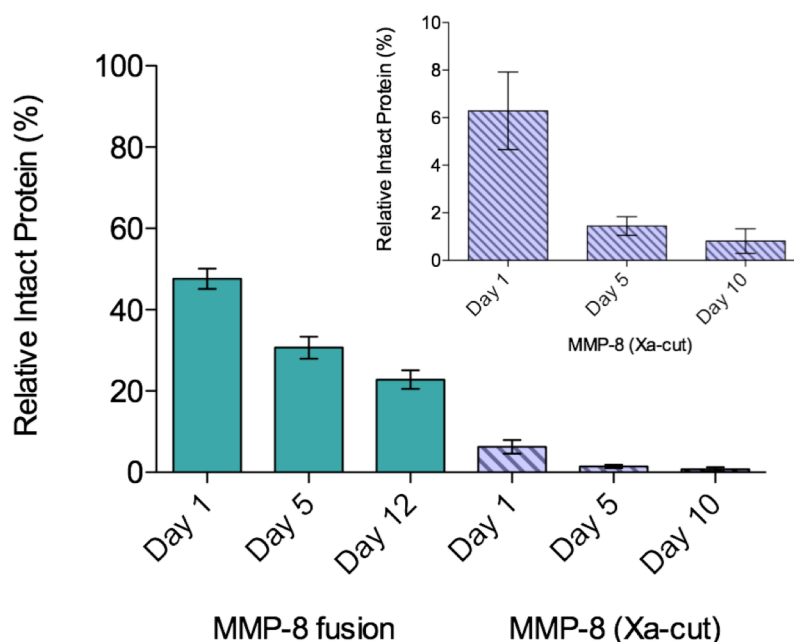
Figure 2.5 Stability analysis of MMP-8 fusion protein and MMP-8 (Xa-cut) protein separated after Factor Xa cleavage. Values were determined using densitometry analysis. Inset is zoomed in bar graph of the isolated MMP-8 protein.

demonstrate that the fusion tags on MMP-8 have a stabilizing effect and autoproteolysis is decreased greatly in the fusion protein compared to MMP-8.

2.3.6 Activity Assay

A fluorescent activity assay for MMP-8 was used to examine the activity of the purified fusion and isolated Xa-cut MMP-8 (Figure 2.6). The enzyme was examined 1 and 10 days after purification and was stored in 50 mM Tris, 60 mM NaCl pH 7.9 with and without (*) 10 μM NNGH, an inhibitor predicted to act as a protective stabilizer against proteolysis. Approximately 100-fold dilution of these protein samples into the assay conditions reduced the inhibitor
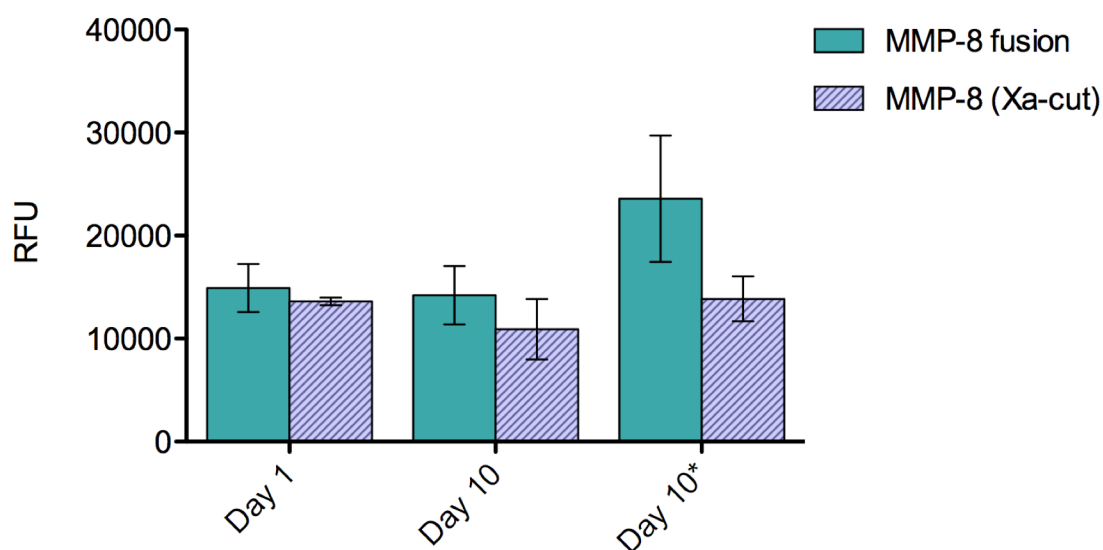
Figure 2.6 Comparison of catalytic activity in relative fluorescence units (RFU) of the MMP-8 fusion protein and its cleaved products as analyzed using MMP-8 Fluorescent Drug Discovery Kit, RED (Enzo Life Sciences) at 25 min. Samples were analyzed immediately after purification (day 1) and on day 10. The proteins were stored with (day 10) or without (day 10*) a protective stabilizer at 4 °C prior to analysis. Solid bars represent the uncut MMP-8 fusion and hashed bars represent isolated MMP-8 following Factor Xa cleavage.

concentration well below the IC50, eliminating its inhibitory effect. After 25 min of incubation with the substrate, MMP-8 fusion emits approximately 15,000 RFU on day 1 and day 10. Although degradation of the polypeptide chain was observed by SDS-PAGE, the MMP-8 fusion

retains activity over 10 days both with and without NNGH indicating that addition of this compound has no effect. When the fusion tags are removed, MMP-8 appears to lose activity compared to MMP-8 fusion when stored without the inhibitor.

The activity of *cla*MP-link-MMP-8 fusion and Xa-cut protein (MMP-8) were obtained to compare to the original MMP-8 fusion and Xa-cut MMP-8 protein lacking the *cla*MP Tag (Figure 2.7). MMP-8 fusion was determined to have 3-times higher activity than *cla*MP-link-MMP-8 fusion when analyzed directly after purification (day 1). Immediately after cleavage with Factor Xa, both MMP-8 and *cla*MP-link-MMP-8 retain comparable activity to their original
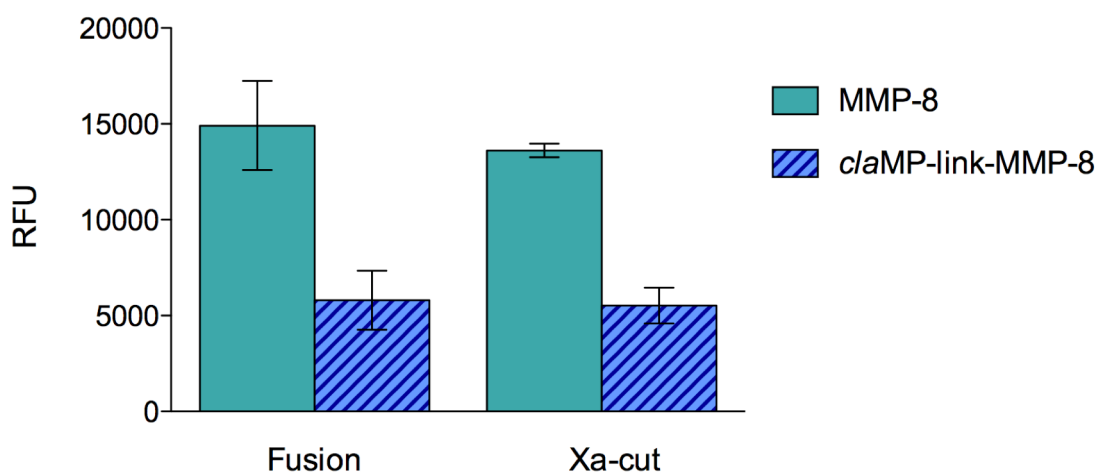
Figure 2.7 Comparison of catalytic activity in relative fluorescence units (RFU) of the MMP-8 and *cla*MP-link-MMP-8 fusion and Xa-cut proteins using MMP-8 Fluorescent Drug Discovery Kit, RED (Enzo Life Sciences) at 25 min. Samples were analyzed immediately after purification (day 1). Solid bars represent the MMP-8 construct and hashed bars represent the *cla*MP-link-MMP-8 construct.

fusion construct. Although the *cla*MP Tag and inserted linker decreases the activity of MMP-8 in both the fusion and Xa-cut constructs, the extent of diminution is within error. A UV-Vis scan of *cla*MP-link-MMP-8 fusion displays all the expected unique spectral features of the Ni-*cla*MP complex (data not shown), including the non-overlapping feature at 425 nm to facilitate quantitation. Comparison of the A425 value with the total protein concentration, as determined by Bradford assay, demonstrated 1:1 binding of the *cla*MP Tag with nickel. The Ni-*cla*MP

complex is extraordinarily stable and its formation in the fusion construct would preclude the tag from interacting with the zinc ion in MMP-8.

Because degradation of MMP-8 proceeds quickly once the fusion partner is cleaved, the impact on catalytic activity of leaving the fusion partner in the sample to avoid additional purification was examined. When the *cla*MP-link-MMP-8 fusion protein was cleaved by Factor Xa, it was either separated from the released tag (purified) or was analyzed as a mixture of thioredoxin and MMP-8 Xa-cut protein (unpurified). Comparing the two methods of protein handling reveals that retention of the fusion partner has an insignificant effect on activity (Figure 2.8). Previous work has shown that the metal-free *cla*MP module effectively inhibits MMP-8,[29] and new data shows that loading *cla*MP with nickel prevents binding to MMP-8 (*manuscript in preparation*). This data indicates that the *cla*MP Tag may be placed inline with a metalloenzyme and when it is loaded with another metal, such as nickel in this study, active enzyme is recovered.
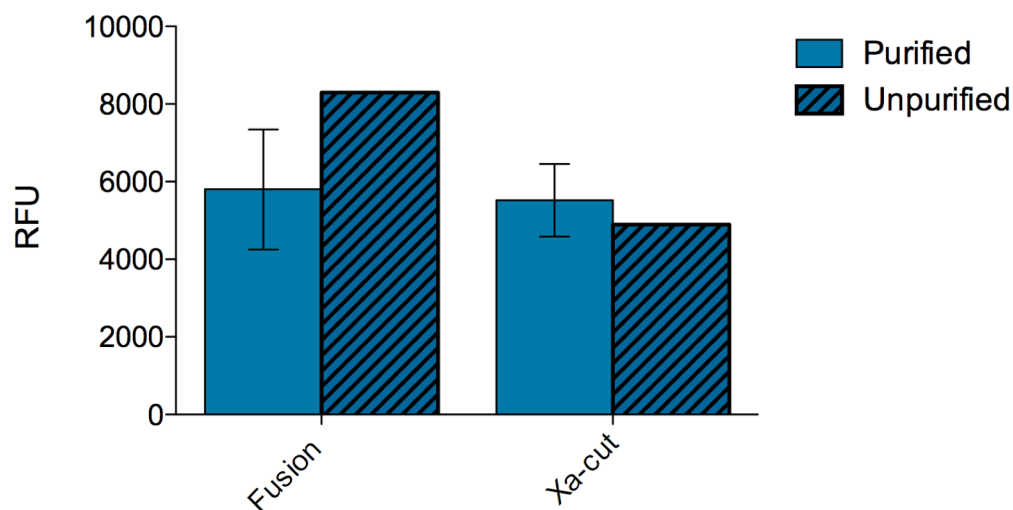
Figure 2.8 Comparison of catalytic activity in relative fluorescence units (RFU) of the claMP-link-MMP-8 fusion and Xa-cut proteins either being purified by SEC after cleavage by Factor Xa or not purified, using MMP-8 Fluorescent Drug Discovery Kit, RED (Enzo Life Sciences) at 25 min. Samples were analyzed immediately after purification (day 1). Solid bars represent the separated claMP-link-MMP-8 construct and hashed bars represent the mixture of cleaved *cla*MP-link-MMP-8 fusion partner and MMP-8 protein.

2.4 DISCUSSION

A fusion construct containing thioredoxin and S Tag N-terminal to MMP-8 resulted in the ability to accumulate large amounts of functional enzyme in the soluble fraction of *E. coli*. Subsequent purification using Ni-IMAC and a single SEC step enabled recovery of 20-40 mg of MMP-8 from 1 L of cell culture and the purified protein retained full activity at 10 days when stored refrigerated at high concentration (~0.5 mM) in a simple buffer solution. The catalytic domain of MMP-8 alone is typically stored in 50% glycerol at -80 °C at very low enzyme concentration to ensure activity remains, which is not optimal because the presence of glycerol can interfere with structural studies and this compound can be difficult to remove. SDS-PAGE shows that proteolysis of the fusion protein occurs over the course of several days but this is vastly improved compared to MMP-8 alone. Because the activity remains constant for at least 10 days, the functional core of the enzyme must remain intact and therefore provides useful material for numerous types of analysis, including structural studies where high concentration is required.

Removal of the fusion tags leads to proteolytic degradation and decreased activity. Inclusion of the inhibitor NNGH with MMP-8 following Factor Xa cleavage acts as a protective stabilizer and improves storage stability of the enzyme. Complete inhibition of MMP-8 is accomplished at 7 μM under the conditions of the catalytic assay (MMP-8 Fluorescent Drug Discovery Kit, RED (Enzo Life Sciences)), but at the much higher enzyme concentrations produced and examined for storage stability herein, 10 μM NNGH was insufficient to prevent cleavage of MMP-8 degradation (Figure 2.6).[34] Because this concentration is near the limit of solubility of NNGH in water, higher concentrations could not be tested. Although NNGH did not provide adequate protection against autoproteolysis, the results indicate that identification of

inhibitors with higher solubility and/or affinity for the enzyme should improve stability and could be used to preserve MMP-8 in the absence of the fusion partner.

The *cla*MP Tag was added to the MMP-8 construct to examine the effect of an additional metal binding entity inline with a metal-containing enzyme. The *cla*MP Tag binds metal extraordinarily tightly at basic pH and this fusion system becomes occupied with nickel during IMAC purification.[30] The metal-free *cla*MP Tag has been shown to inhibit MMP-8 activity and is being investigated as a potential regulator of the activity of MMP-8.[29] *cla*MP-link-MMP-8 was originally designed to contain a linker peptide sequence that would allow the *cla*MP Tag to interact with the active site zinc to potentially inhibit the activity of the enzyme as a pro-moiety that is releasable by adjusting the pH to below neutral or by inserting another metal into the tag. Inclusion of the *cla*MP Tag and linker did not interfere with folding of the enzyme but it did impair catalytic function by three-fold. Investigation of the amount of metal bound to the *cla*MP Tag determined complete occupancy of the *cla*MP Tag with nickel. The rich UV-Vis spectrum of the Ni-*cla*MP complex confirms the *cla*MP Tag is not available to interact with zinc in MMP-8 and therefore cannot inhibit the enzyme in the fusion construct examined. Although demonstrating the reason for this modest decrease in activity is beyond the scope of the present study, it is likely that introducing 13 extra residues between the fusion tags and MMP-8 gives greater flexibility, allowing for better interaction between the enzyme and the stabilizing partner, thereby decreasing activity. Importantly, like the construct that lacks the *cla*MP Tag, the activity remains unchanged with cleavage of the fusion partner (Figure 2.7).

2.5 CONCLUSION

Recombinant MMP-8 fusion was expressed and purified using a straightforward procedure to obtain active enzyme that is much more stable. The fusion protein can be stored

refrigerated in common buffer without glycerol at high concentration and it retains full activity for longer than one week. This approach to preparation of MMP-8 is efficient and sufficiently simply to enable a wide variety of studies on MMP-8. The *cla*MP Tag may be included in the construct and exogenous metal inserted during purification, demonstrating that the inline *cla*MP Tag is compatible for use with metalloproteins.

2.6 REFERENCES

1.   Lu, P.; Takai, K.; Weaver, V. M.; Werb, Z., Extracellular Matrix Degradation and Remodeling in Development and Disease. *Cold Spring Harbor perspectives in biology* **2011,** *3* (12), 10.1101/cshperspect.a005058 a005058.

2.   Nagase, H.; Visse, R.; Murphy, G., Structure and function of matrix metalloproteinases and TIMPs. *Cardiovascular research* **2006,** *69* (3), 562-573.

3.   Gutiérrez-Fernández, A.; Fueyo, A.; Folgueras, A. R.; Garabaya, C.; Pennington, C. J.; Pilgrim, S.; Edwards, D. R.; Holliday, D. L.; Jones, J. L.; Span, P. N., Matrix metalloproteinase-8 functions as a metastasis suppressor through modulation of tumor cell adhesion and invasion. *Cancer research* **2008,** *68* (8), 2755-2763.

4.   Kessenbrock, K.; Plaks, V.; Werb, Z., Matrix Metalloproteinases: Regulators of the Tumor Microenvironment. *Cell* **2010,** *141* (1), 52-67.

5.   Hadler-Olsen, E.; Winberg, J.-O.; Uhlin-Hansen, L., Matrix metalloproteinases in cancer: their value as diagnostic and prognostic markers and therapeutic targets. *Tumor Biol.* **2013,** *34* (4), 2041-2051.

6.   Shapiro, S. D., Matrix metalloproteinase degradation of extracellular matrix: biological consequences. *Current Opinion in Cell Biology* **1998,** *10* (5), 602-608.

7.   Windsor, L. J.; Steele, D. L., Expression of Recombinant Matrix Metalloproteinases in Escherichia coli #. In *T Matrix Metalloproteinase Protocols*, 2009; Vol. 622, pp 67-81.

8.   Oneda, H.; Inouye, K., Refolding and Recovery of Recombinant Human Matrix Metalloproteinase 7 (Matrilysin) from Inclusion Bodies Expressed by Escherichia coli. *Journal of Biochemistry* **1999,** *126* (5), 905-911.

9.   Ye, Q. Z.; Johnson, L. L.; Hupe, D. J.; Baragi, V., Purification and characterization of the human stromelysin catalytic domain expressed in Escherichia coli. *Biochemistry* **1992,** *31* (45), 11231-11235.

10.   Hyun Min, K.; Joo-Hyon, K.; In Kwan, H.; Seo-Jin, L.; Tae-Han, K.; Ki-Hyeong, R.; Seung-Taek, L., Refolding of the Catalytic and Hinge Domains of Human MT1-MMP Expressed in Escherichia coli and Its Characterization. *Molecules & Cells* **2002,** *13* (1), 118.

11.   Vaisar, T.; Kassim, S. Y.; Gomez, I. G.; Green, P. S.; Hargarten, S.; Gough, P. J.; Parks, W. C.; Wilson, C. L.; Raines, E. W.; Heinecke, J. W., MMP-9 Sheds the β(2) Integrin

Subunit (CD18) from Macrophages. *Molecular & Cellular Proteomics : MCP* **2009,** *8* (5), 1044-1060.

12. Palmier, M. O.; Fulcher, Y. G.; Bhaskaran, R.; Duong, V. Q.; Fields, G. B.; Van Doren, S. R., NMR and Bioinformatics Discovery of Exosites That Tune Metalloelastase Specificity for Solubilized Elastin and Collagen Triple Helices. *Journal of Biological Chemistry* **2010,** *285* (40), 30918-30930.

13. Van Doren, S. R., Matrix metalloproteinase interactions with collagen and elastin. *Matrix Biology* **2015,** *44–46*, 224-231.

14. Brandstetter, H.; Grams, F.; Glitz, D.; Lang, A.; Huber, R.; Bode, W.; Krell, H.-W.; Engh, R. A., The 1.8-Å Crystal Structure of a Matrix Metalloproteinase 8-Barbiturate Inhibitor Complex Reveals a Previously Unobserved Mechanism for Collagenase Substrate Recognition. *Journal of Biological Chemistry* **2001,** *276* (20), 17405-17412.

15. Gavuzzo, E.; Pochetti, G.; Mazza, F.; Gallina, C.; Gorini, B.; D'Alessio, S.; Pieper, M.; Tschesche, H.; Tucker, P. A., Two Crystal Structures of Human Neutrophil Collagenase, One Complexed with a Primed- and the Other with an Unprimed-Side Inhibitor: Implications for Drug Design†. *Journal of Medicinal Chemistry* **2000,** *43* (18), 3377-3385.

16. Pochetti, G.; Gavuzzo, E.; Campestre, C.; Agamennone, M.; Tortorella, P.; Consalvi, V.; Gallina, C.; Hiller, O.; Tschesche, H.; Tucker, P. A.; Mazza, F., Structural Insight into the Stereoselective Inhibition of MMP-8 by Enantiomeric Sulfonamide Phosphonates. *Journal of Medicinal Chemistry* **2006,** *49* (3), 923-931.

17. Pochetti, G.; Montanari, R.; Gege, C.; Chevrier, C.; Taveras, A. G.; Mazza, F., Extra Binding Region Induced by Non-Zinc Chelating Inhibitors into the S1′ Subsite of Matrix Metalloproteinase 8 (MMP-8)†. *Journal of Medicinal Chemistry* **2009,** *52* (4), 1040-1049.

18. Spicer, T. P.; Jiang, J.; Taylor, A. B.; Choi, J. Y.; Hart, P. J.; Roush, W. R.; Fields, G. B.; Hodder, P. S.; Minond, D., Characterization of Selective Exosite-Binding Inhibitors of Matrix Metalloproteinase 13 That Prevent Articular Cartilage Degradation in Vitro. *Journal of Medicinal Chemistry* **2014,** *57* (22), 9598-9611.

19. Moy, F. J.; Chanda, P. K.; Cosmi, S.; Pisano, M. R.; Urbano, C.; Wilhelm, J.; Powers, R., High-resolution solution structure of the inhibitor-free catalytic fragment of human

fibroblast collagenase determined by multidimensional NMR. *Biochemistry* **1998,** *37* (6), 1495-1504.

20. Ikejiri, M.; Bernardo, M. M.; Bonfil, R. D.; Toth, M.; Chang, M.; Fridman, R.; Mobashery, S., Potent Mechanism-based Inhibitors for Matrix Metalloproteinases. *Journal of Biological Chemistry* **2005,** *280* (40), 33992-34002.

21. Sulkala, M.; Tervahartiala, T.; Sorsa, T.; Larmas, M.; Salo, T.; Tjäderhane, L., Matrix metalloproteinase-8 (MMP-8) is the major collagenase in human dentin. *Archives of Oral Biology* **2007,** *52* (2), 121-127.

22. McCawley, L. J.; Matrisian, L. M., Matrix metalloproteinases: they're not just for matrix anymore! *Current Opinion in Cell Biology* **2001,** *13* (5), 534-540.

23. Dorman, G.; Cseh, S.; Hajdu, I.; Barna, L.; Konya, D.; Kupai, K.; Kovacs, L.; Ferdinandy, P., Matrix Metalloproteinase Inhibitors: A Critical Appraisal of Design Principles and Proposed Therapeutic Utility. *Drugs* **2010,** *70* (8), 949-964.

24. Gendron, R.; Grenier, D.; Sorsa, T.; Mayrand, D., Inhibition of the Activities of Matrix Metalloproteinases 2, 8, and 9 by Chlorhexidine. *Clinical and Diagnostic Laboratory Immunology* **1999,** *6* (3), 437-439.

25. Vandenbroucke, R. E.; Libert, C., Is there new hope for therapeutic matrix metalloproteinase inhibition? *Nat Rev Drug Discov* **2014,** *13* (12), 904-927.

26. Laurence, J. A. S.; Vartia, A. A.; Krause, M. E., Metal abstraction peptide (MAP) tag and associated methods. Google Patents: 2012.

27. Mills, B. J.; Mu, Q.; Krause, M. E.; Laurence, J. S., claMP Tag: A Versatile Inline Metal-Binding Platform Based on the Metal Abstraction Peptide. *Bioconjugate Chemistry* **2014,** *25* (6), 1103-1111.

28. Krause, M. E.; Glass, A. M.; Jackson, T. A.; Laurence, J. S., MAPping the Chiral Inversion and Structural Transformation of a Metal-Tripeptide Complex Having Ni-Superoxide Dismutase Activity. *Inorganic Chemistry* **2011,** *50* (6), 2479-2487.

29. Dixit, N.; Settle, J. K.; Ye, Q.; Berrie, C. L.; Spencer, P.; Laurence, J. S., Grafting MAP peptide to dental polymer inhibits MMP-8 activity. *Journal of Biomedical Materials Research Part B: Applied Biomaterials* **2015,** *103* (2), 324-331.

30. Mills, B. J.; Laurence, J. S., Stability Analysis of an Inline Peptide-based Conjugate for Metal Delivery: Nickel(II)–claMP Tag Epidermal Growth Factor as a Model System. *Journal of Pharmaceutical Sciences* **2015,** *104* (2), 416-423.

31. Krause, M. E.; Glass, A. M.; Jackson, T. A.; Laurence, J. S., Novel tripeptide model of nickel superoxide dismutase. *Inorganic chemistry* **2009,** *49* (2), 362-364.

32. Yang, H.; Makaroff, K.; Paz, N.; Aitha, M.; Crowder, M. W.; Tierney, D. L., Metal Ion Dependence of the Matrix Metalloproteinase-1 Mechanism. *Biochemistry* **2015,** *54* (23), 3631-3639.

33. Matsuo, K.; Sakurada, Y.; Yonehara, R.; Kataoka, M.; Gekko, K., Secondary-Structure Analysis of Denatured Proteins by Vacuum-Ultraviolet Circular Dichroism Spectroscopy. *Biophysical Journal* **2007,** *92* (11), 4088-4096.

34. Lee, E.-J.; Moon, P.-G.; Baek, M.-C.; Kim, H.-S., Comparison of the Effects of Matrix Metalloproteinase Inhibitors on TNF-α Release from Activated Microglia and TNF-α Converting Enzyme Activity. *Biomolecules & Therapeutics* **2014,** *22* (5), 414-419.

CHAPTER 3. METAL-BOUND *cla*MP TAG INHIBITS PROTEOLYTIC CLEAVAGE

3.1 INTRODUCTION

The specificity provided by a biologic for a target of interest enables delivery of highly potent molecules with fewer side effects.[1-3] Active pharmaceutical ingredients or chelating agents can be conjugated to polypeptides to achieve targeted delivery in therapeutic and diagnostic applications. For effective delivery, the intact conjugate must have an adequate amount of time to accumulate in the target tissue.[4,5] Designing a biologic to remain intact until it reaches the target site is difficult because enzymatic degradation processes are capable of rapid proteolytic degradation.[6-8] Peptides often succumb to short circulation half-lives, either due to their small size, being filtered and removed promptly by the kidney, or proteolytic degradation, rendering them unable to act at their target site,[9-11] such as with the peptide glucagon-like peptide-1 (GLP-1) leading to the development of Exenatide[TM].[12] An appropriate amount of time is necessary for the targeting molecule and its payload to reach the target in both therapeutic and imaging applications where accumulation at the target site is necessary for effective treatment and high-resolution imaging results.[13,14]

The half-life of a small biologic is optimized by increasing the time the biologic has to reach the target site and is routinely accomplished by chemical modifications that increase size, slowing filtration and reducing access by proteases to cleavage sites.[15] Synthetic hydrophilic polymers such as polyethylene glycol (PEG) increase the circulation half-life and solubility as well as decrease proteolysis, demonstrated by PegIntron[TM] (Schering-Plough).[16-18] PEG is a non-metabolized, synthetic compound. A better tolerated and biodegradable partner is desirable.[6,19] Genetic incorporation of an amino acid polymer, known as XTEN, consisting of a sequence of hydrophilic, stable residues creates an inline, homogeneous half-life enhanced molecule.[20] Used

as an alternative to PEG, XTEN is practical to encode biosynthetically and, while resistant to serum proteases, is biodegradable.[21] Conjugation of 288 amino acids of XTEN to the hormone glucagon (Gcg) increased the half-life from 10 min to 9 h[22] and XTEN addition to both termini of recombinant human growth hormone (rhGH) to produce Somavaratan (VRS-317) yields a 30-60-fold increase in plasma half-life, potentially enabling once monthly dosing instead of daily injection.[23] Increasing half-life by enlarging size, however, results in longer exposure time to proteases. Resistance to proteases through strategic engineering is important for combating loss through enzymatic degradation. While amino acid tags used to increase the serum stability of peptides are being developed, none have been consistently reliable. Thus, a method to inhibit proteases across a broad range of peptides is still sought.[24]

The need to extend the half-life of peptides is particularly important when they are used as imaging agents.[15,25] Peptides conjugated to a chelator generate contrast agents for imaging applications to visualize tumors for diagnosis. For example, Sandostatin[TM] (Novartis Pharmaceuticals), a somatostatin analog, has an improved half-life of somatostatin from 2 min to 90 min and when radiolabeled creates a conjugate capable of effectively imaging carcinoid tumors.[26] In applications involving metals, circulating half-life is typically short because dilution into the large volume of a patient leads to rapid loss of the metal from the carrier via transmetallation reactions.[27,28] When metal is lost from the chelator prematurely, free metal ions accumulate in the bone and liver causing changes to normal cellular processes, toxicity and elevated background signal, decreasing the quality of the image.[29-32] Lanthanides are used currently because available chelators are poorly compatible with small transition metals, but small transition metals are preferred because of their biocompatibility and decreased patient toxicity.[33,34] An alternative method for delivery of metals to a target site for imaging is to use the

novel metal-binding tripeptide known as the *cla*MP Tag.[35-37] The *cla*MP Tag has the capability of acting as a contrast agent by binding safe, biocompatible transition metals rather than large, toxic lanthanide ions. Our lab discovered the unique metal abstraction peptide (MAP) chemistry and developed the inline *cla*MP Tag, which is currently being investigated as a targeted delivery method of transition metals for therapeutic and diagnostic applications. The tag consists of the amino acid sequence Asn-Cys-Cys and binds transition metals extraordinarily tightly,[38-40] making it possible to increase effective circulation time and target-specific tissue accumulation for transition metal-based imaging agents. The metal-*cla*MP complex has been shown to not disrupt the overall protein structure, including proteins that depend on formation of multiple, complex disulfide bonds for proper folding and function.[38,41] To investigate susceptibility of the metal-bound *cla*MP Tag to proteolytic cleavage and determine viability of using this tag in targeted imaging applications, an *in-vitro* proof of concept study of a fusion protein was carried out by engineering the *cla*MP Tag adjacent to a known recognition site for the serum protease Factor Xa. A series of spacer residues was added between the protease binding motif and the tag to further examine the ability of the *cla*MP Tag to affect cleavage at the recognition site.

3.2 MATERIALS AND METHODS

3.2.1 Genetic Engineering

Six constructs of *cla*MP-maltose binding protein (MBP) were prepared. Five of the DNA sequences contained the *cla*MP Tag (NCC) each with an increasing number of glycine residues on the N-terminus, from zero to four. In addition, a control was generated in which cysteine residues were replaced by alanine to eliminate metal binding. To create the recombinant DNA, a plasmid containing MBP in the pMAL-C5X vector was obtained (New England Biolabs, Inc.) and the MBP sequence was amplified with the different N-terminal primers (Integrated DNA

Technologies) using PCR. The primers consisted of a region matching the pET-32Xa/LIC vector shown as underlined, followed by the glycine spacers and *cla*MP Tag sequence, and lastly a portion matching the N-terminal MBP sequence shown in bold (Gly4, 5'-<u>ATT GAG GGT CGC</u> GGA GGA GGA GGA AAC TGT TGT GGC **AAA ATC GAA GAA**-3'; Gly3, 5'-<u>GGT ATT GAG GGT CGC</u> GGA GGA GGA AAC TGT TGT GGC **AAA ATC GAA GAA**-3'; Gly2, 5'-<u>GGT ATT GAG GGT CGC</u> GGA GGA AAC TGT TGT GGC **AAA ATC GAA GAA GG**-3'; Gly1, 5'-<u>GGT ATT GAG GGT CGC</u> GGA AAC TGT TGT GGC **AAA ATC GAA GAA GG**-3'; Gly0, 5'-<u>GGT ATT GAG GGT CGC</u> AAC TGT TGT GGC **AAA ATC GAA GAA GG**-3'; Control, 5'-<u>GGT ATT GAG GGT CGC</u> AAC GCA GCA GGC **AAA ATC GAA GAA GG**-3') The PCR reactions were purified using the QIAquick PCR Purification Kit (Qiagen) and the resulting product was inserted into the pET-32Xa/LIC vector via procedure provided by the manufacturer (Novagen). The ligation independent cloning reaction was then transformed into the DH5α *Escherichia coli* (*E. coli*) cell strain using the standard heat shock procedure. The cells were plated on LB agar plates with 100 μg/mL ampicillin and incubated overnight at 37 °C. Colonies were individually grown in 5 mL of LB with 100 μg/mL ampicillin overnight at 37 °C, 250 rpm. Cells were pelleted at 4000 rpm for 15 min and the supernatant discarded. The DNA was harvested using a miniprep kit (Qiagen) and confirmed by DNA sequencing (UC Berkeley DNA Sequencing Facility).

3.2.2 Protein Expression

Plasmids were transformed into BL21 *E. coli* using the standard heat shock technique. The cells were plated on LB agar plates with 100 μg/mL ampicillin and incubated overnight at 37 °C. Starter cultures were prepared using a single colony to inoculate 50 mL of LB with 100 μg/mL ampicillin and grown for 16 h at 37 °C, 250 rpm. Twenty milliliters of starter culture

were used to inoculate 1 L of LB with 100 μg/mL ampicillin in a 3-L Fernbach flask. The cells were grown at 37 °C, 250 rpm until the OD_{600} reached approximately 0.7 and expression was induced by addition of 1 mM isopropyl β-D-1-thiogalactopyranoside (IPTG). The cells were cultured for 4 h more and then harvested by centrifugation. Cell pellets were stored at -80 °C until use.

3.2.3 Protein Purification

Each 1 L pellet was resuspended in 25 mL of freshly made 50 mM Tris-Cl, 200 mM NaCl, pH 7.4 and lysed by three passes through a French press at 21,000 psi. The lysed cells were centrifuged for 1 h at 21,000 x g and 4 °C. The supernatant containing the protein was filtered through a 1.2 μm filter and applied to a nickelated 5 mL Hi-Trap Chelating HP column (GE Lifesciences). The column was washed with 50 mM Tris-Cl, 200 mM NaCl, 40 mM imidazole, pH 7.4 for 20 CV at a flow rate of 1.25 mL/min at 4 °C. The protein was eluted with 25 mL of 50 mM Tris-Cl, 200 mM NaCl, 250 mM imidazole, pH 7.4. Samples were diluted to 100 mL with 50 mM Tris-Cl, 100 mM NaCl, pH 8. The eluent was applied to a 10-mL column of amylose resin (New England Biolabs, Inc.) at 1.5 mL/min using an Econo Pump (BioRad) and MBP proteins were eluted with 40 mL of 50 mM Tris-Cl, 100 mM NaCl, 10 mM Maltose, pH 8. The protein was concentrated using Amicon Ultra 30 kDa MWCO concentrators (Millipore) to a final concentration of approximately 0.5-1 mM.

3.2.4 Nickel Release

Metal was released from the *cla*MP Tag by decreasing the pH and incubating with EDTA. Approximately 1 mL of metal-bound protein was diluted to a final concentration of 10 mM EDTA, 12 mM succinate, 35 mM citrate and 70 mM NaCl, pH 6.8. This diluted the amount of maltose in the sample to approximately 0.2 mM. Protein was incubated at room temperature

for approximately 2 h and either concentrated to 0.5 mM for metal quantification using absorption spectroscopy or applied to amylose resin and eluted with 30 mL of 50 mM citrate, 100 mM NaCl, 10 mM maltose, pH 6.5.

3.2.5 Factor Xa Cleavage

Constructs were prepared in 500 μL aliquots of 0.05 mM. Factor Xa (Novagen, 0.98 mg/mL) was added to a final concentration of 0.3 nM. The reaction was carried out at room temperature and monitored for up to 12 h.

3.2.6 SDS PAGE Analysis

Thirty microliter aliquots of 0.05 mM protein were collected at 0, 1, 2, 4, 6, 8, 10, and 12 h, combined with 30 μL of reducing Laemmli buffer and heated at 90 °C for 10 min. Samples were stored at -20 °C until used. Two microliters of each gel sample were loaded onto standard 15% (v/v) resolving, 4% (v/v) stacking gels and run at 135 V for 4 h. A pre-stained molecular weight ladder was used as a reference (BioRad, #161-0374). Gels were stained with SYPRO Ruby Protein Gel Stain (Life Technologies, cat# S-12000) according to the manufacturer's instructions. Replicates were obtained by adding Factor Xa to three individual aliquots of protein at a concentration of 0.05 mM protein. Samples of equivalent volumes of protein were added to reducing or non-reducing laemmli buffer at each time point. SDS-PAGE was completed for each of the three replicates for each protein construct.

3.2.7 Densitometry Analysis

The analysis was performed using a Typhoon TRIO Variable Mode Imager (Amersham Biosciences) and ImageQuantTL software (Amersham Biosciences). Relative intensity values in RFU were measured for each band and normalized to 100% for each lane in order to eliminate gel-loading variability between samples. The replicates at each time point were averaged and the

time 0 point, before Factor Xa was added, was normalized to 100% intact protein. The intact fusion protein was quantified in each lane of the gel and the relative amount cleaved was determined compared to the time 0 point. Plots of the relative normalized natural log of the relative fluorescent units (RFU) over time displayed a nearly linear relationship with R^2 values displayed in Table 3.1. The relative cleavage rate was determined from the slope and the error analysis displays a 90% confidence interval.

Table 3.1 R^2 Values of the Relative Linear Fit

Construct	R^2 With Nickel	R^2 Without Nickel
Gly4	0.97	0.98
Gly3	0.95	0.99
Gly2	0.96	0.98
Gly1	0.95	0.97
Gly0	0.92	0.99
Control	0.98	0.98

Secondary cleavage at the thrombin recognition site was observed. The relative amount of protein cleaved at the Factor Xa recognition site was quantified as a percentage compared to the total to account for only cleavage at the site adjacent to the *cla*MP Tag and not the minor non-specific cleavage site.

3.3 RESULTS

3.3.1 SDS-PAGE and Densitometry Analysis to Quantify Proteolytic Cleavage

In previous studies of *cla*MP-Tagged proteins embedded in cleavable fusion constructs, inclusion of the metal-bound tag slowed the ability to cleave the fusion partner.[38] Therefore, this *in vitro* proof of concept study was initiated to examine how the proximity of the *cla*MP Tag to a protease recognition site affects cleavage by a serum protease. The *cla*MP Tag was genetically engineered into a fusion protein (Trx-*cla*MP-MBP) adjacent to the serine protease Factor Xa recognition site between thioredoxin (Trx) and maltose binding protein (MBP) (Figure 3.1A), and the extent to which the metal-bound *cla*MP Tag inhibits the ability of Factor Xa to cleave at

Figure 3.1 Depiction of the proof of concept study used to understand the inhibitory nature of the *cla*MP Tag. (A) Cartoon of the fusion construct illustrating the inhibitory effect of the Ni-*cla*MP complex on Factor Xa cleavage. (B) Five of the constructs (three shown) consist of the *cla*MP Tag with a varied number of glycine spacers (1-3). A control without the two-cysteine residues (NAA) responsible for binding nickel was also tested (4). Ni^{2+} is represented by a green circle, which is bound by the *cla*MP Tag (red). The blue box illustrates the spacer positioned between the Factor Xa recognition site (black line) and *cla*MP Tag. (C) Abbreviated names for each of the six protein constructs.

the adjacent site was examined. Five variants of Trx-*cla*MP-MBP were made to examine the effect of changing the spacing between the enzymatic recognition site and the *cla*MP Tag. Zero, one, two, three or four glycine residues were engineered between the cleavage site and the *cla*MP Tag (Figure 3.1B and C). A non-metal binding control (NAA) also was made in which the two Cys in the *cla*MP Tag were substituted with Ala. At basic pH metal is bound to the tag, kinking the protein next to the recognition site, but in acidic conditions metal is released.

SDS-PAGE was used to observe protein cleavage as a function of time and densitometry analysis was performed for quantification. The 58-kDa fusion protein is cleaved after the intended Factor Xa recognition site (Ile-Glu-Gly-Arg) into two fragments of 41 kDa (*cla*MP-

MBP) and 17 kDa (Trx) (Figure 3.2), as verified by ESI-MS. The decrease in the amount of intact fusion protein (58 kDa) over time was quantified. A linear fit was established by plotting the relative normalized natural log of the relative fluorescence units (RFUs) acquired using densitometry vs. time (Figure 3.3).
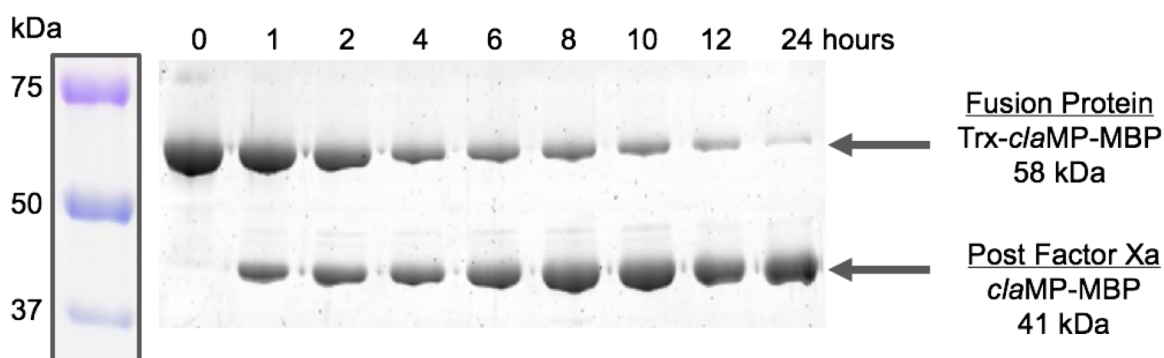
Figure 3.2 Factor Xa cleavage of the fusion protein, Trx-*cla*MP-MBP, over a 24-hour incubation period. Trx-*cla*MP-MBP is cleaved at the Factor Xa recognition site into two fragments, *cla*MP-MBP (41 kDa) and Trx (17 kDa). Trx is not shown because it is too small to be retained on the gel. The gels were stained with SYPRO Ruby Protein Gel Stain, which only allowed visualization of the 75-kDa molecular weight marker. The gel was aligned with the marker set by Coomassie staining and the ladder is shown.
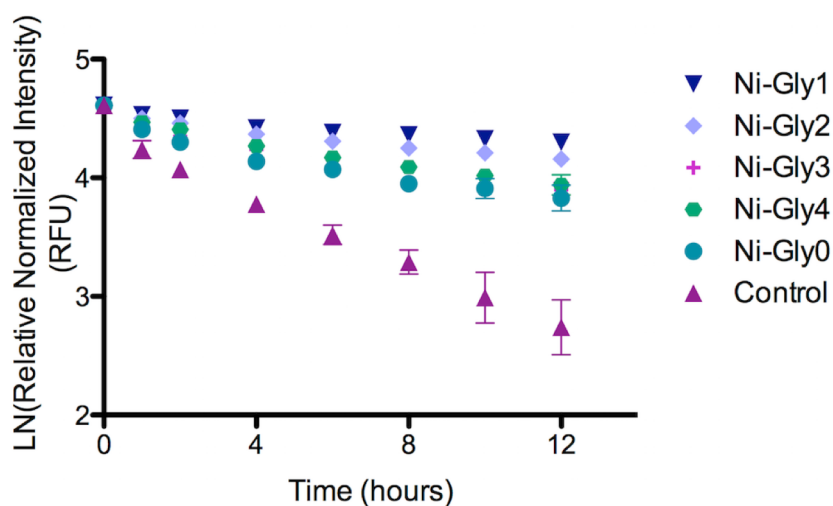
Figure 3.3 Plot of relative cleavage of Ni-*cla*MP Tag constructs demonstrating the inhibitory action of the inline metal-bound *cla*MP Tag. The control, followed by Ni-Gly0 have the fastest cleavage rates as shown by the first order relative rate plot. Error bars reflect a 90% confidence interval with n=3 data points. The R^2 values range from 0.92 to 0.99 indicating the majority of the constructs do not fit precisely to a first order linear function (Table 3.1).

3.3.2 The Metal-bound *cla*MP Tag Inhibits Proteolysis

Ni-Gly1 was determined to inhibit Factor Xa by approximately 3-fold compared to the control at the 12-hr time point showing the most inhibition compared to the other five constructs (Figure 3.4). At the 12-hr time point Factor Xa cleaved 28% of the Ni-Gly1 construct whereas

83% of the control was cleaved. If Ni-*cla*MP occludes access to the site based on steric hindrance, it would follow that the rate of cleavage would be slowest with the shortest spacer Ni-Gly0 and faster with the longest spacer Ni-Gly4. This trend was observed generally among the constructs examined except for one outlier, Ni-Gly0. Starting with Ni-Gly1, the trend held true; Ni-Gly1 had the slowest cleavage rate and increasing the number of glycine residues in the spacer led to increasing cleavage rate

Figure 3.4 The Ni-*cla*MP Tag inhibits proteolysis relative to the control for all five constructs depicted at the 12-hr time point. Ni-Gly1 exhibits the most inhibition with a 3-fold decrease in proteolysis compared to the control. Error bars represent a 90% confidence interval with n=3 data points.

with Ni-Gly3 and Ni-Gly4 having approximately the same rate. At 12 h, 28% of Ni-Gly1, 36% of Ni-Gly2, 51% of Ni-Gly3, and 48% of Ni-Gly4 were cleaved (Figure 3.4). Surprisingly, Factor Xa cleaved similar amounts of Ni-Gly0 (54%) and Ni-Gly4 (48%). Ni-Gly0 displayed a slower rate of cleavage than the control, suggesting the *cla*MP module does impede access to the cleavage site, but this construct's deviation from the trend was unexpected because the protease recognition site directly abuts the Ni-*cla*MP Tag and would be expected to more effectively hinder approach by the enzyme than the Ni-Gly1 and Ni-Gly2 variants.

3.3.3 Partial Metal Release Increases Proteolysis

To understand how metal bound to the *cla*MP Tag impacts proteolysis compared to the empty *cla*MP Tag sequence, the six constructs were subjected to mild acidic conditions in the presence of a chelating agent to release nickel form the *cla*MP Tag and incubated with Factor Xa. The Ni-*cla*MP Tag has spectral features in the UV and visible regions representing the unique structure of the metal-bound tag with identified peak maxima at 418 nm and 530 nm (Figure 3.5).[37,38] As such, UV-Vis absorption spectroscopy was used to quantify the metal remaining bound to the *cla*MP Tag. An extensive screen of conditions and approaches was performed to identify a set of parameters under which comparable and consistent results could be achieved, culminating in the conditions reported herein. All variants shown in Figure 3.5 were analyzed at equivalent protein concentration, highlighting the absorption difference when metal is bound. The absorption

Figure 3.5 Nickel is incorporated and released from constructs containing the *cla*MP Tag. The distinct features in the visible region indicate the unique structure of the metal-bound *cla*MP Tag. Ni-Gly1 is fully occupied and Gly1 is the partially occupied *cla*MP Tag after incubation at low pH with a chelator. The control does not contain the *cla*MP Tag and shows no absorbance in the visible region.

differences between the three constructs in the UV region are due to the Ni-bound *cla*MP Tag absorption at 313 nm.[37] The control protein that does not contain the *cla*MP Tag has no absorbance in the visible region and also lacks the ligand to metal charge transfer band at 313 nm indicative of the metal-bound state, whereas these distinct features are observed with both fully

occupied Ni-Gly1 and partially occupied Gly1, but in different proportions relative to the protein absorbance at 280 nm (Figure 3.5).

Results of the absorption spectroscopy revealed that metal is not released fully nor at equivalent rates and varies among the set of constructs analyzed. Consequently, it was necessary to quantify the percentage of metal retained in the *cla*MP Tag to compare the extent of cleavage by Factor Xa among the constructs (Table 3.2). Metal quantification became increasingly problematic with longer incubation at pH 6.5 due to instability of the samples, which resulted in light scattering, precipitation and protein loss from solution. The amount of metal released after incubation at pH 6.5 with EDTA for 2 h was determined to be the most consistently reliable time point for measuring metal release without interference and ranged from 46.6% to 69.4%. Most constructs released more than 57% of the nickel from the *cla*MP Tag, but Gly0 again was an outlier displaying greater retention of metal with only 46.6% released. Subsequent Factor Xa

Table 3.2 Relative Cleavage of *cla*MP-Tagged Constructs and Metal Bound

Construct	Normalized Percent Protein Cleaved pH 8[a] (%)	Normalized Percent Protein Cleaved pH 6.5[b] (%)	Percent Metal Bound pH 6.5[c] (%)	%cleaved/ %metal bound, pH 8[d]	%cleaved/ %metal bound, pH 6.5[e]	Ratio of amounts cleaved, pH 6.5/pH 8[f]
Gly1	33 ± 1	43 ± 6	43 ± 6	0.33	1.0	3.0
Gly2	43 ± 2	70 ± 10	37 ± 2	0.43	1.8	4.2
Gly3	61 ± 2	82 ± 3	31 ± 4	0.61	2.7	4.4
Gly4	58 ± 3	68 ± 2	43 ± 2	0.58	1.6	2.7
Gly0	65 ± 4	91.3 ± 0.5	50 ± 10	0.65	1.7	2.6
Control	100 ± 3	100 ± 5	N/A	1.0	1.0	1.0

[a]Percent protein cleaved normalized to the control at pH 8. [b]Percent protein cleaved normalized to the control at pH 6.5. [c]Percent metal retained in the *cla*MP Tag after incubation at pH 6.5 with EDTA for 2 h (n=2). [d]Relative ratio of percent protein cleaved to percent metal bound at pH 8, where the percent protein cleaved is divided by 100% metal-bound. [e]Relative ratio of percent protein cleaved to percent metal bound at pH 6.5. [f]Comparison of pH 6.5 to pH 8 of the ratios of percent protein cleaved to % metal bound. Error represents standard deviation of n=2 or 3.

cleavage of the constructs demonstrates Gly1 is the most inhibitory, reducing cleavage more than 2-fold compared to the control. Gly2 and Gly3 have less impact on cleavage as additional Gly

residues are placed between the enzymatic recognition sequence and the *cla*MP Tag. In general, the percentage of apo-*cla*MP Tag and percentage of protein cleaved increased as the number of glycine spacers was increased, with the exception of Gly0 (Figure 3.6). Gly0 is clearly an exception; this construct released appreciably less of the nickel than other constructs and yet had the greatest percentage of proteolysis. This result, however, does make sense because cleavage occurs more rapidly when metal is bound to this construct compared to the others. The data set generally suggests the metal-bound *cla*MP Tag hinders access by the enzyme to the cleavage site, presumably because of its bulky, kinked structure. Clearly with Gly0 proteolysis is not dependent solely on metal-binding to the *cla*MP Tag because it deviates from the trend of increased proteolysis with increased number of Gly spacer residues. The study shows that cleavage by Factor Xa is dependent on the presence of the *cla*MP Tag, its proximity to the hydrolyzed peptide bond and metal occupancy of the tag. On average, the partially metal occupied *cla*MP Tag inhibited proteolysis approximately 2-fold, and the fully occupied Ni-*cla*MP Tag displayed a 3-fold increase in inhibition, leading to the conclusion that the engineered sequence alone may modulate proteolysis and metal binding to the *cla*MP Tag further impedes cleavage.

The six constructs with partial metal release were compared to the nickel-bound constructs that were cleaved at pH 8. Because the rate of cleavage by Factor Xa differs between pH 6.5 and 8.0,[42] the relative results are compared by normalizing cleavage of the control protein at each pH to 100%. A similar trend to the fully metal-bound data set was observed (Figure 3.6A), where Gly1 exhibited the greatest inhibition, followed by Gly2, Gly3 and Gly4. In each case, a greater amount of cleavage was observed at pH 6.5 where metal release from the *cla*MP Tag occurs. The Gly0 construct, which had 54% cleaved at pH 8, demonstrates that proteolytic

susceptibility can be restored upon metal release, as evidenced by a similar amount of cleavage as the control, with 91% cleaved at 12 h (Figure 3.6A). In other samples subjected to conditions of metal release, substantial variability in the amount of protein cleaved was observed for the constructs with more Gly spacers, leading us to suspect differing degrees of instability or metal-release from these molecules, possibly via metal-based crosslinking because non-reducing SDS-PAGE shows insignificant formation of intermolecular disulfide bonds between cysteine residues in the tag sequence following metal release (data not shown). Because a truly quantitative analysis of the metal-free proteins and comparison to their Ni-bound analogs would require larger amounts of pure metal-free starting materials and detailed characterization of differences in chemical and physical stability among the constructs, particularly with respect to the oxidation state of cysteine residues from the tag, herein we first demonstrate that the *cla*MP Tag inhibits proteolysis by a serum protease, indicating subsequent more in-depth studies are warranted.

Because the metal is only partially released and to differing extents among the constructs

(A) (B)
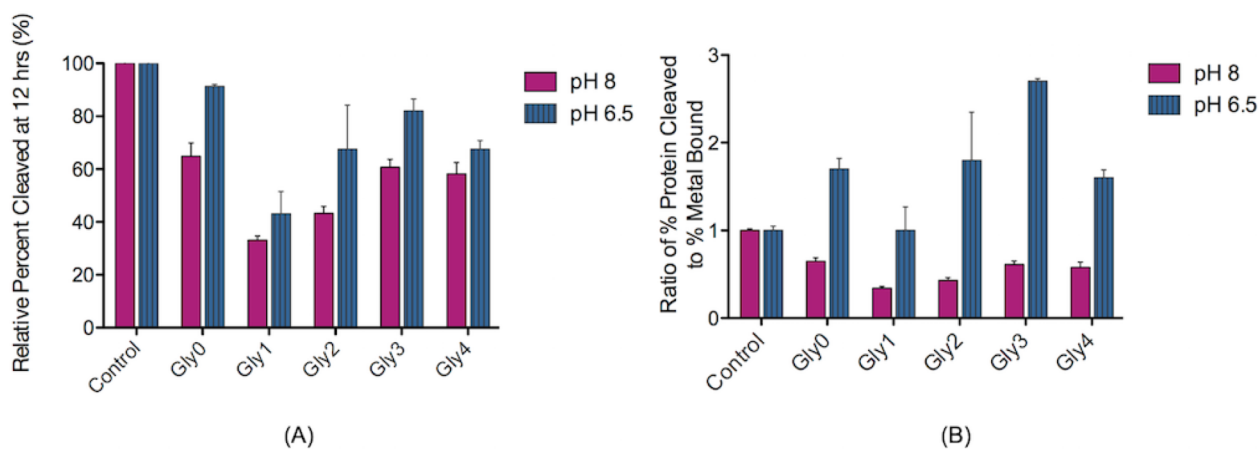
Figure 3.6 Relative cleavage of constructs at pH 6.5 compared to pH 8. (A) The *cla*MP Tag at pH 6.5 shows that metal release increases cleavage relative to the fully metal-bound analog at pH 8 and the control, but that cleavage remains below the level of the pH 6.5 control. Histogram represents the relative percent cleaved at 12 h normalized to the control at the same pH. Error bars reflect a 90% confidence interval with n=3 data points. (B) Comparison of cleavage relative to the amount of metal bound to the *cla*MP Tag. The ratios show that a substantial increase in cleavage occurs when metal is released.

and recovery of metal-free protein is poor, presumably due to instability, and in addition the enzyme cleavage rate slows as a function of time due to product formation, accurate quantitation of cleavage rate for the constructs was not feasible. As such, quantitative values reported herein are intended solely for the purpose of demonstrating relative comparisons and trends. Both the metal-bound and apo *cla*MP Tag constructs demonstrate a decrease in proteolytic cleavage as the spacer length is reduced from four to one glycine (Gly4 to Gly1) and that elimination of a spacer residue partially abrogates the inhibitory effect. The sequence, Gly1 was determined to be the most effective inhibitor of Factor Xa, decreasing cleavage rate by approximately 3-fold compared to the control. The tabulated results at pH 8 reveal a large reduction in the amount of protein cleaved compared to control when metal is bound to the *cla*MP Tag (100% occupancy), whereas at pH 6.5, which is amenable to metal release, substantially more protein is cleaved in the same amount of time. Within each condition, the percent protein cleaved increases from Gly1 to Gly4, indicating more protein is cleaved with an increasing number of glycine residues at both pH 8 and pH 6.5. The values presented in Table 3.2 are relative (normalized to percent of control) and the ratios also are reported proportional to the amount of metal bound to permit comparison of results at the two different pH conditions. Taking the ratio of the amount of protein cleaved relative to the amount of metal bound with each construct at pH 6.5 to pH 8, it is clear substantially more protein is cleaved at pH 6.5 than pH 8 due to metal release (Figure 3.6B). The higher the ratio the greater the amount of protein cleaved at pH 6.5, when the protein is metal free, than at pH 8.

3.4 DISCUSSION

In previous studies, it was determined that the MAP chemistry is compatible with recombinant production of difficult to express proteins having intramolecular disulfide bonds

because the engineered *cla*MP Tag does not interfere with proper folding and protein structure.[38,39] In the preparation of proteins used in these studies, however, slow or incomplete cleavage of the fusion partners was observed for some constructs. Here, an *in vitro* proof of concept study was performed to examine how the proximity of the *cla*MP Tag to a protease recognition site affects cleavage at the known recognition site by the serum protease Factor Xa embedded in a thioredoxin (Trx) - maltose binding protein (MBP) fusion protein as a model system. The nickel-bound *cla*MP complex has been extensively characterized, and therefore, nickel was inserted into the *cla*MP Tag in this investigation because this metal complex has extraordinary stability and its rich spectroscopic properties enable quantitative analysis of metal incorporation.[38,39] Nickel is a suitable substitute for other transition metals such as platinum and copper (unpublished data), which are sought after elements for therapeutic and diagnostic use.

When metal is bound to the tag, there is a 3-fold decrease in cleavage rate compared to the control protein. Figure 3.7 depicts how the metal-bound *cla*MP Tag alters the protein's conformation and flexibility to inhibit proteolysis. When metal is not bound to the *cla*MP Tag, the conformation of the tripeptide sequence and therefore the orientation of the two fusion proteins with respect to each other, is less restricted. In comparison, when the *cla*MP Tag is occupied with metal, the tag becomes constrained by the obligate square planar geometry of the coordinating moieties and access to the adjacent recognition site by Factor Xa is altered, decreasing the ability to cleave the protein. In the metal-bound state, the protein sequence bends around the metal ion forming a tight turn, kinking the protein. Additional glycine residues were included in an effort to increase flexibility adjacent to the recognition site and to increase space between the tag and cleavage site, allowing the enzyme greater ability to approach and cleave the protein.

Based on the structures presented in Figure 3.7, Ni-Gly0 would be expected to have the slowest rate of cleavage if dominated by steric hindrance and the rate would increase as a larger number of glycine residues were placed between the enzyme recognition sequence and the *cla*MP Tag as a spacer. The trend of increasing cleavage rate with increasing number of spacer residues was observed for the constructs assembled with glycine spacers, with the exception of

(a) Gly0   (b) Ni-Gly0   (c) Ni-Gly1
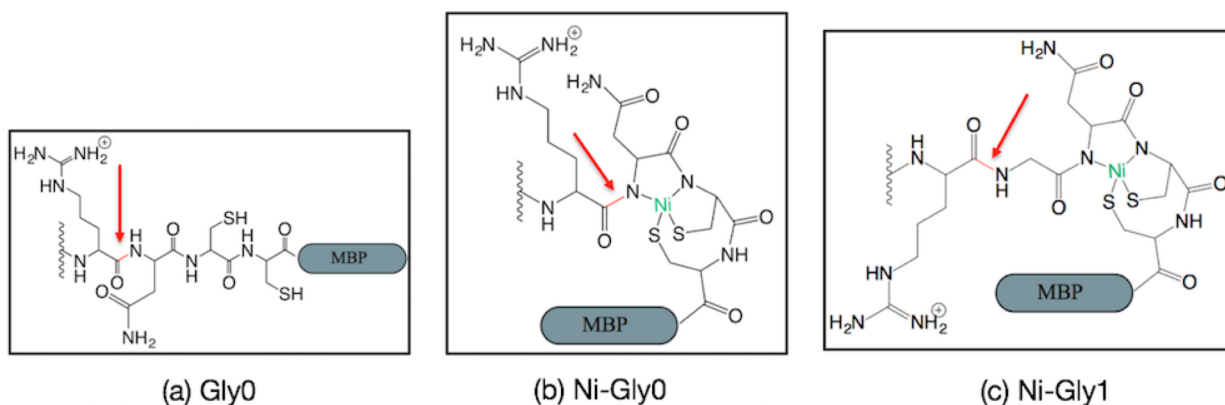
Figure 3.7 Chemical structures indicating the site of hydrolysis by Factor Xa. Arginine is the final residue of the Factor Xa recognition site and adjacent is the *cla*MP Tag (Asn-Cys-Cys). Red arrows and bonds represent the site of peptide bond hydrolysis by Factor Xa. The *cla*MP Tag (a) without metal-bound (Gly0), (b) with metal (Ni-Gly0), and (c) with metal-bound and one glycine residue (Ni-Gly1).

Gly0, which surprisingly has a more rapid rate of cleavage than Gly1-4, indicating that the amount of space is not the only significant influence on cleavage rate. It was expected that metal insertion would affect the structure between the two folded domains, causing the fusion protein to adopt a more protease-resistant conformation when the *cla*MP Tag is loaded, as observed for constructs with 1-4 Gly spacer residues. Because the relative cleavage rate of Gly0 deviates from the expected trend, it is evident that in addition to steric hindrance adjacent or neighboring residues influence the rate of hydrolysis.[43,44] This construct may have a conformation that is preferred by the enzyme, while those with spacer residues are more resistant to proteolysis. However, a notable chemical difference is that Gly0 has metal bound directly to the nitrogen of the peptide bond that is cleaved by the enzyme, and it is reasonable to anticipate direct metal

coordination by the amide nitrogen of the cleaved peptide bond may promote hydrolysis (Figure 3.7b). Metal ions have chemical reactivity and can cause peptide bond breakage either through oxidation or hydrolysis.[45,46] Copper (II) binding within the hinge region of IgG1 monoclonal antibodies (mAbs) can lead to fragmentation, and in some cases, neighboring residues have been shown to alter the rate of hydrolysis of the peptide bond adjacent to the metal binding site.[47] Nickel and other cationic transition metals are Lewis acids with high electron affinity, causing bond polarization and facilitating hydrolysis as well.[48] Metals also can promote hydrolysis by activating a water molecule that can be deprotonated by an adjacent basic side chain, mimicking natural metalloproteinases that use metals in their active site for the purpose of proteolytic hydrolysis.[49,50] Importantly, because the nickel-bound *cla*MP Tag and fusion protein is stable in the absence of Factor Xa, the presence of metal alone does not account for the observed increase in cleavage of the Gly0 construct. It is more likely that displacement of the proton from the backbone amide nitrogen by Ni(II) in the *cla*MP Tag complex accelerates cleavage by altering the electronic properties of this peptide bond, making the enzymatic reaction more favorable. This could be accomplished by a preferred orientation that permits greater access to the recognition site or through the provision of a chemical moiety that facilitates the reaction or a combination of both. Because the adjacent residue is Gly in all of the constructs examined, the result is likely because another nearby residue in this construct presents a functional group in a structurally favorable position to facilitate more effectively the hydrolytic reaction. Although hydrolysis of the Gly0 construct occurs faster than the other *cla*MP Tag constructs, Gly0 still offers significant protection compared to the control, indicating that inclusion of the metal-bound *cla*MP Tag inhibits proteolysis and that the construct's stability can be tuned by placement and composition of neighboring residues.

In order for Factor Xa to attack the carbonyl of the stable amide bond in the peptide backbone of the substrate, residues within the substrate pocket of Factor Xa act as a general acid by hydrogen bonding to the carbonyl of the substrate, creating a more electrophilic carbon center for nucleophilic attack.[51,52] Metal bound adjacent to the hydrolyzing peptide bond will increase the electron withdrawing effects, resulting in a more electrophilic center for nucleophilic attack by the serine residue, increasing the rate of peptide bond cleavage compared to when metal is not bound adjacently. This explanation would account for the anomalously fast rate of cleavage for Gly0, while steric occlusion explains the overall trend among the series of Gly-containing constructs with protonated rather than metal-bound adjacent nitrogen atoms. Once the kinked Ni-claMP Tag and the folded domains of the fusion partners are sufficiently separated in space from the protease recognition site, cleavage rates are expected to become more similar as more glycine residues are added. The rates of cleavage of Gly3 and Gly4 with and without metal are statistically equivalent. This result suggests that the metal-bound claMP Tag is directly responsible for inhibition when fewer than three residues separate the tag from the recognition site. Although a much larger series of variants would need to be examined to verify the mechanism, when three or more spacer residues are present, it seems that the size of the folded domains instead may limit diffusional access to the binding site to restrict approach by the enzyme.

Control of proteolysis is crucial and knowing both where and when cleavage occurs enables design of effective therapeutics. Prodrugs and antibody drug conjugates (ADCs) are designed to use proteolysis to their advantage. Such biologics aim to be stable and inaccessible to proteases in the serum yet degraded through proteolytic cleavage in the lysosomal compartment of the target cell to release the payload.[53,54] The activity of Factor Xa was examined to gain an

initial understanding of the inhibitory action of the *cla*MP Tag when exposed to a serum protease, but during conditions of stress, such as disease, protease activity can increase. Disease states, specifically tumor metastasis, are typically associated with upregulation of proteases, which is the main concern when protection is needed until the biologic is internalized into the target cell.[55,56] It is particularly important for ADCs to contain a stable linker to avoid proteolysis and release of the conjugated toxin before reaching the target because they can be in circulation for days.[57,58] The site of release of the toxin will impact the toxicity profile and premature, untargeted release may cause unwanted toxicity.[59-61] The ability to slow proteolysis in the serum by 3-fold or more would provide significant protection against premature release. As demonstrated in this proof of concept study, inclusion of the metal-bound *cla*MP Tag can protect proteins from proteolytic degradation and by inference should decrease side effects due to premature release of a toxic payload in serum. ADCs target extracellular receptors and are taken up via endocytosis.[62] A commonly employed ADC delivery approach relies on enzymatic release of the toxic payload in lysosomes by cathepsin B.[63] pH decreases with endocytosis and the acidic environment facilitates enzymatic cleavage. The *cla*MP Tag has been demonstrated to be both stable and protease resistant in mildly basic conditions, including those that emulate serum.[41] Importantly, metal release from the *cla*MP Tag occurs solely below pH 7.00 in acidic conditions[40] such that once a targeted molecule is directed to the lysosome[62], cleavage would not be impeded because the tag would empty concomitantly. For practical reasons of analysis pH 8 was chosen for this study instead of serum pH with knowledge that the structure of the Ni-*cla*MP complex remains unaltered above neutral pH up to at least pH 9.[40] Although actual enzyme rates of cleavage differ with pH, *relative* differences in cleavage of the constructs at pH 8.0 and 7.4 are expected to be similar and to follow the same trends. Previous stability characterization at pH

7.3 of *cla*MP-Tagged protein showed the complex remains stable for at least 12 weeks.[39] Examining proteolysis at a mildly basic pH where metal is retained and at acidic pH where metal is released allowed initial comparison of proteolysis among a series of *cla*MP-Tagged constructs within a simple system. Once a clinical candidate is identified, further experiments in serum would enable identification of all fragments and cleavage sites relevant for *in vivo* degradation.

Although all constructs with the metal-bound *cla*MP Tag slowed proteolysis, it is evident that the specific amino acid sequence surrounding the tag affects cleavage. Further exploration of the adjacent sequence, specifically substitution of the glycine residues to more bulky groups, should be pursued to determine to what extent residue choice in neighboring positions offers greater protection. The presented data demonstrate clearly the *cla*MP Tag reduces proteolysis at an existing recognition site. The *cla*MP Tag not only provides protection from unwanted degradation, but this finding provides support for its use for the targeted delivery of metals. As such, further exploration of the amino acid residues surrounding the *cla*MP Tag is warranted to determine the optimal sequence for resisting cleavage by Factor Xa and other serum proteases.

3.5 SUPPLEMENTAL DATA

3.5.1 Probing the Amino Acid Sequence Surrounding the *cla*MP Tag

The amino acid sequence surrounding the *cla*MP was varied to identify residues that are able to improve inhibition. Either the Asn residue of the *cla*MP Tag within Ni-Gly0 or the Gly residue preceding the *cla*MP Tag within Ni-Gly1 were mutated to different residues (Supplementary Figure 3.1). Asn was mutated to either Gly or Val and both Gly and Val improved inhibition by 1.8-fold compared to Ni-Gly0 (Supplementary Figure 3.1a). The Gly residue preceding the *cla*MP Tag was changed to either Pro, Arg, Lys, Val, Phe, or Thr within Ni-Gly. Other than Pro, Gly was determined to be the most inhibitory compared to the other five

mutations (Supplementary Figure 3.1b). Pro is known to inhibit Factor Xa, so this inhibition is not due to the *cla*MP Tag, but is due to the proline residue itself.[64]

(a)   (b)
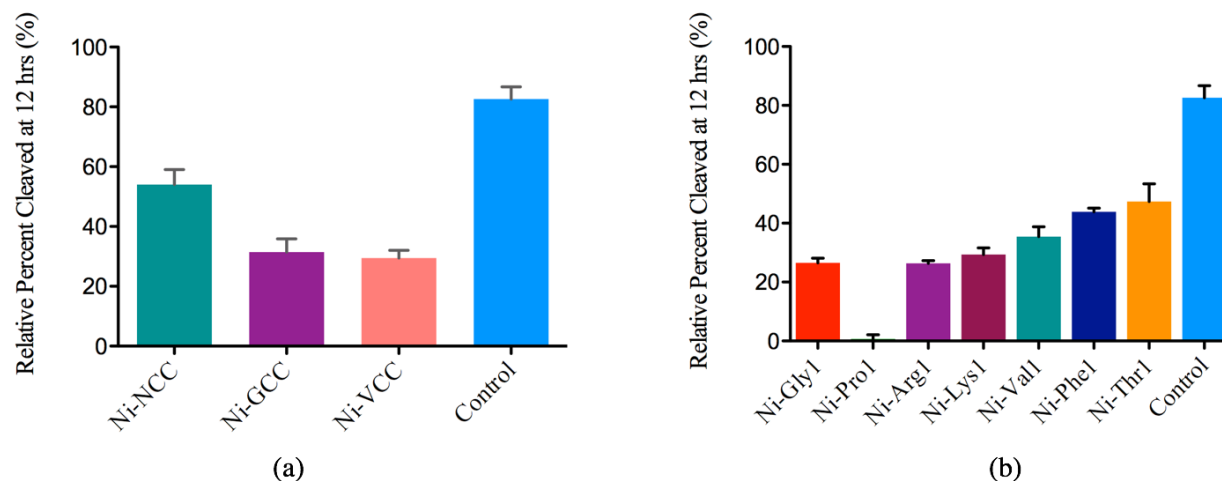
Supplementary Figure 3.1 Varying the amino acid sequence surrounding the metal-binding site of the *cla*MP Tag showed small improvements in proteolytic stability. (a) Mutation of Asn residue within Ni-Gly0 showed small improvement in proteolytic stability. (b) Mutation of Gly residue within Ni-Gly1 and the only improvement in stability was by Pro. Control for Ni-NAA are placed on each graph as a reference.

3.6 REFERENCES

1.   Srinivasarao, M.; Galliford, C. V.; Low, P. S., Principles in the design of ligand-targeted cancer therapeutics and imaging agents. *Nat Rev Drug Discov* **2015,** *14* (3), 203-219.

2.   Thundimadathil, J., Cancer Treatment Using Peptides: Current Therapies and Future Prospects. *Journal of Amino Acids* **2012,** *2012*, 13.

3.   Fosgerau, K.; Hoffmann, T., Peptide therapeutics: current status and future directions. *Drug Discovery Today* **2015,** *20* (1), 122-128.

4.   Carter, P. J.; Senter, P. D., Antibody-Drug Conjugates for Cancer Therapy. *The Cancer Journal* **2008,** *14* (3), 154-169.

5.   Hamley, I. W., PEG–Peptide Conjugates. *Biomacromolecules* **2014,** *15* (5), 1543-1559.

6.   Mitragotri, S.; Burke, P. A.; Langer, R., Overcoming the challenges in administering biopharmaceuticals: formulation and delivery strategies. *Nat Rev Drug Discov* **2014,** *13* (9), 655-672.

7.   Craik, D. J.; Fairlie, D. P.; Liras, S.; Price, D., The Future of Peptide-based Drugs. *Chemical Biology & Drug Design* **2013,** *81* (1), 136-147.

8.   Bruno, B. J.; Miller, G. D.; Lim, C. S., Basics and recent advances in peptide and protein drug delivery. *Therapeutic delivery* **2013,** *4* (11), 1443-1467.

9.   Daugherty, A. L.; Mrsny, R. J., Formulation and delivery issues for monoclonal antibody therapeutics. *Advanced Drug Delivery Reviews* **2006,** *58* (5–6), 686-706.

10.   Torchilin, V., Intracellular delivery of protein and peptide therapeutics. *Drug Discovery Today: Technologies* **2008,** *5* (2–3), e95-e103.

11.   Werle, M.; Bernkop-Schnürch, A., Strategies to improve plasma half life time of peptide and protein drugs. *Amino Acids* **2006,** *30* (4), 351-367.

12.   Pratley, R. E.; Gilbert, M., Targeting Incretins in Type 2 Diabetes: Role of GLP-1 Receptor Agonists and DPP-4 Inhibitors. *The Review of Diabetic Studies : RDS* **2008,** *5* (2), 73-94.

13.   Bae, Y. H.; Park, K., Targeted drug delivery to tumors: Myths, reality and possibility. *Journal of Controlled Release* **2011,** *153* (3), 198-205.

14.   Kwon, I. K.; Lee, S. C.; Han, B.; Park, K., Analysis on the current status of targeted drug delivery to tumors. *Journal of controlled release : official journal of the Controlled Release Society* **2012,** *164* (2), 10.1016/j.jconrel.2012.07.010.

15.   Pollaro, L.; Heinis, C., Strategies to prolong the plasma residence time of peptide drugs. *MedChemComm* **2010,** *1* (5), 319-324.

16.   Kozlowski, A.; Milton Harris, J., Improvements in protein PEGylation: pegylated interferons for treatment of hepatitis C. *Journal of Controlled Release* **2001,** *72* (1–3), 217-224.

17.   Harris, J. M.; Chess, R. B., Effect of pegylation on pharmaceuticals. *Nat Rev Drug Discov* **2003,** *2* (3), 214-221.

18.   Chapman, A. P., PEGylated antibodies and antibody fragments for improved therapy: a review. *Advanced Drug Delivery Reviews* **2002,** *54* (4), 531-545.

19.   Strohl, W. R., Fusion Proteins for Half-Life Extension of Biologics as a Strategy to Make Biobetters. *BioDrugs* **2015,** *29* (4), 215-239.

20.   Schellenberger, V.; Wang, C.-w.; Geething, N. C.; Spink, B. J.; Campbell, A.; To, W.; Scholle, M. D.; Yin, Y.; Yao, Y.; Bogin, O.; Cleland, J. L.; Silverman, J.; Stemmer, W. P. C., A recombinant polypeptide extends the in vivo half-life of peptides and proteins in a tunable manner. *Nat Biotech* **2009,** *27* (12), 1186-1190.

21.   Haeckel, A.; Appler, F.; Figge, L.; Kratz, H.; Lukas, M.; Michel, R.; Schnorr, J.; Zille, M.; Hamm, B.; Schellenberger, E., XTEN-Annexin A5: XTEN Allows Complete Expression of Long-Circulating Protein-Based Imaging Probes as Recombinant Alternative to PEGylation. *Journal of Nuclear Medicine* **2014,** *55* (3), 508-514.

22.   Geething, N. C.; To, W.; Spink, B. J.; Scholle, M. D.; Wang, C.-w.; Yin, Y.; Yao, Y.; Schellenberger, V.; Cleland, J. L.; Stemmer, W. P. C.; Silverman, J., Gcg-XTEN: An Improved Glucagon Capable of Preventing Hypoglycemia without Increasing Baseline Blood Glucose. *PLOS ONE* **2010,** *5* (4), e10175.

23.   Moore, W. V.; Nguyen, H. J.; Kletter, G. B.; Miller, B. S.; Rogers, D.; Ng, D.; Moore, J. A.; Humphriss, E.; Cleland, J. L.; Bright, G. M., A Randomized Safety and Efficacy Study of Somavaratan (VRS-317), a Long-Acting rhGH, in Pediatric Growth Hormone Deficiency. *The Journal of Clinical Endocrinology & Metabolism* **2016,** *101* (3), 1091-1097.

24.   Jambunathan, K.; K Galande, A., Design of a serum stability tag for bioactive peptides. *Protein and peptide letters* **2014,** *21* (1), 32-38.

25.   Lee, S.; Xie, J.; Chen, X., Peptide-Based Probes for Targeted Molecular Imaging. *Biochemistry* **2010,** *49* (7), 1364-1376.

26.   Critchley, M., Octreotide scanning for carcinoid tumours. *Postgraduate Medical Journal* **1997,** *73* (861), 399-402.

27.   Cacheris, W. P.; Quay, S. C.; Rocklage, S. M., The relationship between thermodynamics and the toxicity of gadolinium complexes. *Magnetic resonance imaging* **1990,** *8* (4), 467-481.

28.   Frenzel, T.; Lengsfeld, P.; Schirmer, H.; Hütter, J.; Weinmann, H.-J., Stability of Gadolinium-Based Magnetic Resonance Imaging Contrast Agents in Human Serum at 37°C. *Investigative Radiology* **2008,** *43* (12), 817-828.

29.   Ersoy, H.; Rybicki, F. J., Biochemical Safety Profiles of Gadolinium-Based Extracellular Contrast Agents and Nephrogenic Systemic Fibrosis. *Journal of magnetic resonance imaging : JMRI* **2007,** *26* (5), 1190-1197.

30.   Aime, S.; Caravan, P., Biodistribution of gadolinium-based contrast agents, including gadolinium deposition. *Journal of magnetic resonance imaging : JMRI* **2009,** *30* (6), 1259-1267.

31.   Sieber, M. A.; Lengsfeld, P.; Frenzel, T.; Golfier, S.; Schmitt-Willich, H.; Siegmund, F.; Walter, J.; Weinmann, H.-J.; Pietsch, H., Preclinical investigation to compare different gadolinium-based contrast agents regarding their propensity to release gadolinium in vivo and to trigger nephrogenic systemic fibrosis-like lesions. *European radiology* **2008,** *18* (10), 2164-2173.

32.   Morawski, A. M.; Lanza, G. A.; Wickline, S. A., Targeted contrast agents for magnetic resonance imaging and ultrasound. *Current Opinion in Biotechnology* **2005,** *16* (1), 89-92.

33.   Yang, J. J.; Yang, J.; Wei, L.; Zurkiya, O.; Yang, W.; Li, S.; Zou, J.; Zhou, Y.; Maniccia, A. L. W.; Mao, H.; Zhao, F.; Malchow, R.; Zhao, S.; Johnson, J.; Hu, X.; Krogstad, E.; Liu, Z.-R., Rational Design of Protein-Based MRI Contrast Agents. *Journal of the American Chemical Society* **2008,** *130* (29), 9260-9267.

34.   Franz, K. J.; Nitz, M.; Imperiali, B., Lanthanide-Binding Tags as Versatile Protein Coexpression Probes. *ChemBioChem* **2003,** *4* (4), 265-271.

35. Krause, M. E.; Glass, A. M.; Jackson, T. A.; Laurence, J. S., Novel Tripeptide Model of Nickel Superoxide Dismutase. *Inorganic Chemistry* **2010,** *49* (2), 362-364.

36. Krause, M. E.; Glass, A. M.; Jackson, T. A.; Laurence, J. S., MAPping the Chiral Inversion and Structural Transformation of a Metal-Tripeptide Complex Having Ni-Superoxide Dismutase Activity. *Inorganic Chemistry* **2011,** *50* (6), 2479-2487.

37. Krause, M. E.; Glass, A. M.; Jackson, T. A.; Laurence, J. S., Embedding the Ni-SOD Mimetic Ni-NCC within a Polypeptide Sequence Alters the Specificity of the Reaction Pathway. *Inorganic Chemistry* **2013,** *52* (1), 77-83.

38. Mills, B. J.; Mu, Q.; Krause, M. E.; Laurence, J. S., claMP Tag: A Versatile Inline Metal-Binding Platform Based on the Metal Abstraction Peptide. *Bioconjugate Chemistry* **2014,** *25* (6), 1103-1111.

39. Mills, B. J.; Laurence, J. S., Stability analysis of an inline peptide-based conjugate for metal delivery: nickel(II)-claMP Tag epidermal growth factor as a model system. *J Pharm Sci* **2015,** *104* (2), 416-23.

40. Laurence, J. A. S.; Vartia, A. A.; Krause, M. E., Metal abstraction peptide (MAP) tag and associated methods. Google Patents: 2012.

41. Mills, B. J.; Laurence, J. S., Stability Analysis of an Inline Peptide-based Conjugate for Metal Delivery: Nickel(II)–claMP Tag Epidermal Growth Factor as a Model System. *Journal of Pharmaceutical Sciences* **2015,** *104* (2), 416-423.

42. Qiagen, I.; Valencia, C., The QIA Expressionist: A Handbook for High-level Expression and Purification of $6\times$ His-tagged Proteins. *Qiagen Inc: Chatsworth, CA* **2003**.

43. Supattapone, S.; Nguyen, H.-O. B.; Muramoto, T.; Cohen, F. E.; DeArmond, S. J.; Prusiner, S. B.; Scott, M., Affinity-Tagged Miniprion Derivatives Spontaneously Adopt Protease-Resistant Conformations. *Journal of Virology* **2000,** *74* (24), 11928-11934.

44. Ewart, K. V.; Yang, D. S. C.; Ananthanarayanan, V. S.; Fletcher, G. L.; Hew, C. L., Ca2+-dependent Antifreeze Proteins MODULATION OF CONFORMATION AND ACTIVITY BY DIVALENT METAL IONS. *Journal of Biological Chemistry* **1996,** *271* (28), 16627-16632.

45. Allen, G.; Campbell, R. O., Specific cleavage of histidine-containing peptides by copper (II). *International journal of peptide and protein research* **1996,** *48* (3), 265-273.

46. Grant, K. B.; Kassai, M., Major advances in the hydrolysis of peptides and proteins by metal ions and complexes. *Current Organic Chemistry* **2006,** *10* (9), 1035-1049.

47. Glover, Z. K.; Basa, L.; Moore, B.; Laurence, J. S.; Sreedhara, A., Metal ion interactions with mAbs: Part 1 pH and conformation modulate copper-mediated site-specific fragmentation of the IgG1 hinge region. *Mabs* **2015,** *7* (5), 901-911.

48. Haas, K. L.; Franz, K. J., Application of Metal Coordination Chemistry to Explore and Manipulate Cell Biology. *Chemical reviews* **2009,** *109* (10), 4921-4960.

49. Andberg, M.; Jäntti, J.; Heilimo, S.; Pihkala, P.; Paananen, A.; Koskinen, A. M. P.; Söderlund, H.; Linder, M. B., Cleavage of recombinant proteins at poly-His sequences by Co (II) and Cu (II). *Protein science* **2007,** *16* (8), 1751-1761.

50. Humphreys, D. P.; King, L. M.; West, S. M.; Chapman, A. P.; Sehdev, M.; Redden, M. W.; Glover, D. J.; Smith, B. J.; Stephens, P. E., Improved efficiency of site-specific copper (II) ion-catalysed protein cleavage effected by mutagenesis of cleavage site. *Protein engineering* **2000,** *13* (3), 201-206.

51. Hedstrom, L., Serine Protease Mechanism and Specificity. *Chemical Reviews* **2002,** *102* (12), 4501-4524.

52. Perona, J. J.; Craik, C. S., Structural basis of substrate specificity in the serine proteases. *Protein Science : A Publication of the Protein Society* **1995,** *4* (3), 337-360.

53. Ducry, L.; Stump, B., Antibody− drug conjugates: linking cytotoxic payloads to monoclonal antibodies. *Bioconjugate chemistry* **2009,** *21* (1), 5-13.

54. Law, B.; Tung, C.-H., Proteolysis: a biological process adapted in drug delivery, therapy, and imaging. *Bioconjugate chemistry* **2009,** *20* (9), 1683-1695.

55. Duffy, M. J., The role of proteolytic enzymes in cancer invasion and metastasis. *Clinical & experimental metastasis* **1992,** *10* (3), 145-155.

56. Gabriel, D.; F Zuluaga, M.; Van Den Bergh, H.; Gurny, R.; Lange, N., It is all about proteases: From drug delivery to in vivo imaging and photomedicine. *Current medicinal chemistry* **2011,** *18* (12), 1785-1805.

57. Xu, K.; Liu, L.; Saad, O. M.; Baudys, J.; Williams, L.; Leipold, D.; Shen, B.; Raab, H.; Junutula, J. R.; Kim, A.; Kaur, S., Characterization of intact antibody–drug conjugates from plasma/serum in vivo by affinity capture capillary liquid chromatography–mass spectrometry. *Analytical Biochemistry* **2011,** *412* (1), 56-66.

58. Teicher, B. A.; Chari, R. V. J., Antibody Conjugate Therapeutics: Challenges and Potential. *Clinical Cancer Research* **2011,** *17* (20), 6389-6397.

59. Kamath, A. V.; Iyer, S., Challenges and advances in the assessment of the disposition of antibody-drug conjugates. *Biopharmaceutics & Drug Disposition* **2015**, n/a-n/a.

60. Lin, K.; Tibbitts, J., Pharmacokinetic considerations for antibody drug conjugates. *Pharmaceutical research* **2012,** *29* (9), 2354-2366.

61. Gébleux, R.; Wulhfard, S.; Casi, G.; Neri, D., Antibody Format and Drug Release Rate Determine the Therapeutic Activity of Noninternalizing Antibody–Drug Conjugates. *Molecular Cancer Therapeutics* **2015,** *14* (11), 2606-2612.

62. Ritchie, M.; Tchistiakova, L.; Scott, N., Implications of receptor-mediated endocytosis and intracellular trafficking dynamics in the development of antibody drug conjugates. *mAbs* **2013,** *5* (1), 13-21.

63. Ducry, L.; Stump, B., Antibody−Drug Conjugates: Linking Cytotoxic Payloads to Monoclonal Antibodies. *Bioconjugate Chemistry* **2010,** *21* (1), 5-13.

64. Ludeman, J. P.; Pike, R. N.; Bromfield, K. M.; Duggan, P. J.; Cianci, J.; Le Bonniec, B.; Whisstock, J. C.; Bottomley, S. P., Determination of the P 1′, P 2′ and P 3′ subsite-specificity of factor Xa. *The international journal of biochemistry & cell biology* **2003,** *35* (2), 221-225.

CHAPTER 4. DESIGN AND CHARACTERIZATION OF A *cla*MP-TAGGED EGFR TARGETING MOLECULE WITH INCREASED PROTEOLYTIC STABILITY

4.1 INTRODUCTION

Non-invasive imaging techniques provide means of visualizing biological processes to aid in early diagnosis and treatment, ultimately improving patient prognosis.[1-4] Targeted molecular imaging probes consist of a targeting molecule, such as a peptide, protein, or antibody, conjugated to a chelator. These molecular probes are coupled with imaging techniques, such as positron emission tomography (PET) and single-photon emission computed tomography (SPECT) to provide functional information and enable quantification of disease-related biochemical processes, adding more detail to currently used anatomical techniques such as MRI and CT.[5,6] Aspects such as ligand affinity, ligand properties (molecular weight, lipophilicity and charge), tissue uptake, and background signal must be considered in designing a molecular probe.[7] Stability in the systemic circulation is necessary for the molecule to reach the target tissue and accumulate in it, while rapid clearance from sites that do not contain the target is necessary to achieve high contrast images.[8] Often, molecular probes are specifically designed with a half-life that achieves these desired pharmacokinetic properties. For example, Octreotide was designed as a proteolytic-resistant prototype of the native somatostatin hormone that has a half-life of only 3 min caused by enzymatic degradation.[9] Incorporation of unnatural amino acids and disulfide crosslinking increased the half-life to approximately 100 min,[10] and rapid tumor uptake and background clearance enabled successful imaging of neuroendocrine tumors.[11]

In pharmaceutical applications, radioactive metals are used for PET and SPECT imaging. The half-life of the radioisotope should be long enough for the synthesis and administration time span, but not so long that it causes damage to the patient's tissues. Ideally, the half-life of the

isotope should match that of the final bioactive complex.[12] Most often the half-lives of peptides and proteins must be increased for accumulation in the target tissue; this goal can be accomplished by addition of synthetic polymers such as PEG.[13] Although PEG has been used successfully in many cases, addition of an inline fusion protein, such as XTEN, simplifies production and creates a natural and biodegradable molecule.[14,15] XTEN has been fused to annexin A5 (AnxA5) to detect phosphatidylserine-exposing cells, which indicate that apoptosis is occurring in disease states. AnxA5 has a short half-life of less than 7 min in mice; however, inline addition of 288 amino acids of XTEN increases the half-life to 1 h.[16] This new technology provides the desired pharmacokinetic properties and creates a simplified and well-tolerated molecule.

Currently used contrast agents consist of the chemical conjugation of a chelator that binds large lanthanide metals such as gadolinium.[17] Gadolinium is often released from the chelator upon dilution into the body causing toxicity due to accumulation in the kidney.[18] Therefore, a tight-binding chelator from a native protein sequence is desired. A successful chelator is the calcium-binding sites of the rat α-parvalbumin; these calcium-binding sites were converted to Gd^{3+} binding sites to target tumor tissue with prostate-specific membrane antigen (PSMA).[19] Transition metals are a more biocompatible and safer alternative to lanthanide metal ions; however, their use is limited because of the lack of availability of strong chelators. Commonly used chelators, such as DOTA, do not bind small transition metals very tightly. For example, DOTA was conjugated to an antibody, cetuximab, and complexed with Gd^{3+} to target and block signal transduction of EGFR. Incorporation of Cu^{2+} rather than Gd^{3+} created a weak metal coordination complex, and the loss of copper from the chelator decreased the quality of the

image due to a high background.[20,21] The released copper was observed to accumulate in the liver.[20,21]

Presented here is the design of a homogenous and site-specific EGFR-targeting imaging agent. A novel metal-binding tripeptide, known as the *cla*MP Tag, was created inline with epidermal growth factor (EGF), the natural ligand to target EGFR. Inline addition of the *cla*MP Tag simplified production of the conjugate compared to chemical conjugation of a synthetic moiety to a protein. The *cla*MP Tag consists of the amino acid sequence, Asn-Cys-Cys, and is used for transition metal binding with targeting proteins for diagnostic and therapeutic applications. Previously, the *cla*MP Tag has been shown to bind tightly to nickel;[22,23] described here is the first application of using the *cla*MP Tag to complex cobalt. The *cla*MP Tag was placed inline with EGF followed by addition of 14, 34, or 57 amino acids of XTEN to create EGF-*cla*MP-XTEN fusions with longer half-lives than that of EGF (i.e., longer than $t_{1/2}$ of 3–7 min).[24,25] The degradation sites of EGF-*cla*MP-XTEN fusion proteins were evaluated when incubated with serum proteases. The effect of single amino acid mutation to increase proteolytic stability was also investigated.

4.2 MATERIALS AND METHODS

4.2.1 Genetic Engineering

Three EGF-*cla*MP-XTEN genes were custom designed to include EGF followed by a glycine residue preceding the *cla*MP Tag and varying lengths of XTEN[26] (XTEN14, Ser-Ala-Ala-Ser-Pro-Glu-Ser-Thr- Glu-Glu-Gly-Thr-Ser-Thr; XTEN34, Ser-Ala-Ala-Ser-Pro-Ala-Ser-Pro-Ala-Gly-Ser-Pro-Thr-Ser-Thr-Glu-Glu-Gly-Thr-Ser-Glu-Ser-Ala-Thr-Pro-Glu-Ser-Thr-Glu-Glu-Gly-Thr-Ser-Thr; XTEN57, Ser-Ala-Ala-Ser-Pro-Ala-Ser-Pro-Ala-Gly-Ser-Pro-Thr-Ser-Thr-Glu-Glu-Gly-Thr-Ser-Glu-Ser-Ala-Thr-Pro-Glu-Ser-Gly-Pro-Gly-Thr-Ser-Thr-Glu-Pro-Ser-

Glu-Gly-Ser-Ala-Pro-Gly-Ser-Pro-Ala-Gly-Ser-Pro-Thr-Ser-Thr-Glu-Glu-Gly-Thr-Ser-Thr).

The custom-order genes were purchased from Genescript and user instructions were followed to prepare the purchased DNA. To obtain the desired recombinant DNA, primers were used to amplify the sequence of interest. Primers contained a region matching the EGF-*cla*MP-XTEN sequence shown in bold and a region matching the pET32Xa/LIC vector shown as underlined (forward primer, 5'-TCC GGT ATT GAG GGT CGC **AAC AGC GAT AGC GAA TGC**-3' and reverse primer, 5'-AGA GGA GAG TTA GAG CCT TA**G GTG CTG GTG CCT TCT TCG GT**-3'). The QIAquick PCR Purification Kit (Qiagen) was used to purify the PCR reaction, and the product was inserted into the pET-32Xa/LIC vector following the manufacturer's procedure (Novagen). Unexpectedly, the EGF-*cla*MP-XTEN57 construct contained two reverse primer annealing sequences on the N-terminus. To purify only the desired recombinant DNA sequence, the EGF-*cla*MP-XTEN5 PCR reaction was loaded into a 2% agarose gel. The desired product was cut from the gel and placed in an Eppendorf tube. The QIAquick Gel Extraction Kit procedure was followed to purify the PCR product, and the manufacturer's procedure was followed in the same way as with the other constructs. Standard heat shock procedures were used to transform the LIC reaction into DH5α *Escherichia coli* (*E. coli*) cell strain. Cells were plated on LB agar plates containing 100 μg/mL ampicillin and incubated at 37 °C overnight. Colonies were grown overnight in 5 mL LB with 100 μg/mL ampicillin at 250 rpm, 37 °C. Cells were centrifuged at 4000 rpm for 15 min, and the supernatant was discarded. A miniprep kit (Qiagen) was used to exploit the DNA, and the sequences were confirmed (UC Berkeley DNA Sequencing Facility).

4.2.2 Expression of EGF-*cla*MP-XTEN

Expression and purification of these constructs was highly similar to previously reported EGF expression and purification methods.[22] Standard heat shock methods were used to transform the recombinant DNA into the Origami B (DE3) *E. coli* strain (Novagen). Colonies were grown for approximately 24 h on LB agar plates containing 100 µg/mL ampicillin, 30 µg/mL kanamycin, and 12.5 µg/mL tetracycline. Starter cultures were inoculated with individual colonies consisting of 50 mL of LB with 100 µg/mL ampicillin for 16 h at 37 °C, 250 rpm. Twenty milliliters of starter culture was inoculated into 1 L of LB containing 100 µg/mL ampicillin was grown at 37 °C, 250 rpm, until OD reached between 0.6–0.8 (~ 4 h). The protein expression was then induced with the addition of 1 mM isopropyl β-D-1-thiogalactopyranoside (IPTG). The cells were cultured at 25 °C, 200 rpm, for 16 h and then harvested via centrifugation and stored at –80 °C until used.

4.2.3 Purification of EGF-*cla*MP-XTEN

Twenty-five milliliters of lysis buffer (50 mM sodium phosphate, 300 mM NaCl, pH 7.4) was used to resuspend a 1 L pellet. Three passes through a French press at 21,000 psi were used to lyse the cells, followed by centrifugation for 1 h at 21,000 x g and 4 °C. The soluble fraction containing the protein was filtered through a 1.2 µm filter followed by a 0.45 µm filter and applied to a cobalt-charged HiTrap TALON crude 5 mL column (GE Healthcare Life Sciences) equilibrated in lysis buffer. The protein was left on the column at room temperature for approximately 1 h to allow metal transfer into the tag. The column was washed with wash buffer (50 mM sodium phosphate, 300 mM NaCl, 5 mM imidazole pH 7.4) at 1.25 mL/min for 10 CV. The protein was eluted from the column using 25 mL of elution buffer (50 mM sodium phosphate, 300 mM NaCl, 150 mM imidazole, pH 7.4). The protein was diluted 100-fold into

wash buffer to decrease the imidazole concentration and was concentrated to approximately 4 mL using an AMICON Ultra 10 kDa MWCO concentrator (Millipore). Eight units of thrombin (Fisher Scientific BP254310) per mg protein was incubated with the protein at 16 °C for 9.5 h. The protein was diluted to a final volume of 15 mL in wash buffer and re-applied to a regenerated Co-TALON column. The flow-through as well as an additional 5 CV of wash buffer was collected and diluted 100-fold into 50 mM Tris, 10 mM NaCl pH 7.3. The protein was concentrated to 1.8 mL, and calcium chloride at a final concentration of 5 mM was added prior to Factor Xa (Novagen, 1.1 mg/mL) being added at a final concentration of 4 µg/mL and incubated at room temperature for 16 h. The reaction was applied to a Superdex75 column (GE Lifesciences), and the fractions containing the final product were concentrated to approximately 1 mL.

4.2.4 Mass Spectrometry

ESI spectra were acquired on a Waters Synapt G2 hybrid Quadrupole time-of-flight mass spectrometer operated in MS mode and acquiring data with the time-of-flight analyzer. The instrument was operated in resolution, 22K, mode. The cone voltage was 45eV, and Ar was admitted to the collision (trap) cell. Spectra were acquired at the auto pusher frequency covering the mass range 50–3000 u. Time to mass calibration was made with NaI cluster ions acquired under the same conditions and lock mass corrected with an auxiliary sprayer presenting the doubly charged ion, 785.84265, from Glu-fibrinogen peptide. Lock mass spectra were acquired every 30 s.

Capillary HPLC/MS experiments were performed with a chromatograph that develops gradients at 28 µL/min on 0.3 mm ID × 5cm C4 RP medium with a Waters Nano Acquity. The solvents are: A H_2O, B 80% CH_3CN, 20% isopropanol, both 0.08% formic acid. The gradient

was held at 1% B for 0.5 min, stepped to 15% by 1 min, and then ramped to 70% by 12 min. Column effluent was directed through a 32-gauge needle operated at 2800 V on a standard Waters ESI source probe. "Zero" charge spectra for molecular weight information from ESI-presented charge states were obtained using "Transform" or "MaxEnt I" routines in Masslynx software.

4.2.5 Cell Culture

The protocol for the cell viability assay was previously described.[22] Human epidermoid carcinoma cells (A-431 ATCC CRL-1555) and Dulbecco's Modified Eagle's Medium (DMEM) (ATCC-30-2002) were purchased from ATCC. A-431 cells were cultured in DMEM supplemented with 10% fetal bovine serum (FBS), 1% penicillin, and 1% streptomycin. The culture method recommended by ATCC was followed and the cells were grown in an incubator at 37 °C and 5% CO_2.

4.2.6 EGF Cell Viability Assay

After the A-431 cells reached confluency, they were passaged, and plated at a density of 10,000 cells per well were plated in a 96-well clear-bottom black plate. The cells were placed in the incubator overnight, and the following day the medium was replaced with medium containing the treatments and controls. The treatments were diluted into the medium at the appropriate concentrations and added to the wells, after which they were placed in the incubator for 72 h. Resazurin was added to A-431 cultures at a final concentration of 0.09 mg/mL and was incubated for 3 h before measuring the fluorescence (560 nm excitation, 590 nm emission) using a fluorescence plate reader (BioTek).

4.2.7 Stability Samples

Immediately after purification, stability analysis of the protein was started. Each day 20 µL samples of a 0.1 mM stock solution of protein were mixed with 20 µL of non-reducing lamelli buffer and incubated at 90 °C for 10 min to create the samples for SDS-PAGE. Samples were left at room temperature or 4 °C and stability was analyzed at both temperatures.

4.2.8 Enzymatic Incubation

Factor Xa or thrombin were added to a 0.1 mM protein sample to a final concentration of 11 µg/mL Factor Xa (Novagen, 1.1 mg/mL) or 50 U/mL thrombin (Fisher Scientific BP254310). Incubation occurred at room temperature and samples were taken at time points 0, 10, 12, 14, 16, 18, 20, 22, and 36 h. At the specified time points, 25 µL of the protein sample was mixed with 25 µL reducing lamelli buffer and incubated at 90 °C for 10 min to create samples for SDS-PAGE.

4.2.9 SDS-PAGE

SDS-PAGE consisting of 4% (v/v) stacking and 20% (v/v) resolving gels was used to visualize the stability and proteolysis over time. A prestained molecular weight ladder (Biorad #161-0374) was used as a reference, and the gels were stained with coomassie.

4.2.10 Densitometry Analysis

Protein bands on the SDS-PAGE gels were quantified using the Odyssey CLx Imaging System (Li-cor). Gels were imaged and quantified using the fluorescence emission of coomassie at 700 nm (excitation ~ 650 nm).[27]

4.3 RESULTS

4.3.1 Design of EGF-*cla*MP-XTEN Constructs

Three variants of a *cla*MP-Tagged EGFR-targeting molecule were designed as inline fusion proteins and characterized with respect to metal-binding and stability. Epidermal growth

factor (EGF), which is the natural ligand of epidermal growth factor receptor (EGFR), and was ideal to use as a target to EGFR (+) tumor cells. EGF was genetically engineered inline with the *cla*MP Tag followed by either 14, 34, or 57 amino acids of XTEN (Figure 4.1). Previously, a *cla*MP-Tagged EGF molecule was expressed and purified as a fusion protein;[22] here the fusion protein was modified by the addition of XTEN (Supplementary Figure 4.1 and 4.2). Prior purification efforts have utilized nickel-immobilized metal affinity chromatography (Ni-IMAC) for both purification through the His6 tag and incorporation of metal into the *cla*MP Tag. Primarily, previous efforts to characterize the *cla*MP Tag have been accomplished using nickel because of the unique properties of the Ni-*cla*MP Tag, such as tight metal-binding and rich spectroscopic features. Described here is the first exploration of cobalt complexed to the *cla*MP Tag for SPECT and PET imaging.
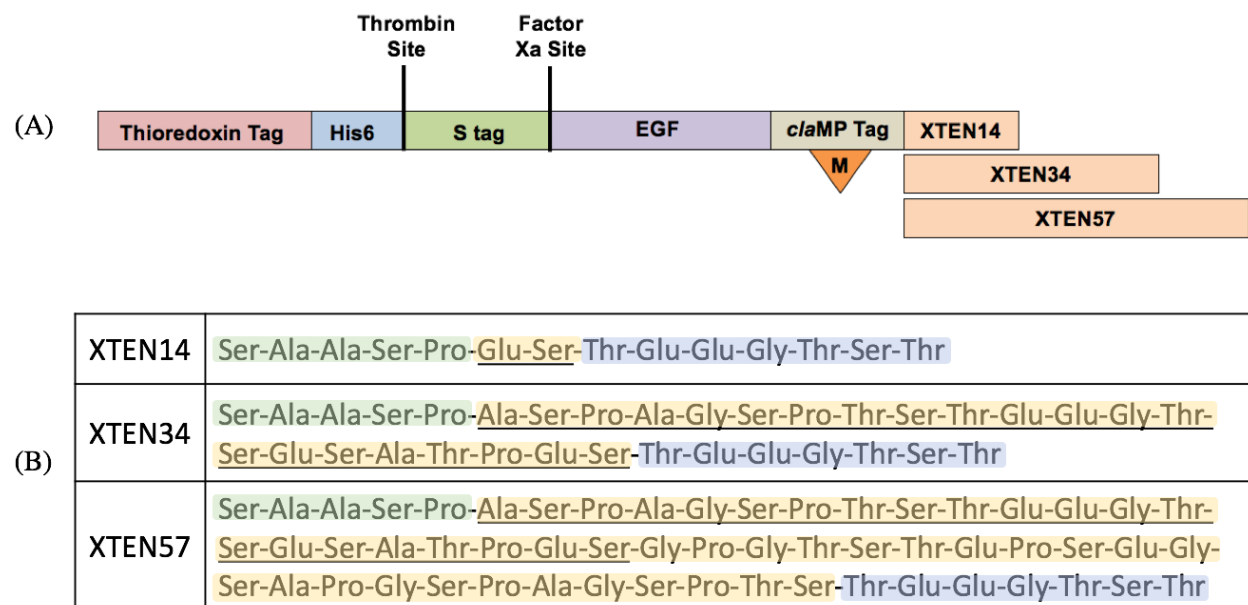
Figure 4.1 Cartoon of EGF-*cla*MP-XTEN fusion constructs. (A) The fusion partner of each construct consists of Thioredoxin, His Tag and S-Tag followed by EGF and the *cla*MP Tag (Asn-Cys-Cys) and either 14, 34 or 57 amino acids of XTEN. Enzymatic recognition sequences are built into the fusion protein to enable removal of the fusion partners upon purification. (B) Sole comparison of XTEN sequences with identical sequences highlighted or underlined.

4.3.2 Investigation of the Co-*cla*MP Tag Complex

While the nickel-bound *cla*MP Tag has been extensively studied and is known to form an extraordinarily stable complex,[28] the Co-*cla*MP Tag has yet to be investigated. Cobalt was compared to nickel to understand relative differences between the two metal-bound *cla*MP Tag complexes. Cobalt was introduced into the *cla*MP Tag in a manner similar to that previously completed with nickel. The *cla*MP-Tagged conjugates were placed on a 5-mL cobalt-charged TALON column to permit exchange of cobalt into the *cla*MP Tag. The expectation was that cobalt and nickel would behave very similarly as both have a +2-charge and are located adjacent on the periodic table. Initial comparisons between cobalt and nickel consisted of investigating the EGF-*cla*MP-XTEN34 fusion protein purified by either nickel or cobalt affinity chromatography. Absorption spectroscopy was used to determine metal uptake by the *cla*MP Tag (Figure 4.2). Metal binding occurred in both nickel- and cobalt-purified samples and was confirmed by a visual color change from a clear protein solution to a rusty orange/brown color upon exposure to metal (Supplementary Figure 4.3). Spectroscopic features have yet to be characterized for the cobalt-*cla*MP Tag. To determine the extent of cobalt binding to the *cla*MP Tag, the Co-*cla*MP Tagged protein sample was placed over a nickelated column. Unoccupied *cla*MP Tag sites will readily incorporate nickel, allowing quantification of cobalt occupation of the *cla*MP Tag. Specifically, the Ni-*cla*MP Tag can be quantified by a peak in the visible region at approximately 410 nm, and the 280/410 nm ratio aligns with complete occupancy (Table 4.1). Spectroscopic features at 410 nm were observed for both nickel- and cobalt-purified samples (Figure 4.2). The ratio of the 280 nm to 410 nm peak was unchanged when placed over the nickelated column, indicating that cobalt fully occupies the *cla*MP Tag (Table 4.1). A peak in the visible region of the cobalt-purified sample was also identified, however with a lower intensity than the Ni-*cla*MP

Tag. Comparing the Co-*cla*MP Tag intensity at 410 nm to the Ni-*cla*MP Tag shows that the relative molar absorptivity is approximately three-fourths of that of the Ni-*cla*MP Tag (Table 4.1).
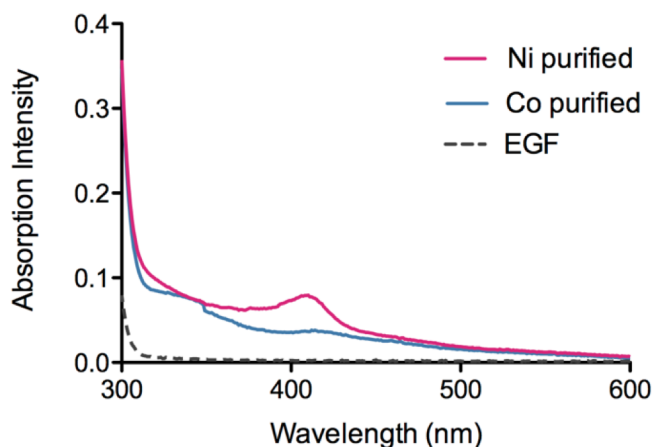
Figure 4.2 Comparison of nickel and cobalt *cla*MP Tag complexes within the EGF-*cla*MP-XTEN34 fusion protein. Absorption spectrum of nickel-bound and cobalt-bound *cla*MP Tag and identification of similar peaks at 410 nm. EGF is shown as a control that does not contain the *cla*MP Tag and therefore does not bind metal.

Table 4.1 Comparison of Nickel and Cobalt Binding to the *cla*MP Tag

Purification Method	Ratio of 280/410	Relative Molar Absorptivity[a]
Ni purified	39 ± 3	1.00 ± 0.09
Co purified	52 ± 4	0.75 ± 0.05
Co followed by Ni	53 ± 4	0.73 ± 0.06

[a]Molar absorptivity at 410 nm compared to the nickel purified sample.

Non-reducing SDS-PAGE and mass spectrometry indicate covalent disulfide dimerization occurring in the EGF-*cla*MP-XTEN constructs. Dimerization was confirmed by mass spectrometry (monomer 11769.59 Da and dimer 23539.41 Da) (Supplementary Figure 4.4). Reducing SDS-PAGE eliminated higher molecular weight species (data not shown), indicating that covalent disulfide bonds are formed. Quantification of the higher molecular weight, dimeric, and monomeric species was completed using non-reducing SDS-PAGE and densitometry

analysis (Figure 4.3). Dissociation of higher molecular weights species to monomeric species occurs after the concentration and dilution step; at higher temperature, dissociation occurs more

(A)   (B)
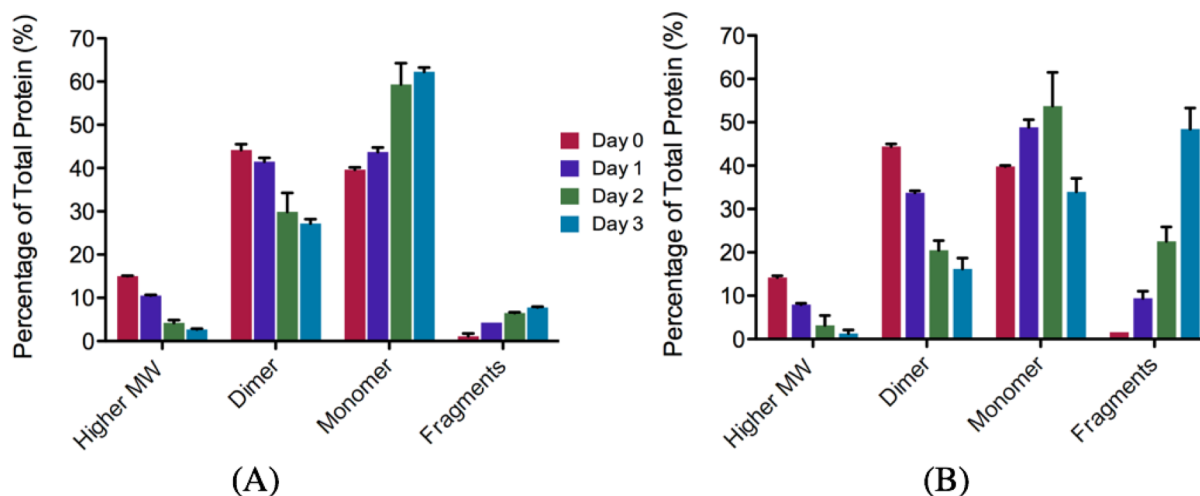
Figure 4.3 Quantification of higher molecular weight, dimer, monomer and fragment species of EGF-claMP-XTEN34. Stability was analyzed at (A) 4 °C and (B) room temperature (approximately 25 °C). Quantification was completed using a densitometry analysis of SDS-PAGE. Error bars represents standard deviation of n=2.

rapidly (Figure 4.3). EGF-claMP-XTEN constructs contain eight Cys residues, six Cys residues within EGF forming three disulfide bonds, and two Cys residues within the claMP Tag, any of which could be responsible for dimerization. Removal of the claMP Tag Cys residues was completed using site-directed mutagenesis of the two Cys residues to Ala and, upon purification, dimerization no longer occurred. Therefore, dimerization is through the claMP Tag Cys residues and not the three disulfide bonds within EGF.

Fragmentation of the protein over time was also observed and, at 4 °C, less than 10% fragmentation occurred, while at room temperature almost 50% of the protein is fragmented after three days. To understand this further, a control protein consisting of only EGF was purified using the cobalt purification method. EGF remains monomeric and stable for at least one week (longest time examined) and non-reducing SDS-PAGE lacks dimerization. A fragment of EGF consisting of EGF without the C-terminal Arg53 residue was identified by mass spectrometry.

Cleavage at this site was also observed with EGF-Ni-*cla*MP constructs, but only a small amount accumulated over 2 months, with the initial identification after 8 weeks.[29] Purification using cobalt may impact the stability of EGF, causing more rapid cleavage between Leu52 and Arg53.

4.3.3 Addition of XTEN Does Not Impact EGF Yield or Function

Addition of XTEN to the C-terminus of EGF is expected to have little to no impact on the structure or function of EGF-*cla*MP. Expression and purification of the XTEN constructs resulted in similar yields at each purification step for both nickel and cobalt purifications (Table 4.2).

Table 4.2 Addition of XTEN Does Not Impact Yield of EGF-*cla*MP-XTEN Constructs

Construct	Post IMAC (mg)[a]	Post Thrombin Cleavage (mg)[a]	Post Factor Xa Cleavage (mg)[a]	Average Percent Yield (%)[b]
Ni-purified EGF	30 ± 10	17 ± 1	4.2 ± 0.9	16 ± 5
Co-purified EGF	13.3	10.2	2.5	18.8
Ni-EGF-*cla*MP-XTEN14	40 ± 10	16 ± 5	4.1 ± 0.9	11 ± 1
Co-EGF-*cla*MP-XTEN14	24 ± 9	14 ± 6	2.5 ± 0.6	11 ± 2
Co-EGF-*cla*MP-XTEN34	30 ± 10	14 ± 6	1.2 ± 0.4	5 ± 1
Co-EGF-*cla*MP-XTEN57	19 ± 6	9 ± 1	1.5 ± 0.4	9 ± 4

[a]Reported as mass equivalents of EGF-*cla*MP-XTEN construct and were calculated by taking the final EGF-*cla*MP XTEN mass as a fraction of the fusion protein. [b]Yield was calculated by taking the post Factor Xa cleavage mass as a fraction of the initial post IMAC mass.

Conjugation of a fusion protein or polymer to a targeting protein can interfere with the ability of the molecule to target the receptor by blocking receptor binding. The functionality of the EGF-*cla*MP-XTEN was examined using an A431 epidermoid carcinoma cell line, which overexpresses EGFR on the surface of the cells (Figure 4.4). Addition of EGF to the A431 cell line causes the previously established, albeit unexpected result of cell death.[30] The control protein, EGF, was compared to the Co-EGF-*cla*MP-XTEN constructs. Cell viability decreased at similar rates for all constructs, with 25% of the cells remaining viable at doses greater than 10

nM indicating that addition of Co-*cla*MP-XTEN does not impact the functionality of EGF (Figure 4.4).
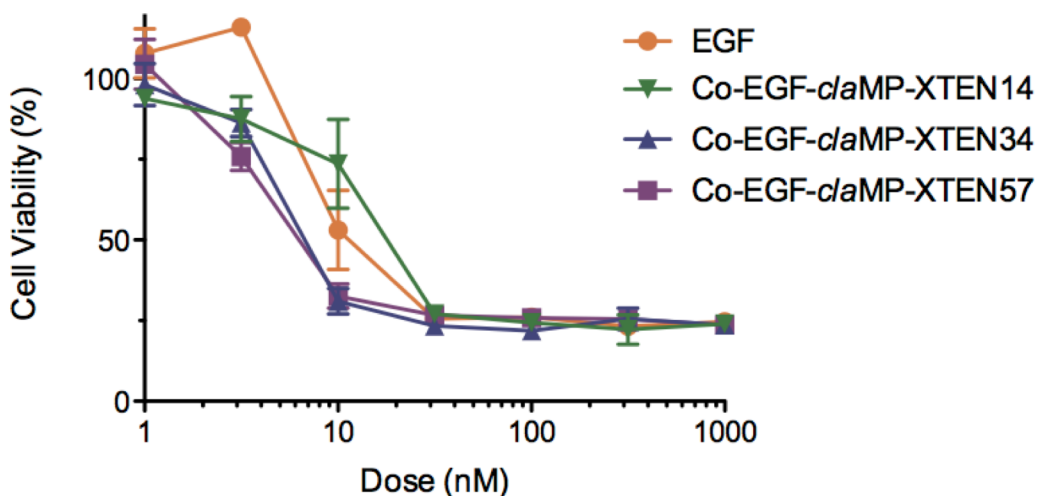
Figure 4.4 Inline addition of XTEN residues on the C-terminus of EGF has no influence on the function of EGF. The three EGF-*cla*MP-XTEN constructs decreased cell viability similar to the control protein, EGF.

4.3.4 Investigation of Proteolytic Stability of EGF-*cla*MP-XTEN

EGF-*cla*MP-XTEN constructs were exposed to two serum proteases, thrombin and Factor Xa, and their proteolytic susceptibility was examined. Degradation of the intact molecule into smaller molecular weight fragments was visualized using SDS-PAGE (Supplementary Figure 4.5) and quantified with a densitometry analysis. The decrease in the intensity of the intact protein was quantified and the constructs were compared at the 0, 12, 22, and 36 h time points (Figure 4.5). The three constructs behaved in a highly similarly manner when cleaved with Factor Xa or thrombin. After 36 h, thrombin cleaved 73.9% of EGF-*cla*MP-XTEN14, 63.5% of EGF-*cla*MP-XTEN34, and 71.1% of EGF-*cla*MP-XTEN57, while Factor Xa cleaved 33.3% EGF-*cla*MP-XTEN14, 48.3% of EGF-*cla*MP-XTEN34, and 42.5% of EGF-*cla*MP-XTEN57.
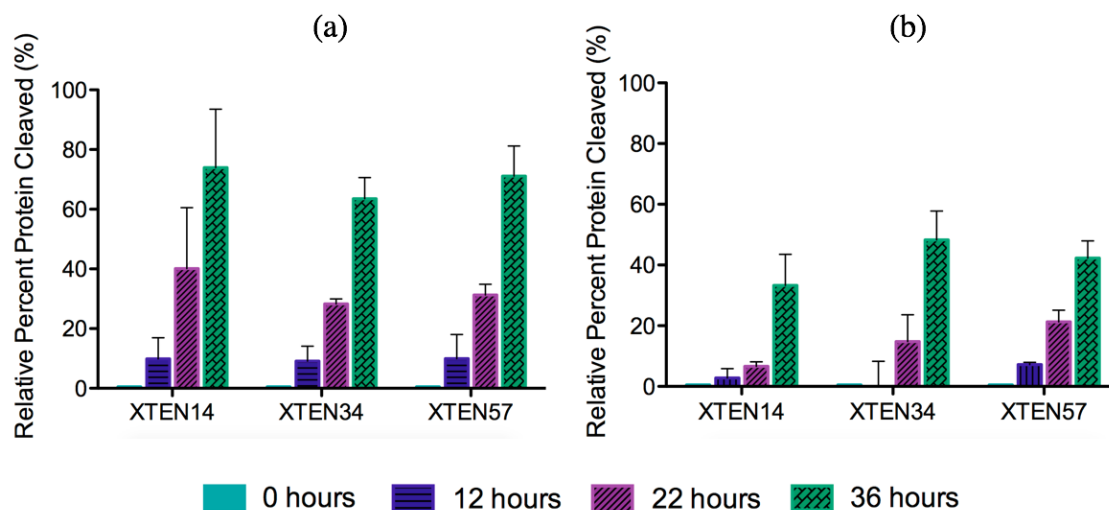
Figure 4.5 Comparison of the enzymatic cleavage of EGF-*cla*MP-XTEN14 (XTEN14), EGF-*cla*MP-XTEN34 (XTEN34), and EGF-*cla*MP-XTEN57 (XTEN57) constructs by (a) thrombin and (b) Factor Xa at 0, 12, 22, and 36 h incubation. Error bars represent standard deviation between two separate protein purifications.

Identification of cleavage sites within EGF-*cla*MP-XTEN34 and EGF-*cla*MP-XTEN57 was completed using mass spectrometry (Table 4.3, Figure 4.6). Cleavage sites within EGF-*cla*MP-XTEN34 and EGF-*cla*MP-XTEN57 were highly similar, and multiple cleavage sites within XTEN were identified. Both constructs showed cleavage between Leu52 and Arg53, the terminal amino acid of EGF. Proteolysis prior to Arg53 was observed by Factor Xa, but not by thrombin within the EGF-*cla*MP-XTEN34 construct. Both thrombin and Factor Xa cleaved EGF-*cla*MP-XTEN57 prior to Arg53, indicating that it is a site of proteolysis by both thrombin and Factor Xa; however, thrombin does not prefer this site within EGF-*cla*MP-XTEN34.

An amino acid mutation of Arg53 to Ala (Arg53Ala, R53A) was completed within EGF-*cla*MP-XTEN34. Arg53Ala showed vast improvement in the proteolytic stability of EGF-*cla*MP-XTEN34 with 17.5% of the protein cleaved compared to 48.3% cleaved without the mutation. Proteolytic stability was improved 2.8-fold by a single amino acid mutation with respect to Factor Xa (Figure 4.7a). Thrombin was not influenced by the amino acid mutation, as 63.5% of the original protein compared to 62.7% of the mutated construct was cleaved (Figure

4.7b). This is consistent with the mass spectrometry analysis that indicated that Leu52-Arg53 is not a site of proteolysis for thrombin within EGF-*cla*MP-XTEN34, and that proteolysis is occurring at other sites, specifically within XTEN. Mass spectrometry was used to identify major cleavage sites within EGF-*cla*MP-XTEN34 Arg53Ala (Table 4.3, Figure 4.6), most prominently within XTEN.

Table 4.3 Fragmentation of EGF-*cla*MP-XTEN Constructs Identified by Mass Spectrometry

Fragment	Description of Molecule	Theoretical Mass (Da)	Observed Mass (Da)	Enzyme		Construct Cleavage Occurs[a]
				Thrombin	Factor Xa	
F1	EGF-*cla*MP-XTEN[1-46]	10642.5	10635.4 ± 0.17	x	x	✷
F2	EGF-*cla*MP-XTEN[1-10]	7311.2	7302.6 ± 2.7	x	x	✓
F3	EGF-*cla*MP-XTEN[1-3]	6828.7	6820.03 ± 0.12	x	x	⊠, ✓, ✷
F4	EGF[1-52]	6065.8	6059.27 ± 0.01		x	⊠, ✷
F5	XTEN[4-31]	2969.9	2969.2	x	x	⊠, ✓
F6	XTEN[18-34]	1613.6	1615.3	x	x	✓
F7	XTEN[23-34]	1138.1	1137.7	x	x	⊠

[a]Symbols represent: (⊠) EGF-*cla*MP-XTEN34 and (✓) EGF-*cla*MP-XTEN34 with the Arg53Ala mutation, (✷) EGF-*cla*MP-XTEN57
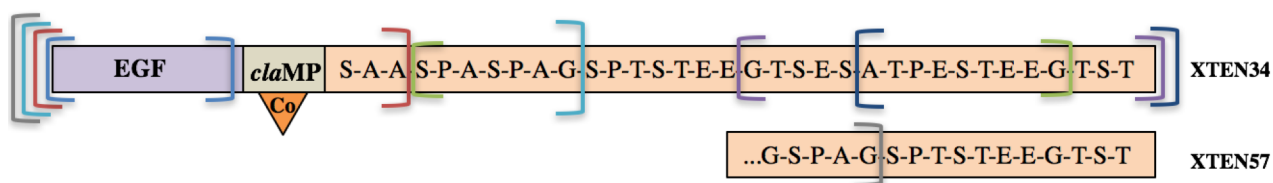
Figure 4.6 Cartoon of EGF-*cla*MP-XTEN34 and EGF-*cla*MP-XTEN57 with labeled cleavage sites identified by mass spectrometry. Table 4.3 describes the fragments identified by mass spectrometry that are referred to in this figure. Proteolysis occurred at site indicated by the bracket within the protein sequence to yield the fragments within each color-coded bracket. One site was found only in EGF-*cla*MP-XTEN57 and is represented by a highlighted segment of the XTEN57 sequence within EGF-*cla*MP-XTEN57.
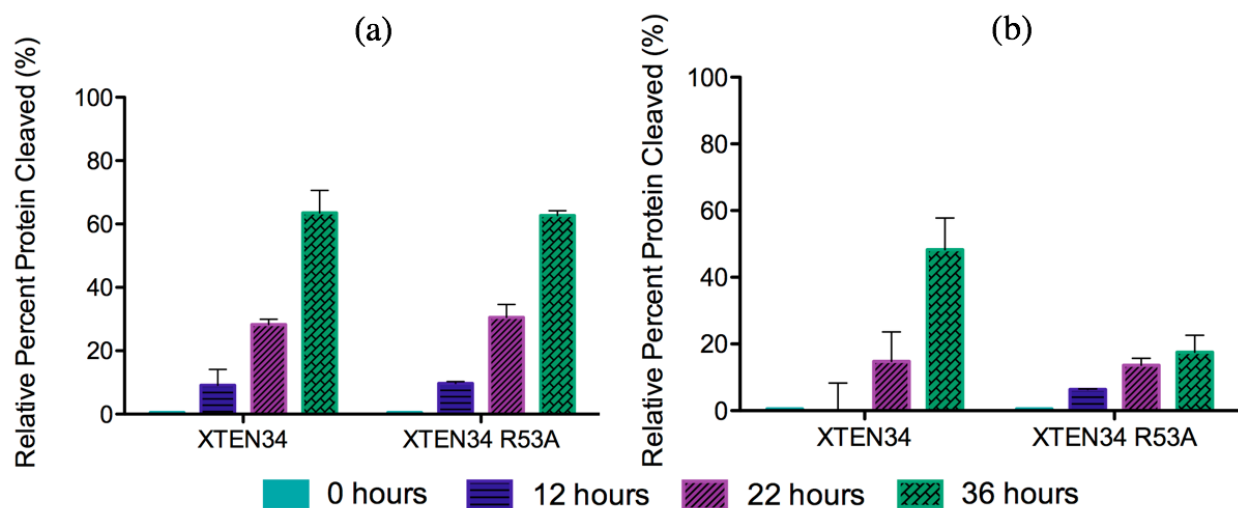
Figure 4.7 Enzymatic cleavage of EGF-*cla*MP-XTEN34 Arg53Ala incubated with either (a) thrombin or (b) Factor Xa. Enzymatic reactions were completed at room temperature and samples were taken at 0, 12, 22, and 36 h.

4.4 DISCUSSION

A candidate molecule for molecular imaging applications was designed; it consisted of three functional segments: (1) the targeting protein: epidermal growth factor (EGF), (2) a metal-binding entity: the *cla*MP Tag, and (3) a hydrophilic polymer of amino acids used to extend the half-life of recombinant proteins: XTEN. Inline addition of these molecules creates a targeted molecular imaging agent with a tunable half-life, and the synchronization of these three entities was characterized to understand the stability of the molecule. Here, cobalt was explored within the *cla*MP Tag as a safer metal for imaging than the currently used lanthanide ions. The most commonly used contrast agents are gadolinium-based, which have proven to be toxic to patients with renal impairment. Further studies have shown retention of Gd^{3+} in critical tissues such as the brain.[31,32] Cobalt was chosen to study because incorporation of cobalt into chelators such as DOTA has been successful at probing tumors; for example, a [57]Co-labeled octreotide analog was effective at imaging neuroendocrine tumors.[33] The preliminary characterization of the Co-*cla*MP

Tag resulted in determination of complete occupy of cobalt in the *cla*MP Tag (Figure 4.2, Table 4.1). Further characterization identified higher molecular weight covalently linked species (Figure 4.3) that are formed through the Cys residues within the *cla*MP Tag. This was confirmed by lack of dimerization upon mutation of the *cla*MP Tag Cys residues to Ala residues. Dimerization occurs through the *cla*MP Tag and is most likely caused by partial loss of cobalt from the *cla*MP Tag over time.

Rather than chemical conjugation of a synthetic polymer such as PEG to EGF-*cla*MP, XTEN was genetically engineered to the C-terminus of the protein sequence. Three different lengths of XTEN were examined here as an initial analysis of the effect of XTEN on the structure and function of both EGF and the *cla*MP Tag. The number of XTEN amino acids can be easily manipulated to create the desired half-life of the molecule and 14, 34, and 57 amino acids were chosen as initial lengths. XTEN did not affect the expression or purification of EGF-*cla*MP, and did not inhibit receptor binding (Table 4.2, Figure 4.4). Addition of more amino acids of XTEN may decrease interaction of EGF with the receptor, and this must be considered when designing molecules with longer XTEN polymers. A decrease in receptor binding is not necessarily undesirable; for example, Somavaratan (VRS-317, Versartis) utilizes XTEN on both the N- and C-termini of recombinant human growth hormone (rhGh) to both decrease renal clearance and reduce receptor binding affinity to delay receptor-mediated clearance mechanisms. Somavaratan exhibits a 30–60-fold increase in half-life compared to rhGh, allowing once monthly dosing.[34,35] The ability to easily tune the length of XTEN was a desirable feature that warranted investigation of the use of XTEN in this system.

Finally, the proteolytic stability of the three molecules was analyzed and compared to identify critical cleavage sites. Knowledge of potential sites of cleavage will prevent degradation

of the intact protein and create a more stable and effective molecule. Enzymatic incubation studies incubated that proteolysis by Factor Xa and thrombin occurred at multiple sites within XTEN. Although proteolysis occurs within XTEN, this is not a main concern as XTEN is known to be biodegradable and, over time, will be degraded by proteolysis. The main area of concern is proteolysis at the C-terminus of EGF, ultimately separating the targeting protein from the imaging modality and rendering the imaging agent ineffective. The primary site of concern is cleavage between Leu52 and Arg53, where the Co-*cla*MP Tag is separated from EGF. Previous stability studies of EGF-Ni-*cla*MP indicated cleavage at this same site and hypothesized that this was due to an enzymatic contaminant or metal-catalyzed chemical reaction.[29] Mutation of Arg53 to Ala inhibited Factor Xa cleavage, although thrombin cleavage still persisted (Figure 4.6). Thrombin and Factor Xa are known to have broad specificity and to cleave at multiple sites. Both thrombin and Factor Xa cleave after Arg residues within the recognition sequences Ile-Glu-Gly-Arg and Leu-Val-Pro-Arg-Gly, respectively.[36,37] Proteolysis within XTEN was the major source of proteolysis within both EGF-*cla*MP-XTEN34 and EGF-*cla*MP-XTEN57. Cleavage within XTEN was of less concern, as XTEN is known to be biodegradable. Three of the seven fragments within XTEN were caused by cleavage after Gly residues and, since Gly is a flexible residue, this is not surprising. The half-life will decrease as XTEN is degraded, and very similar sites of proteolysis were identified in EGF-*cla*MP-XTEN34 and EGF-*cla*MP-XTEN57. Analyzing proteolysis by two serum proteases, Factor Xa and thrombin, is a place to begin the analysis of degradation. Complete analysis of degradation in serum would yield further fragmentation and amino acid mutations that could potentially be used to create a more stable molecule.

4.5 CONCLUSION

Here, an improved molecular probe was investigated by using the *cla*MP Tag inline with a targeting protein to accomplish the targeted delivery of transition metals. This molecule was designed to have site-specific engineering of metal binding to the protein and formed a homogeneous molecule that could be easily produced in *E. coli*. A relevant SPECT and PET metal was investigated in this system and cobalt was determined to fully occupy the *cla*MP Tag. The XTEN fusion partner can be added to the protein and can be tuned to increase the size and ultimately the half-life of the molecule. XTEN does not have an impact on functionality with as large an addition as 57 amino acids to the C-terminus. The initial analysis of EGF-*cla*MP-XTEN constructs proved promising, and further research is warranted to investigate the ability of this molecule to probe EGFR (+) tumor cells.
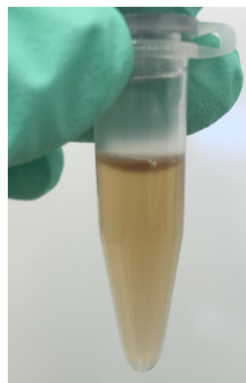
4.6 SUPPLEMENTARY FIGURES
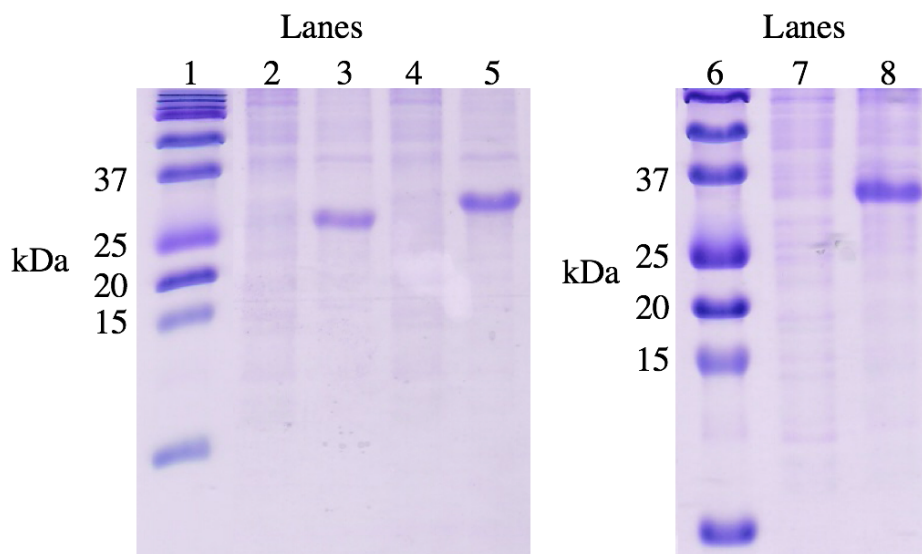
Supplementary Figure 4.1 Expression of EGF-*cla*MP-XTEN14 (lanes 2 and 3), EGF-*cla*MP-XTEN34 (lanes 4 and 5) and EGF-*cla*MP-XTEN57 (lanes 7 and 8) represented by Coomassie-stained SDS-PAGE. Lane 1 and 6 are molecular weight ladders, lanes 2, 4, and 7 are pre-induction samples and lanes 3, 5, and 8 are post-induction samples.
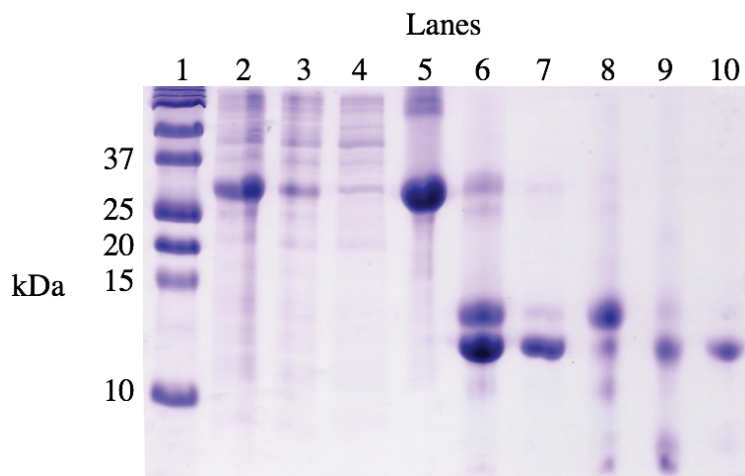
Supplementary Figure 4.2 Purification of EGF-*cla*MP-XTEN34. Molecular weight ladder (lane 1), soluble fraction of the cell lysate (lane 2), flow through of application of the cell lysate to Co-TALON (lane 3), flow through of the 5 mM imidazole wash buffer (lane 4), elution of fusion protein (lane 5), after incubation for 9.5 h with thrombin (lane 6), separation of thioredoxin-tag (lane 7), separation of thrombin-cleaved protein (lane 8), after incubation for 16 h with Factor Xa (lane 9), after SEC separation of final EGF-*cla*MP-XTEN34 (lane 10). EGF-*cla*MP-XTEN34 appears at a higher mass than expected because of XTEN, which increases the hydrodynamic radius of the molecule.[15]

(A)   (B)

Supplementary Figure 4.3 Visual inspection of incorporation of either (A) nickel or (B) cobalt into the *cla*MP Tag.
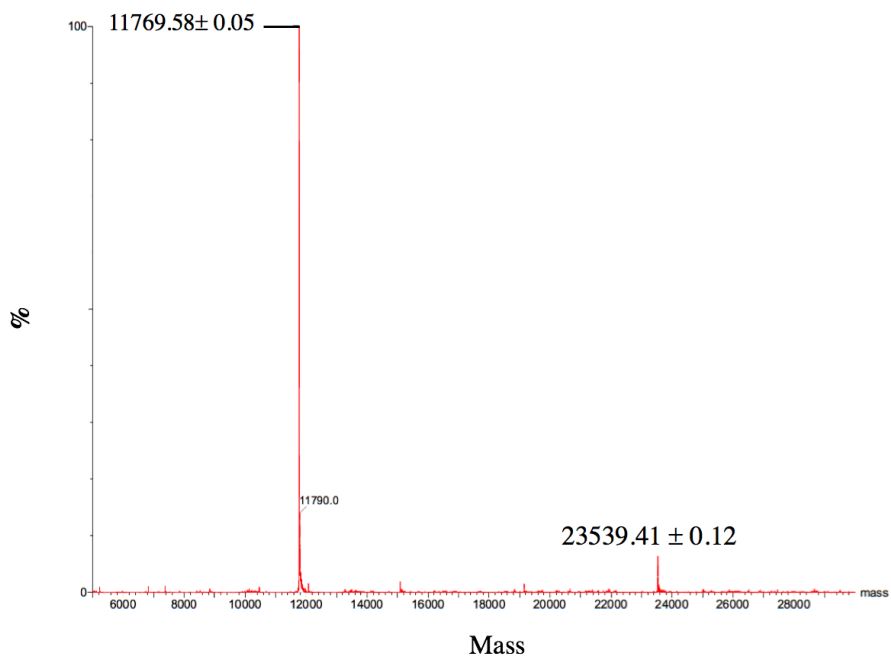
Supplementary Figure 4.4 Mass spectrometry identifies the presence of the monomer and dimer of EGF-*cla*MP-XTEN57. Monomer average theoretical mass is 11777.6 Da and dimer average theoretical mass is 23537.2 Da.

(A)   (B)
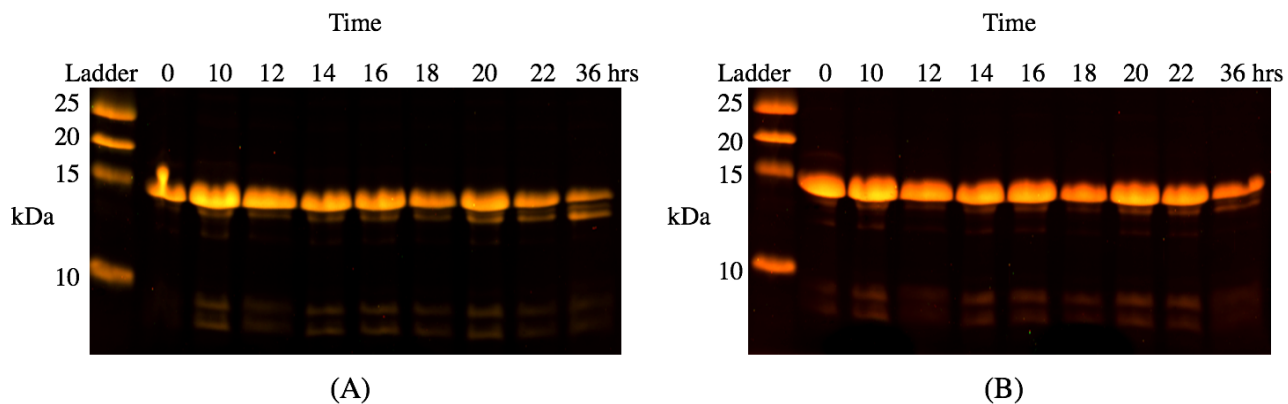
Supplementary Figure 4.5 Example SDS-PAGE of EGF-*cla*MP-XTEN57 treated with (A) Thrombin or (B) Factor Xa.

4.7 REFERENCES

1.   Herschman, H. R., Molecular Imaging: Looking at Problems, Seeing Solutions. *Science* **2003,** *302* (5645), 605.

2.   Pimlott, S. L.; Sutherland, A., Molecular tracers for the PET and SPECT imaging of disease. *Chemical Society Reviews* **2011,** *40* (1), 149-162.

3.   Chu, T.; Huang, H., Opportunities and Challenges of Radiolabeled Molecular Probes. In *Molecular Imaging: Fundamentals and Applications*, Tian, J., Ed. Springer Berlin Heidelberg: Berlin, Heidelberg, 2013; pp 473-482.

4.   Lu, F.-M.; Yuan, Z., PET/SPECT molecular imaging in clinical neuroscience: recent advances in the investigation of CNS diseases. *Quantitative Imaging in Medicine and Surgery* **2015,** *5* (3), 433-447.

5.   Spencer, S. S.; Theodore, W. H.; Berkovic, S. F., Clinical applications: MRI, SPECT, and PET. *Magnetic Resonance Imaging 13* (8), 1119-1124.

6.   Louie, A., Multimodality Imaging Probes: Design and Challenges. *Chemical reviews* **2010,** *110* (5), 3146-3195.

7.   Zhang, L.; Bhatnagar, S.; Deschenes, E.; Thurber, G. M., Mechanistic and quantitative insight into cell surface targeted molecular imaging agent design. *Scientific reports* **2016,** *6*.

8.   Chen, K.; Chen, X., Design and development of molecular imaging probes. *Current topics in medicinal chemistry* **2010,** *10* (12), 1227-1236.

9.   Kwekkeboom, D. J.; Krenning, E. P. In *Somatostatin receptor imaging*, 2002; Elsevier: pp 84-91.

10.   Chanson, P.; Timsit, J.; Harris, A. G., Clinical Pharmacokinetics of Octreotide. *Clinical Pharmacokinetics* **1993,** *25* (5), 375-391.

11.   Wester, H.; Schottelius, M.; Scheidhauer, K.; Meisetschläger, G.; Herz, M.; Rau, F.; Reubi, J.; Schwaiger, M., PET imaging of somatostatin receptors: design, synthesis and preclinical evaluation of a novel 18F-labelled, carbohydrated analogue of octreotide. *European journal of nuclear medicine and molecular imaging* **2003,** *30* (1), 117-122.

12.   Alford, R.; Ogawa, M.; Choyke, P. L.; Kobayashi, H., Molecular probes for the in vivo imaging of cancer. *Molecular BioSystems* **2009,** *5* (11), 1279-1291.

13. Backer, M. V.; Levashova, Z.; Patel, V.; Jehning, B. T.; Claffey, K.; Blankenberg, F. G.; Backer, J. M., Molecular imaging of VEGF receptors in angiogenic vasculature with single-chain VEGF-based probes. *Nature medicine* **2007,** *13* (4), 504-509.

14. Schellenberger, V.; Wang, C.-w.; Geething, N. C.; Spink, B. J.; Campbell, A.; To, W.; Scholle, M. D.; Yin, Y.; Yao, Y.; Bogin, O.; Cleland, J. L.; Silverman, J.; Stemmer, W. P. C., A recombinant polypeptide extends the in vivo half-life of peptides and proteins in a tunable manner. *Nat Biotech* **2009,** *27* (12), 1186-1190.

15. Podust, V. N.; Balan, S.; Sim, B.-C.; Coyle, M. P.; Ernst, U.; Peters, R. T.; Schellenberger, V., Extension of in vivo half-life of biologically active molecules by XTEN protein polymers. *Journal of Controlled Release* **2016,** *240*, 52-66.

16. Haeckel, A.; Appler, F.; Figge, L.; Kratz, H.; Lukas, M.; Michel, R.; Schnorr, J.; Zille, M.; Hamm, B.; Schellenberger, E., XTEN-Annexin A5: XTEN Allows Complete Expression of Long-Circulating Protein-Based Imaging Probes as Recombinant Alternative to PEGylation. *Journal of Nuclear Medicine* **2014,** *55* (3), 508-514.

17. Caravan, P.; Ellison, J. J.; McMurry, T. J.; Lauffer, R. B., Gadolinium (III) chelates as MRI contrast agents: structure, dynamics, and applications. *Chemical reviews* **1999,** *99* (9), 2293-2352.

18. Rogosnitzky, M.; Branch, S., Gadolinium-based contrast agent toxicity: a review of known and proposed mechanisms. *Biometals* **2016,** *29* (3), 365-376.

19. Pu, F.; Salarian, M.; Xue, S.; Qiao, J.; Feng, J.; Tan, S.; Patel, A.; Li, X.; Mamouni, K.; Hekmatyar, K., Prostate-specific membrane antigen targeted protein contrast agents for molecular imaging of prostate cancer by MRI. *Nanoscale* **2016,** *8* (25), 12668-12682.

20. Cai, W.; Chen, K.; He, L.; Cao, Q.; Koong, A.; Chen, X., Quantitative PET of EGFR expression in xenograft-bearing mice using 64Cu-labeled cetuximab, a chimeric anti-EGFR monoclonal antibody. *European journal of nuclear medicine and molecular imaging* **2007,** *34* (6), 850-858.

21. Mishani, E.; Abourbeh, G.; Eiblmaier, M.; Anderson, C. J., Imaging of EGFR and EGFR tyrosine kinase overexpression in tumors by nuclear medicine modalities. *Current pharmaceutical design* **2008,** *14* (28), 2983-2998.

22. Mills, B. J.; Mu, Q.; Krause, M. E.; Laurence, J. S., claMP Tag: A Versatile Inline Metal-Binding Platform Based on the Metal Abstraction Peptide. *Bioconjugate Chemistry* **2014,** *25* (6), 1103-1111.

23. Krause, M. E.; Glass, A. M.; Jackson, T. A.; Laurence, J. S., Embedding the Ni-SOD Mimetic Ni-NCC within a Polypeptide Sequence Alters the Specificity of the Reaction Pathway. *Inorganic Chemistry* **2013,** *52* (1), 77-83.

24. Senekowitsch-Schmidtke, R.; Steiner, K.; Haunschild, J.; Möllenstädt, S.; Truckenbrodt, R., In vivo evaluation of epidermal growth factor (EGF) receptor density on human tumor xenografts using radiolabeled EGF and anti-(EGF receptor) mAb 425. *Cancer Immunology, Immunotherapy* **1996,** *42* (2), 108-114.

25. Chung, K. H.; Park, S. H.; Kim, M. K.; Park, H. D.; Son, T. I., Stabilization of epidermal growth factor on thermal and proteolytic degradation by conjugating with low molecular weight chitosan. *Journal of applied polymer science* **2006,** *102* (5), 5072-5082.

26. Schellenberger, V.; Podust, V.; Wang, C. W.; McLaughlin, B.; Sim, B. C.; Ding, S.; Gu, C., Xten conjugate compositions and methods of making same. Google Patents: 2013.

27. Butt, R. H.; Coorssen, J. R., Coomassie Blue as a Near-infrared Fluorescent Stain: A Systematic Comparison With Sypro Ruby for In-gel Protein Detection. *Molecular & Cellular Proteomics* **2013,** *12* (12), 3834-3850.

28. Laurence, J. A. S.; Vartia, A. A.; Krause, M. E., Metal abstraction peptide (MAP) tag and associated methods. Google Patents: 2012.

29. Mills, B. J.; Laurence, J. S., Stability analysis of an inline peptide-based conjugate for metal delivery: nickel(II)-claMP Tag epidermal growth factor as a model system. *J Pharm Sci* **2015,** *104* (2), 416-23.

30. Gill, G. N.; Lazar, C. S., Increased phosphotyrosine content and inhibition of proliferation in EGF-treated A431 cells. **1981**.

31. Perazella, M. A., Current Status of Gadolinium Toxicity in Patients with Kidney Disease. *Clinical Journal of the American Society of Nephrology* **2009,** *4* (2), 461-469.

32. Ramalho, J.; Semelka, R. C.; Ramalho, M.; Nunes, R. H.; AlObaidy, M.; Castillo, M., Gadolinium-Based Contrast Agent Accumulation and Toxicity: An Update. *American Journal of Neuroradiology* **2016,** *37* (7), 1192.

33. Thisgaard, H.; Olsen, B. B.; Dam, J. H.; Bollen, P.; Mollenhauer, J.; Høilund-Carlsen, P. F., Evaluation of Cobalt-Labeled Octreotide Analogs for Molecular Imaging and Auger Electron–Based Radionuclide Therapy. *Journal of Nuclear Medicine* **2014,** *55* (8), 1311-1316.

34. Moore, W. V.; Nguyen, H. J.; Kletter, G. B.; Miller, B. S.; Rogers, D.; Ng, D.; Moore, J. A.; Humphriss, E.; Cleland, J. L.; Bright, G. M., A Randomized Safety and Efficacy Study of Somavaratan (VRS-317), a Long-Acting rhGH, in Pediatric Growth Hormone Deficiency. *The Journal of Clinical Endocrinology & Metabolism* **2016,** *101* (3), 1091-1097.

35. Yuen, K. C. J.; Conway, G. S.; Popovic, V.; Merriam, G. R.; Bailey, T.; Hamrahian, A. H.; Biller, B. M. K.; Kipnes, M.; Moore, J. A.; Humphriss, E.; Bright, G. M.; Cleland, J. L., A Long-Acting Human Growth Hormone With Delayed Clearance (VRS-317): Results of a Double-Blind, Placebo-Controlled, Single Ascending Dose Study in Growth Hormone–Deficient Adults. *The Journal of Clinical Endocrinology & Metabolism* **2013,** *98* (6), 2595-2603.

36. Gallwitz, M.; Enoksson, M.; Thorpe, M.; Hellman, L., The Extended Cleavage Specificity of Human Thrombin. *PLOS ONE* **2012,** *7* (2), e31756.

37. Jenny, R. J.; Mann, K. G.; Lundblad, R. L., A critical review of the methods for cleavage of fusion proteins with thrombin and factor Xa. *Protein Expression and Purification* **2003,** *31* (1), 1-11.

CHAPTER 5. CONCLUSIONS AND FUTURE WORK

5.1 MAJOR CONCLUSIONS

Reported in this work is the first exploration of the influence of the *cla*MP Tag on proteolysis. The *cla*MP Tag is a novel metal-binding tripeptide that can be placed inline with a targeting protein to specifically deliver transition metals to cells of interest. Applications of the *cla*MP Tag are being explored in the areas of therapy and diagnosis of cancer. One application consisted of determining the implications of the *cla*MP Tag inline with a matrix metalloproteinase (MMP). MMP-8 is known to degrade extracellular matrix proteins and its activity is often dysregulated in disease states. Investigation of MMP-8 led to determination of a method to express and purify large quantities of soluble and active MMP-8. Ultimately, the *cla*MP Tag exhibited no structural or functional implications on MMP-8. The ability to place the *cla*MP Tag within a protease with a metal-binding active site presents opportunities to use the *cla*MP Tag to modulate metalloenzymatic activity.

An alternative application was investigating the ability of the *cla*MP Tag to inhibit adjacent proteolysis. When designing biologics, one major limitation is rapid degradation of the biologic by proteases upon administration. Biologics are most commonly delivered by injection directly to the systemic circulation in an effort to overcome absorption and enzymatic barriers at alternative sites of administration. However, the systemic circulation is home to active proteases as well. Proteolytic cleavage adjacent to the *cla*MP Tag was investigated with respect to a relevant serum protease that is most likely encountered upon administration. A proof-of-concept study was designed to probe the ability of the *cla*MP Tag to inhibit adjacent proteolysis. Addition of a single Gly residue between the *cla*MP Tag and the enzymatic recognition sequence

was able to inhibit Factor Xa 3-fold compared to the control. In addition to providing site-specific, inline addition of transition metals, the *cla*MP Tag is able to resist adjacent proteolysis.

Additionally, the use of the *cla*MP Tag as a complex to enable molecular imaging was of interest. This work describes the first attempts to bind cobalt to the *cla*MP Tag. Complete occupancy upon exposure to cobalt was confirmed by visual inspection and quantification of spectroscopic features. XTEN was also placed inline with the *cla*MP Tag to improve the half-life of the small protein EGF. XTEN did not impact the structure or function of EGF, and was determined to be a desirable way to easily tune the size of the molecule to achieve the desired half-life. Accessible sites of proteolysis were identified, most of which were within the XTEN sequence. Cleavage between Leu52 and Arg53 was particularly important as these are the terminal residues of EGF and cleavage separates the targeting protein from the metal-bound *cla*MP Tag and XTEN. An amino acid mutation improved stability and decreased Factor Xa proteolysis by 2.8-fold.

5.2 FUTURE DIRECTIONS

5.2.1 Investigation of the *cla*MP Tag's Ability to Regulate Metalloproteinase Activity

The compatibility of the *cla*MP Tag placed inline with a matrix metalloproteinase was investigated. The *cla*MP Tag followed by an eight-amino acid linker sequence was placed on the N-terminus of MMP-8. The goal was for the *cla*MP Tag to have enough flexibility at the end of the linker sequence to reach in and bind the Zn^{2+} ion in the active site of MMP-8. It has been previously reported that the *cla*MP Tag binds the Zn^{2+} active site within MMP-8, inhibiting its activity.[1] Initial structural analysis of the MMP-8 fusion protein has been completed previously. NMR was used to probe the ability of the metal abstraction peptide (MAP) (Asn-Cys-Cys) to interact with the fusion protein and NCC was observed to interact in a localized region within

MMP-8, most likely at the Zn^{2+} active site. Further studies using alternative protein-labelling techniques are necessary to elucidate these structural interactions.

The linker sequence designed in our initial studies was not long enough to reach the active site of MMP-8 as nickel was incorporated into the *cla*MP Tag. Upon purification, it was revealed that the *cla*MP Tag was not bound to the Zn^{2+} active site. An engineered enzymatic recognition sequence was placed between the linker and MMP-8 to allow release of the *cla*MP Tag when it encountered Factor Xa. This prodrug approach allows release of the *cla*MP Tag from the enzyme once it reaches a particular enzymatic environment. The ability to control the activity of MMP-8 would be a great advantage for diseases where MMP-8 activity is dysregulated.

5.2.2 Investigation of the Co-*cla*MP Tag Complex

The Ni-*cla*MP Tag complex has been extensively characterized, and many applications using the Ni-*cla*MP Tag as a proof-of-concept have been completed because of the ideal qualities of this complex, such as rich spectroscopic features and tight metal-binding.[2,3] Initial studies with solely the metal abstraction peptide (MAP) (Asn-Cys-Cys) bound to nickel were completed.[4] The *cla*MP Tag has been shown to bind nickel with 100% occupancy when placed within a small protein and to remain stable for months at a time.[5,6] Nickel lacks molecular imaging capabilities; thus applying SPECT-active metals such as cobalt will provide insight into the use of the *cla*MP Tag as a molecular probe. Because cobalt is adjacent to nickel on the periodic table and also carries a +2 charge, incorporation of cobalt was hypothesized to be fairly similar to that of nickel. Thus, a *cla*MP-Tagged protein was exposed to cobalt affinity chromatography to successfully occupy the *cla*MP Tag with cobalt. Initial studies determined full occupancy of the *cla*MP Tag with cobalt. Similar spectroscopic features in the visible region, for example at 410

nm, was observed for both nickel and cobalt, albeit cobalt with approximately three-fourths the intensity of nickel (Table 4.2). To fully characterize the Co-*cla*MP Tag complex, studies using the Asn-Cys-Cys peptide and cobalt binding can provide insight into geometry and strength of metal-binding. Stability analysis with respect to other chelators such as EDTA and pH titrations to understand the pH range of metal-binding can be completed to fully characterize this complex. Additional analytical techniques such as ICP-MS can be used to quantify metal within the *cla*MP Tag.

Dimerization and higher molecular weight species formed upon purification of these constructs and were determined to occur through covalent disulfide bonds. EGF without *cla*MP-XTEN is stable, and previous experiments with EGF-Ni-*cla*MP Tag proved that it is stable and monomeric as well.[5] Cobalt purification and loss of metal from the *cla*MP Tag over time most likely causes dimerization to occur in these samples. Further analysis of the stability of the EGF-Co-*cla*MP Tag constructs will identify ways to prevent dimerization. Fragmentation also occurred within these fusion proteins, primarily between Leu52 and Arg53 prior to the addition of enzymes. Fragmentation could be due to a metal-catalyzed cleavage event or the presence of an enzymatic contaminant. Further investigation of the Co-*cla*MP Tag will elucidate many of the instabilities encountered with the EGF-*cla*MP-XTEN constructs.

5.2.3 *In vivo* Studies of a *cla*MP-Tagged Molecular Probe

The overall goal of investigating the stability of the *cla*MP-Tagged EGFR targeting molecules is to create an improved imaging agent. Receptor recognition and binding of the EGF-*cla*MP-XTEN constructs was confirmed using an epidermoid carcinoma cell line that overexpresses epidermal growth factor receptor (EGFR) on the surface of the cell. Often when large polymers are added to the N- or C-terminus of a targeting molecule, activity decreases due

to a decrease in receptor binding. Some pharmaceuticals take advantage of this prospect and add polymers to both the N- and C-termini of the targeting protein to reduce receptor-mediated clearance and further increase the half-life. For example, Somavaratan (Versartis) consists of an N- and C-terminal XTEN fusion to accomplish half-life enhancement.[7,8] The addition of XTEN to EGF did not impact the function of EGF, but does increase its size and thus its circulating half-life. More XTEN amino acids can be added to the N- or C-terminus to increase the half-life further to achieve the desired pharmacokinetics.

Here, the design and characterization of a preliminary imaging molecule was completed with the over-arching goal of creating a biologically relevant *cla*MP-Tagged molecular probe. The benchtop application investigated here, used cobalt scavenged from a 5-mL TALON column charged with $CoCl_2$. For SPECT and PET imaging, radioactive metal ions are required. The EGF-*cla*MP-XTEN constructs would need to be produced in the empty or apo *cla*MP Tag form and then prior to administration, loaded with the radioactive metal. Different cobalt isotopes could be used for different purposes. For example, ^{57}Co or ^{58m}Co can be used for imaging or therapeutic purposes, respectively.[9] The molecule would need to be stable in the body only hours before degradation occurred, meaning that some of the instabilities seen over days become irrelevant. Dosing this imaging agent to animals with head and neck tumors that overexpress EGFR and using SPECT imaging would be useful in characterizing how the molecule behaves *in vivo*.

5.3 REFERENCES

1.   Dixit, N.; Settle, J. K.; Ye, Q.; Berrie, C. L.; Spencer, P.; Laurence, J. S., Grafting MAP peptide to dental polymer inhibits MMP-8 activity. *Journal of Biomedical Materials Research Part B: Applied Biomaterials* **2015,** *103* (2), 324-331.

2.   Krause, M. E.; Glass, A. M.; Jackson, T. A.; Laurence, J. S., MAPping the Chiral Inversion and Structural Transformation of a Metal-Tripeptide Complex Having Ni-Superoxide Dismutase Activity. *Inorganic Chemistry* **2011,** *50* (6), 2479-2487.

3.   Laurence, J. A. S.; Vartia, A. A.; Krause, M. E., Metal abstraction peptide (MAP) tag and associated methods. Google Patents: 2012.

4.   Krause, M. E.; Glass, A. M.; Jackson, T. A.; Laurence, J. S., Embedding the Ni-SOD Mimetic Ni-NCC within a Polypeptide Sequence Alters the Specificity of the Reaction Pathway. *Inorganic Chemistry* **2013,** *52* (1), 77-83.

5.   Mills, B. J.; Mu, Q.; Krause, M. E.; Laurence, J. S., *cla*MP Tag: A Versatile Inline Metal-Binding Platform Based on the Metal Abstraction Peptide. *Bioconjugate Chemistry* **2014,** *25* (6), 1103-1111.

6.   Mills, B. J.; Laurence, J. S., Stability analysis of an inline peptide-based conjugate for metal delivery: nickel(II)-claMP Tag epidermal growth factor as a model system. *J Pharm Sci* **2015,** *104* (2), 416-23.

7.   Cleland, J. L.; Geething, N. C.; Moore, J. A.; Rogers, B. C.; Spink, B. J.; Wang, C.-W.; Alters, S. E.; Stemmer, W. P. C.; Schellenberger, V., A Novel Long-Acting Human Growth Hormone Fusion Protein (VRS-317): Enhanced In Vivo Potency and Half-Life. *Journal of Pharmaceutical Sciences* **2012,** *101* (8), 2744-2754.

8.   Moore, W. V.; Nguyen, H. J.; Kletter, G. B.; Miller, B. S.; Rogers, D.; Ng, D.; Moore, J. A.; Humphriss, E.; Cleland, J. L.; Bright, G. M., A Randomized Safety and Efficacy Study of Somavaratan (VRS-317), a Long-Acting rhGH, in Pediatric Growth Hormone Deficiency. *The Journal of Clinical Endocrinology & Metabolism* **2016,** *101* (3), 1091-1097.

9.   Thisgaard, H.; Olsen, B. B.; Dam, J. H.; Bollen, P.; Mollenhauer, J.; Høilund-Carlsen, P. F., Evaluation of Cobalt-Labeled Octreotide Analogs for Molecular Imaging and Auger Electron–Based Radionuclide Therapy. *Journal of Nuclear Medicine* **2014,** *55* (8), 1311-1316.